Technische Universität Berlin

Master-thesis

Computation of the Impulse Response of small rooms with the time domain Boundary Element Method

---

Fakultät V: Verkehrs- und Maschinensysteme
Institut für Strömungsmechanik und Technische Akustik

Ernest Granados Granados
March, 2011

Supervisors: Dipl.-Ing. Michael Stütz
Prof. Dr.-Ing. Michael Möser

Berlin, March 11, 2011 Ernest Granados Granados

Abstract

Nowadays there are many techniques that deal with the estimation of room's properties, however most of them present only good results when working in a high range of the frequency spectrum.

This thesis presents the time domain boundary element method as another way for estimating the room impulse response in small rooms, which is useful when working in the low range of the frequency spectrum.

It has been proved whether this method is suitable for this task and it has been demonstrated that it manifests some weaknesses due to instabilities in the results and because it requires a big computational expense.

The outcome of this thesis describes the causes of these problems in order to understand the reason of the unstable simulation results. It is shown that the level of accuracy on the mesh of a room will affect the eigenvalues of the coefficient matrix to be more or less distant than the unit circle. Therefore, the results are unstable.

Knowing the fundament of the problem, two different solutions, which diminish the instabilities, are developed and presented. First one will lower these values by multiplying the matrix coefficient by a low parameter, what will cause all eigenvalues to decrease as well. Second method, which has proved to offer better results, consists on applying a digital filter to lower the effect of those eigenvalues above the unit circle.

When implementing these solutions into the method, an improvement is recognized on the results. They prove to be more accurate, because results have been compared on one hand with analytical results, and on the other hand with a measurement of the impulse response of the small room.

Acknowledgements

I would like to offer my heartfelt thanks to my supervisor Michael Stütz for his enthusiasm and for his extensive support during this thesis. I especially wish to thank him for helping during the whole procedure of the realization of this thesis, where he always welcomed my questions with the best possible hints and helps. Thank you for your time, and specially for your patience and for your understanding during this time.

Furthermore, I wish to thank all friends and fellow students accompanying me during these hard years of study, Xavi Higuera, Sergi Collado, Anna Echegaray, Cristina Mairal, Gemma Morral, Anna Roma, Roger Escolá, Carla Ufano, Jesús Collado, Francisco Rodríguez, David Fernández, César Mira and Aventí Bonsón, who during these years have become my step-family, because of the time we have spent together suffering the hard times in the library in Barcelona.

To all my friends I have known during this last year in the city of Berlin. This experience helped me to discover that world has no limit for anything; great people exist everywhere and it is always a pleasure to meet people like I have met.

Also to thank all the other people I have met in these last years from all around the world. Although time with some of you could have been short or longer, I remind you all because of advices, moments and good memories. Thank you.

To Albert Morgenstern, because life is a bag of random moments.

I won't also forget Álex González and Samuel Abeijón, with who one day I sat with in a chair still in High School, and we decided to start this career together. Now it has come to an end and I will not forget all great moments from the beginning until the end.

At end I would like to thank my family and especially my parents, who in good times and bad times have been with me. They have always supported and advised all my choices thinking with their best heart. Thank you for enabling this study I have chosen, thank you for helping me afford this marvelous time in Berlin, and thank you for showing me the greatness of life.

Contents

List of Figures

1 Introduction

The subject that deals with the design of spaces in order to improve its sound quality is called Room acoustics.

Room acoustics is a field of acoustical physics, which is related to the consequences caused by the conditions of a room where lots physical events can happen. Those physical events are for instance, the propagation of the sound waves, the reflections of the sound when hitting an obstacle's boundaries, the absorption coefficient that as well affects the incident wave, etc. Mainly it is the research in relation to the acoustics of concert halls, theaters, meeting halls, classrooms, television and radio studios, churches and other spaces where acoustic performances with many listeners will be made available.

Room acoustics are based in the principle that listeners must have a good reception from the signal. That is why it must be taken into account the characteristics of human hearing, the specific features of speech perception and subjective listening habits and also with the aesthetics of music.

In order to have a good reception, the sound must travel through a channel, in the case of room acoustics, obviously a room. Because rooms are steady places that don't evolve in time, rooms act like time invariant systems and by definition, these systems transmit always the sound in the same way, independently of the time or kind of the acoustic excitation.

For this reason a room has to have a transfer function that defines it. The transfer function will be the function that converts and input signal (for example a note played by an instrument) to an output signal (the note heard by a listener).

When working in signal processing, there is an easy way to parameterize that room and obtain its qualities. It is called the "Room Impulse Response" and it denotes the output that the channel will have to an impulse in the input of the system.

This information that is obtained from a room impulse response show an estimation estimation of a sound field in a room. It describes the transmission properties the system analyzed and shows how the channel is able to transport and transform energy around it. As the name suggests, the impulse response is the response in time when the input signal is an impulse. The room impulse response (RIR) is very useful for handling this kind of signal, because with a convolution operation in the time domain, or even easier, with the multiplication operation in the frequency domain (using the frequency properties), the response to another input signal can be computed fast with the actual computational machinery.

Nowadays there are many different kinds of methods designed for this labor. Because of the rapid development of computers in the last decade, new numerical methods, suited for this exercises, have been developed in order to achieve better results in the field of acoustic simulations. These have become an important develop-

ment tool in the acoustic field, because they allow to perform series of measurements, which are quick, easy and moreover permit to vary different design parameters so that results can be optimized to a maximum.

1.1 Numerical methods for sound radiation acoustics

Nowadays there are many different kinds of methods designed for this labor. Because of the rapid development of computers in the last decade, new numerical methods, suited for this exercises, have been developed in order to achieve better results in the field of acoustic simulations. These have become an important development tool in the acoustic field, because they allow performing series of measurements, which are quick, easy and moreover permit to vary different design parameters so that results can be optimized to a maximum.

Geometric Acoustic Models

Until now the most current kind of simulation were based on modeling observed properties of sound instead of analyzing the physical effects beyond. Due to this fact, results are just approximations adjusted to observed results. For this reasons, at high frequencies these approximations are reasonably accurate but at low frequencies, where the wavelength of the sound waves is close to or greater than the dimensions of the room, they become inaccurate, because parameters must be found by trial and error, comparing simulated results with measured results.
The most common model is the "ray-tracing model", which is not only used in the acoustics, but also in the optics.

Statistical Acoustic Models

Statistical acoustic models are based on the reverberation theory, which mainly says, that in an invariant place, sound travels in all directions with same probability and intensity.

Again, this model is another approximation found by trial and error, and does not assure good results on small rooms. The method is just an approximation that works well in diffused fields, rooms with equiprobability of sound distribution and well-distributed absorption on the room boundaries. Results are taken by observation, where a formula based on the evolution on energy decay can be established and will show a probable model of the room. However, very large halls or really small ones, are not the case.

Schroeder Frequency

When in the case of analyzing a room, it is interesting which of these methods is more suitable for one case or for another. For instance, in this work, it is desired to implement an accurate method, which will work in small rooms and low frequencies.

So there is a compromise between which models to use in when working with which frequencies. In order to decide, a critical frequency establishes two regions, which will indicate which method to use. That critical frequency is named as the "Schroeder transition Frequency" and is based on using the reverberation time RT_{60} given by Sabine's equation,

In large or high reverberant rooms, which present high diffuse sound fields, the transition frequency is well established, however, in small listening rooms, this equation results in a wrong prediction of the transition frequency, because Sabine's equation is less reliable for small and absorptive rooms. Because Schroeder's frequency f_c is based on statistical room acoustics theory, another more accurate formulas are used.

In this work, the problem will be dealt in a small room and interest will be on working in a low frequency region, because non of the previous methods fulfill this conditions, wave based models are introduced.

Wave Based Models

Wave based models are, as the name says, based in the wave equation. This models are therefore designed by going to the most fundamental wave equation laws of the physics, and for this reason, the solution shows an exact estimation of the room integrities. However, due to all parameters that participate in the exact description of the room, like the sound pressure or sound velocity, actual computers limit the calculation of the wave acoustic theory to the low frequencies. Within these models there are two main families: Finite Element Method (FEM) and Boundary Element Method (BEM).

As mentioned before, wave based models are based into the most fundamental wave theory of the physics. Nowadays, wave equation calculations are being performed in the frequency domain (FD), because some results are obtained in a faster way. However, when the whole frequency spectrum is desired to be analyzed, all calculations must be done one by one for each frequency. That's why, with the new technologies, calculations done in the time domain (TD) can be more useful.

There are various numerical methods that allow simulations to be done in time domain. Today, the most used method for numerical acoustical simulations is the Finite Element Method (FEM). This method is well aimed for computations in enclosed places. The Finite Element Method (FEM) is a numerical technique for solving models in differential form. For a given design, the FEM requires the entire model, including the surrounding region, to be modeled with a finite number of elements. Once the region has been determined, with a system of linear equations one is able to calculate the potential at the nodes of each element of the object.

However, with the increase of computational machinery, there's another method which is gaining importance in the calculation of sound radiation, which is the Boundary Element Method (BEM).

The Boundary Element Method

The Boundary Element Method (BEM) is a numerical computational method for solving linear partial differential equations, that have been formulated as integral equations. This means, the method basically considers the boundary conditions of the elements, so it is not only a tool specifically designed for calculating sound pressure, but also for many areas of engineering and science like mechanics, electromagnetics, etc.

When making a study for room acoustics, what is interesting to find is the room impulse response of a room. As mentioned before, the impulse response will show the characteristics of the room by showing how the energy is distributed along the frequency range. However, when there is an input of acoustic energy into the room, this will cause that standing waves appear and peaks in the amplitude are created at the modal frequencies. These resonant frequencies are called room modes.

Room Modes are an important acoustical phenomenon, that creates an impact on sound reproduction in rooms. In general room modes are modal frequencies of a room with any shape, this means any room has got room modes at certain frequencies, where a standing wave appears. Standing waves are caused by a perfect constructive interferences of sound waves, which are traveling between two or more room boundaries.

Room modes show resonances, which are distributed in the lower audible frequencies and cause large amplitude variations at specific frequencies and long decays of sound in this range. These variations will cause the reproduction of sound in the room to be altered in such a way that transmission from source to its destination is no longer accurate. The repercussions of this effect are important, as they create a disturbance in the performance of such rooms.

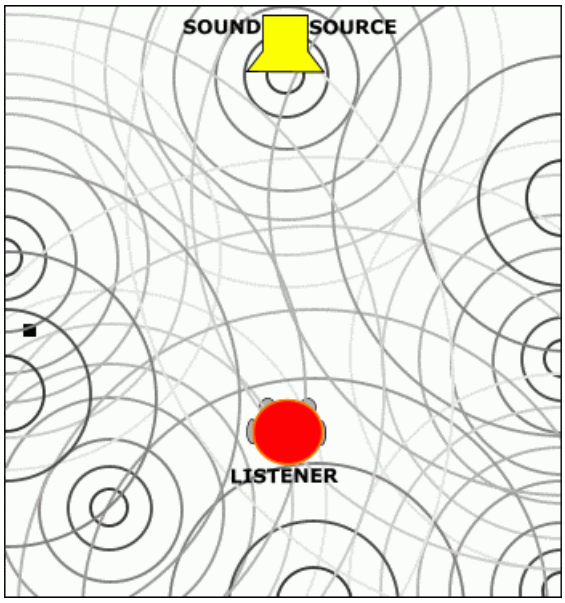

Figure 1: Design of the room affects on the reception

The topic about room modes is not a new one. It has been researched for many decades by many people, for instance Bolt (1939) and Louden (1971). Recently, room designers and loudspeaker manufacturers have been researching into it, like Farnsworth et al. (1985) or Makivirta et al. (2003). There number of solutions proposed varies from a wide spectrum. It ranges from the use of room aspect ratios (e.g. Louden 1971 or Bonello 1981), through passive absorption (e.g. Newell et al. 1997; Fuchs et al. 2000). As it can be seen there is certainly interest in the scientific and industrial fields and this indicates the importance of such a problem. And because of this problem in room acoustics, authors frequently publish studies and express the requirement for more dedicated knowledge on the perception of room modes that could guide the selection of control targets and suggest subjectively accurate reproduction conditions (e.g. Makivirta 2003, Antsalo 2003).

The room to be analyzed has also specific frequencies, where eigenfrequencies are brought up. As it has been seen, the solution of the acoustic wave equation leads to the solution of these eigenfrequencies, always that some conditions have to be met, e.g. the room has to have rigid boundaries, what means that the sound velocity v, being the normal component on the surfaces of the walls, has to be zero.

Because more knowledge is needed, new metrics have to be introduced. The motivation for this thesis is to prove the capabilities of the Boundary Element Method (BEM). This method is applied for room acoustics and is the numerical method for obtaining the room impulse response, which will be presented in the following work.

1.2 Objectives of this work

The objectives of this work and motivation for this project is double:

1. First of all, to try the precision of the BEM method to see the room impulse response. The results will be evaluated to know which is the order of error. Results of the acoustic simulation will be validated according to a comparison with acoustics measures. For this, an small room from the acoustic institute of the TU-Berlin was specifically chosen for the acoustic analysis. The room has been modeled. Although there are lots of software options for modeling and meshing a room, it choice has been FEMLAB Multiphysics. On the other hand, simulation of the room has been done with MATLAB. The realization of the measure has been realized with the system of acoustic measurement OROS System 34. Once the simulation and measure have been realized, the results will be compared with the measures in order to obtain the error committed in the simulation.

2. Second of all, demonstrate the causes of the results of simulations. Because of this, it will be important to present which are the acoustic parameters permit to improve precision in the results, so that future estimations of the acoustic conditions that the rooms can be optimal.

Plan of advance

The plan of advance will have the following steps. After this introductory chapter, where the motivation and background has been explained, section 2 will expose briefly the most important basic concepts utilized in this work in order to understand the principle of the analysis of the rooms. Later on, on section 3 the test room will be designed to prove the numerical results. This design will have different levels of geometric details, in order to see the difference between parameters. Using MATLAB, an acoustic simulation will be held. This results will be evaluated and compared with the theoretical results in order to see the differences, errors in conjectures, hypothesis and causes of those results. Next section number 4 will deal with an empirical detailed explanation of the obtention of the room impulse response of a room. It will as well held the results of the measure of acoustic behavior of the room and its results. Those results will be also compared with both analytical and simulation results, in order to see the difference between them. At last, section 5 will sum up the task realized in this work. The results obtained and the steps followed to improve results will be explained. This section will deal with what future studies could improve in the method. After the main part, this work presents an appendix where more results can be found in order to have another point of view of the evaluation of the method.

2 Theoretical fundaments

This section will describe the basic theory about the principles of room acoustics. The metric used for obtaining the room impulse response of the room will be studied, starting from its principles in the theory and its implementation in the computer.

2.1 The Room Impulse-Response

Main motivation of this work is to see how a room responses when a sound source is emitting a sound inside it. Rooms resonate just like every other kind of object do. Because of this resonation, undesired frequencies may be affected in a room. How the sound reverbs depends on the size of the room, the material of the walls, objects between the source and the receiver, etc. For this reason, in room acoustics, it is always necessary to make a study before any room is designed. Minimizing these problems is the goal when designing a good music room is to, which effects are even greater when working at low frequencies. At higher frequencies the room still has an influence, but resonances are much less of a problem since it is much easier to obtain high absorption at higher frequencies.

Modes in a rectangular room

Considered for this study is a "rectangular room", a chamber which boundaries are parallel to each other. Lecture rooms, for example, have close look in shape to a rectangular room than to any other of simple geometry, and so the results obtained in this study for strictly rectangular rooms can be applied at least qualitatively to many rooms encountered in practice. Therefore this example is not only intended for proving the theory discussed, but also can even have some practical use.

The room to be tested, will have an extension from x=0 to x = L_x in the x-direction, from y=0 to y=L_y in the y-direction and obviously, also from z=0 to z = L_z in the z-direction. The properties of the room is principally the simplest case, indeed that of that the two pair of walls are, first of all rigid, parallel to each other and lastly they are perpendicular to the other pair. With this conditions, the normal components of the particle velocity at the surface of the walls will equal zero.

In cartesian coordinates the Helmholtz equation may be written as:

$$\frac{\delta^2 p}{\delta x^2} + \frac{\delta^2 p}{\delta y^2} + \frac{\delta^2 p}{\delta z^2} = 0 \tag{1}$$

As the three variables are independent from each other, the solution can be also written as follows:

$$p(x, y, z) = p_x(x) \cdot p_y(y) \cdot p_z(z) \tag{2}$$

where each variables depends independently from a space coordinate. Inserting this product into the Helmholtz equation would lead to get three ordinary differential equations. For instance, p_x will have to satisfy the equation

$$\frac{\delta^2 p_x}{\delta x^2} + k_x^2 + p_x = 0 \tag{3}$$

together with the boundary condition

$$\frac{\delta p_x}{\delta x} \quad \text{for x=0 and x=}L_x \tag{4}$$

and taking into account the relation

$$k^2 = k_x^2 + k_y^2 + k_z^2 \tag{5}$$

Analogous equations are hold for $p_y(y)$ and $p_z(z)$.

In order to solve the differential equation following theorem is applied

$$p_x(x) = A_1 cos(k_x x) + B_1 sin(k_x x) \tag{6}$$

The constants A_1 and B_1 are used for adapting this solution to the boundary conditions.

At x=0 the sine function equals zero, this means coefficient B_1 will also equal zero. To obtain a horizontal tangent at x = L_x, it is required that $cos(k_x L_x) = \pm 1$. This means $k_x L_x$ must be a multiple of π and for this reason the solution comes when

$$k_x = \frac{n_x \pi}{L_x} \quad \text{with } n_x \in \mathbb{N} \tag{7}$$

As it was done before, the result for the other variables k_x and k_y is analogue to the previous case, what means that

$$k_y = \frac{n_y \pi}{L_y} \tag{8}$$

$$k_z = \frac{n_z \pi}{L_z} \tag{9}$$

Applying these results to formula (5) it is obtained:

$$k_{n_x n_y n_z} = \pi \left[\left(\frac{n_x}{L_x}\right)^2 + \left(\frac{n_y}{L_y}\right)^2 + \left(\frac{n_z}{L_z}\right)^2 \right]^{\frac{1}{2}} \tag{10}$$

The eigenfunctions associated with these eigenvalues are simply obtained by multiplication of the three cosines, each of which describes the dependence of the pressure on one coordinate:

$$p_{n_x n_y n_z}(x, y, z) = C \cdot cos\left(\frac{n_x \pi x}{L_x}\right) \cdot cos\left(\frac{n_y \pi y}{L_y}\right) \cdot cos\left(\frac{n_z \pi z}{L_z}\right) \tag{11}$$

where C is an arbitrary constant.

To this formula should also be added the time dependent term $e^{j\omega t}$ but it has been purposely skipped due to avoiding obvious repetitions.

Formula (11) presents a "normal mode" of the room, corresponding to a three-dimensional standing wave. The pressure amplitude is zero at all points at which at least one of the cosines becomes zero. This occurs for all values of x which are odd integers of $\frac{L_x}{2n_x}$, and for the analogous values of y and z. The numbers n_x, n_y and n_z indicate the numbers of nodal planes perpendicular to the x-axis, the y-axis and the z-axis, respectively.
The eigenfrequencies corresponding to the eigenvalues of equation (11), are given by the relation of the wave number:

$$k = \frac{w}{c} \text{ with } w = 2\pi f \text{ and } c = 340\frac{m}{s} \tag{12}$$

Which follows to

$$f_{n_x n_y n_z} = \frac{c}{2\pi} k_{n_x n_y n_z} \tag{13}$$

Transforming the cosine function into a sum of exponentials

$$p_{n_x n_y n_z} = \frac{C}{8} \sum \exp\left[\pi i \left(\pm\frac{n_x}{L_x}x \pm \frac{n_y}{L_y}y \pm \frac{n_z}{L_z}z\right)\right] \tag{14}$$

This formula represents a plane wave, whose direction of propagation is defined by the angles β_x, β_y and β_z, which it makes with the coordinate axes, where

$$cos\beta_x : cos\beta_y : cos\beta_z = \left(\pm\frac{n_x}{L_x}x\right) : \left(\pm\frac{n_y}{L_y}y\right) : \left(\pm\frac{n_z}{L_z}z\right) \tag{15}$$

If one of the three values of n, for example n_z, equals zero, then the corresponding angle (β_z for this example is makes a right angle, what means that the propagation takes place perpendicularly to the respective axis, parallel to all planes which are perpendicular to that axis. This vibration pattern is frequently referred to as a "tangential mode". If there is only one non-zero integer n, the propagation is parallel to one of the coordinate axes, then this is called an "axial mode". Modes with all integers different from zero are called "oblique modes".

1. **Axial modes:** The axial modes lay in the lower frequencies. This is so, because two of the three order numbers n_x, n_y, n_z equal zero, what means that the sound wave propagation is parallel to one room boundary and is perpendicular on two opposite walls. Because they lay in lower frequencies, the impact on a room is really affected by these modes.

2. **Tangential modes:** In this case, the wave propagation is perpendicular on one room wall but moves tangential to the other pair of walls. Because in this case two out of the three order numbers n_x ,n_y, n_z are different to zero the sound wave hits another pair of walls with oblique incidence.

3. **Oblique modes:** Last kind of modes are the oblique modes occur only when all order numbers n_x, n_y, n_z are not zero. Because all of the coefficient are not zero, this modes are located in even higher frequency regions than the tangential modes. As its name shows, in this case, the sound wave hits each wall with oblique incidence.

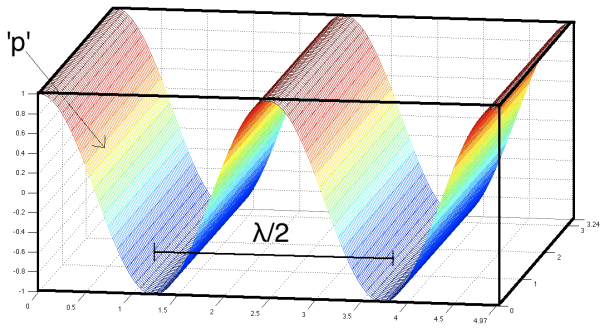

Figure 2: Sketch of the Axial Modes with $n_x = 4$

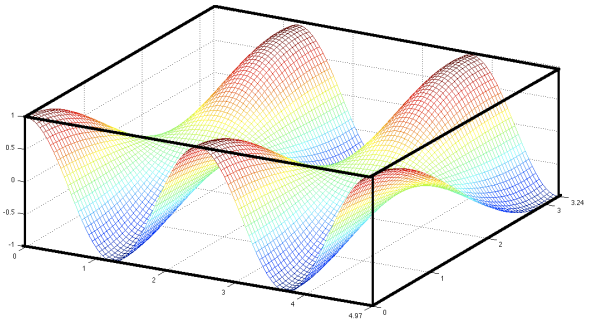

Figure 3: Sketch of the Tangential Modes with $n_x = 4$ and $n_y = 1$

It is demonstrated that number of eigenfrequencies which are located between the zero frequency and some other given frequency can be estimated by the following formula.

$$N_f = \frac{Vk^3}{6\pi^2} = \frac{4\pi}{3} V \left(\frac{f}{c}\right)^3 \tag{16}$$

where V is the geometrical volume of the room under consideration.

The number of points corresponding to tangential modes can be also calculated:

$$N_{tan} = \frac{1}{4\pi} k^2 (L_x L_y + L_y L_z + L_z + L_x) = \frac{k^2 S}{8\pi} = \frac{\pi S}{2} \left(\frac{f}{c}\right)^2 \tag{17}$$

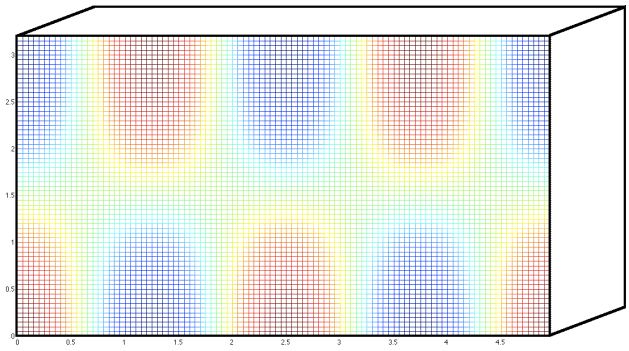

Figure 4: Sketch of the Oblique Modes

where we introduced the total area of all walls, $S = 2(L_x L_y + L_y L_z + L_z L_x)$.

With a correction term due to the axial modes and a corrected expression of the number of modes with eigenfrequencies, the formula becomes:

$$N_f = \frac{4\pi}{3} V \left(\frac{f}{c}\right)^3 + \frac{\pi}{4} S \left(\frac{f}{c}\right)^2 + \frac{L}{8}\frac{f}{c} \tag{18}$$

with $L = 4(L_x + L_y + L_z)$

It can be shown that in the limiting case $f \to \infty$ is valid not only for rectangular rooms but also for rooms of arbitrary shape. This is not too surprising since any enclosure can be conceived as being composed of many rectangular rooms. For each of them it yields the number of eigenfrequencies.

2.2 The Boundary Element Method

After the theoretical explanation, it will be described the numerical method which wants to simulate this behavior.
The Boundary Element Method's (BEM) principle takes point from the fundamental solution of the wave equation: a field of a punctual source, also known as monopole:

$$p(r,t) = \frac{\rho ckQ}{4\pi} e^{j(\omega t - kr)} \tag{19}$$

Where:

- p - acoustic pressure
- r =|x-y| - distance between the source and the observation point
- ρ - density of the fluid
- c - speed of sound propagation
- ω - angular frequency
- k - wave number = ω / c
- Q - the source strength

The main idea of BEM is to find the pressure caused by the vibration on a surface. That surface to be calculated, will be divided into various smaller surfaces (called elements) and those elements will be interpreted as monopoles. For every monopole there will be a normal vector which will point to the direction of the field; that will show the pressure radiated inside the room.

As in another wave based methods, like FEM, the starting point to the derivation of the formula is the basic wave equation. The wave equation is deduced on the basis of fluid continuity, Newton's second law for a differential element of the fluid, the relationship between fluid density and the sound pressure level, assuming a relative small variation of density.
The wave equation can be written also as follows:

$$\frac{\delta^2}{\delta t^2} p(r,t) = c^2 \nabla^2 p(r,t), \text{ with } \nabla \text{ as the Laplace operator.} \tag{20}$$

Supposing harmonic behavior of the acoustic pressure:

$$p(r,t) = \underbrace{\hat{p}(r)}_{\text{amplitude}} \underbrace{e^{j\omega t}}_{\text{phase}} \tag{21}$$

Using the Fourier Transform, equation (2) turns into the Helmholtz equation in the frequency domain:

$$\nabla^2 \hat{p}(r,\omega) + k^2 \hat{p}(r,\omega) = 0, \text{ with k}=\frac{\omega}{c} \tag{22}$$

As mentioned, BEM requires to know the velocities in the boundaries of the subject. From the acoustic pressure one is able to calculate the vibrating velocity in every point of the field. The relation between velocity and pressure and the pressure in a field comes determined by the Euler's equation, which is the consequence from the second Newton's law.

$$\frac{\delta \hat{p}}{\delta x_i} = -j\omega\rho_0\hat{v}_i, \text{ i=1,2,3} \tag{23}$$

So that the general solution of equation (25) describes the real situation it is necessary that all boundary conditions are satisfied in the borders that limit the volume. Moreover, an acoustic field decreases as long as it gets farer of the source, and in the end disappears when the distance is infinitely big. The mathematical expression of this property is Sommerfeld's radiations condition:

$$\lim_{r\to\infty}\left(\frac{\delta p}{\delta r} + jkp\right) = 0 \tag{24}$$

This is a necessary condition to reject the solutions of Equation (24) which do not disappear into infinity.

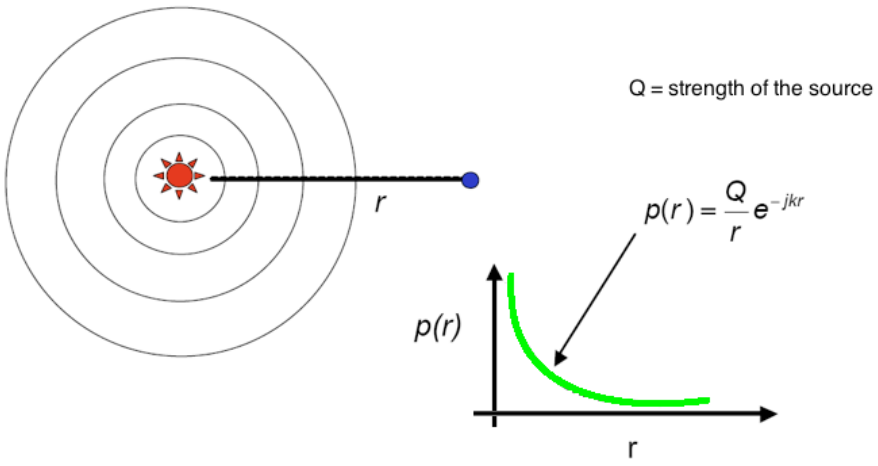

Figure 5: Equation of the monopole

As an example, there is a solid surface 'S' and volume 'V' occupied by a fluid. The volume may be both inside and outside the surface. The vibration of the surface creates a sound field in the fluid. The process can be represented, as a sum of smaller radiation surface elements. Each element will create the field of Equation (22). Another form of Equation (22) is the "fundamental solution", or "Green function" $G(x, y)$:

$$G(x,y) = \frac{e^{-jk|x-y|}}{4\pi|x-y|} \text{ , with 'x' a point in the field and 'y' in the surface.} \tag{25}$$

Assuming that the pressure $p(x)$ satisfies the Helmholtz Equation (25) within the fluid, it can be multiplied by the function $G(x, y)$ and afterward, this product integrated throughout the whole volume:

$$\int_V G(x,y)\left(\nabla^2\hat{p}(x) + k^2\hat{p}(x)\right)dx = 0 \tag{26}$$

Applying to this integral Gauss's theorem for any f(x) function:

$$\int_V f dV = \oint_s f dS \tag{27}$$

and taking into account that G(x,y) has the solution for a point source:

$$\nabla^2 G(x,y) + k^2 G(x,y) = \delta(x-y) \tag{28}$$

it can be demonstrated with Equation (27) that Equation (28) is transformed into the Helmholtz Integral Equation:

$$\int_S \left[p(y)\frac{\delta G(x,y)}{\delta n} - \frac{\delta p(y)}{\delta n}G(x,y)\right]dy = \begin{cases} p(x) & \text{if } x \text{ outside of the boundary} \\ \frac{1}{2}p(x) & \text{if } x \text{ in the boundary} \\ 0 & \text{if } x \text{ inside the boundary} \end{cases} \tag{29}$$

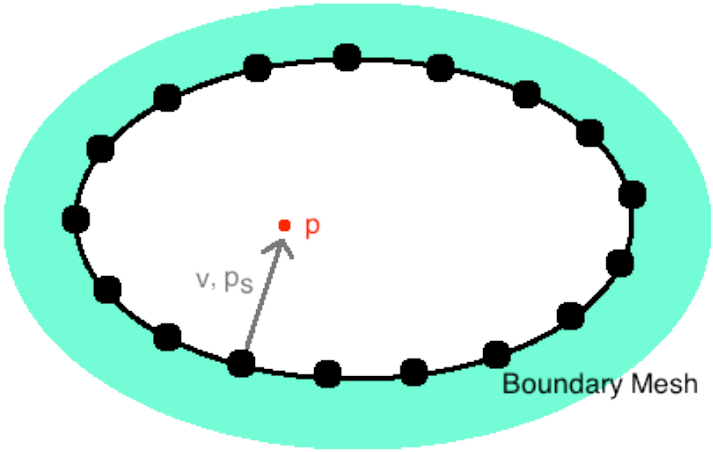

Figure 6: Pressure of the interior of the boundary

As it can be seen, the result of this equation depends on where x is located.

The resolution of discretizing the surface will transform the integral equation into a system of linear equations, which in matrix form will look like this:

$$\underline{\underline{A}}\underline{p_s} = \underline{\underline{B}}\underline{v} \tag{30}$$

Being 'A' and 'B' known matrices, 'p_s' and 'v' are the velocity vectors and pressure at the nodes of the mesh surface, respectively.

After solving this system (the largest computational effort), the pressure at any point in the field can be calculated by the same equation (29). Later on, it will be described how to obtain this result.

The Frequency-Domain to Time-Domain transition

As it was mentioned before, in this work BEM will be used in the time domain (TD-BEM). When using BEM in the frequency domain, results have to be calculated for every frequency of interest, what for obtaining the whole frequency spectrum, would make it calculate all the frequencies. Because of the Fourier Theorem with just one calculation in the time domain, the results can be shown in all frequencies for the slot of time chosen. This means, that it will not be necessary to calculate the response for all frequencies.

In order to achieve this one may start from the Fourier Transform equation:

$$h(t) = \frac{1}{2\pi} \int_{-\infty}^{\infty} h(\tau) e^{i\omega\tau} t\tau \tag{31}$$

When applying this into the Kirchhoff-Helmholtz equation it will result to

$$4\pi d(x_0)\Phi(x_0, t_0) = -\int_S \int_{-\infty}^{\infty} \frac{e^{-ikr}}{r} \frac{\delta\phi_\omega}{\delta n} e^{i\omega t_0} d\omega dV + \tag{32}$$

$$+ \int_S \int_{-\infty}^{\infty} \phi_\omega \frac{\delta}{\delta n} \frac{e^{-ikr}}{r} e^{i\omega t_0} d\omega dV \tag{33}$$

$\phi_\omega(x)$ denotes the Fourier transform of the field $\phi(x,t)$.

First integral results to be

$$\int_{-\infty}^{\infty} \frac{e^{-ikr}}{r} \frac{\delta\phi_\omega}{\delta n} e^{i\omega t_0} d\omega dV = \frac{1}{r} \frac{\delta\Phi}{\delta n} \left(x, t_0 - \frac{r}{c}\right) \tag{34}$$

Here, use was made of the following relationship

$$\phi(x, t + \Delta t) = \int_{-\infty}^{\infty} \phi_\omega(x) e^{i\omega t + \Delta t} d\omega = \int_{-\infty}^{\infty} e^{i\omega\Delta t} \phi_\omega(x) e^{i\omega t} d\omega \tag{35}$$

With Δt =-$\frac{r}{c}$ gives the retarded time

$$t_r = t_0 - \frac{r}{c} \tag{36}$$

Equation (37) which shows the equation in the field can be solved by splitting it into two integrals.
For this one first forms the normal derivative of the field of a monopole. The partial integrals from the addition can now be treated separately, because of the distributive property. A more extended description can be found in M.Stütz doctor's dissertation[5].

So results for the second part of this integral:

$$\int_{-\infty}^{\infty} -\frac{i\omega}{cr} e^{-ikr} \frac{\delta r}{\delta n} \phi_\omega e^{i\omega t_0} \delta w = -\frac{1}{cr} \frac{\delta r}{\delta n} \int_{-\infty}^{\infty} i\omega \Phi_\omega e^{i\omega(t_0 - r/c)} \delta w = \tag{37}$$

$$= -\frac{1}{cr} \frac{\delta r}{\delta n} \frac{\delta \Phi}{\delta t}(x, t_0 - \frac{r}{c}) \tag{38}$$

This results may be substituted in the previous equation and follows to the the Kirchhoff Integral.

$$4\pi d(x_0)\Phi(x_0, t_0) = \int_V \left[\frac{1}{r} \frac{\delta \Phi}{\delta n} + \frac{1}{r^2} \frac{\delta r}{\delta n} \Phi + \frac{1}{cr} \frac{\delta r}{\delta n} \frac{\delta \Phi}{\delta t} \right]_{ret} dV \tag{39}$$

which follows to the following equation:

$$4\pi d(x_0)\Phi(x_0, t_0) = \int_V \left[\frac{\rho_0}{r} \frac{\delta^2 \Phi}{\delta n \delta n} + \frac{1}{r^2} \frac{\delta r}{\delta n} \frac{\delta \Phi}{\delta t} + \frac{\rho_0}{cr} \frac{\delta r}{\delta n} \frac{\delta^2 \Phi}{\delta t^2} \right]_{ret} dV \tag{40}$$

Replacing pressure 'p' and velocity 'v' it results:

$$4\pi d(x_0)p(x_0, t_0) = -\int_V \left[\frac{\rho_0}{r} \frac{\delta v_n}{\delta t} - \frac{p}{r^2} \frac{\delta r}{\delta n} - \frac{1}{cr} \frac{\delta r}{\delta n} \frac{\delta p}{\delta t} \right]_{ret} dV \tag{41}$$

And lastly with the introduction of the sound flux q:

$$q = -\rho_0 \frac{\delta v_n}{\delta t} \tag{42}$$

equation (41) may be further simplified to:

$$4\pi d(x_0)\Phi(x_0, t_0) = \int_V \left[\frac{1}{r} \frac{\delta \Phi}{\delta n} + \frac{1}{r^2} \frac{\delta r}{\delta n} \Phi + \frac{1}{cr} \frac{\delta r}{\delta n} \frac{\delta \Phi}{\delta t} \right]_{ret} dV \tag{43}$$

This is the solution of the Kirchhoff-Helmholtz Integral obtained in the time domain.

2.2.1 Numerical implementation

In the previous section, the Kirchhoff integral was derived. It allows the calculation of the sound field in a region S where the speed and the pressure of the boundary are given. However, for a numerical treatment of the boundary integral equation, it is necessary to discretize the equation. This section will deal with the discretization of the parameters in order the stated theorem to be manipulated with numerical tools.

Time discretization

It is defined an initial time t_0 and simulated the passage of time by adding the constant time step Δ t, which will create a series of time points. It makes sense to be set $t_0 = 0$ for an invariant system and therefore obtain:

$$t_i = i\Delta t \tag{44}$$

and as mentioned before, so remains the retarded time:

$$t_{ri} = i\Delta t - \frac{r}{c} \tag{45}$$

For this numerical implementation, time has to be divided into equidistant time steps. This is mandatory step to follow, which will bring problems later on for the accuracy of the system and will be later on treated. The time course of the sound flux q per time step is regarded as constant.

$$q(x, t_{ri}) = \sum_{m=1}^{i} q_m \Psi(_{tri}). \tag{46}$$

$$\Psi(t_{ri}) = \begin{cases} 1 & \text{if } t_{ri} \in [t_{m-1}, t_m) \\ 0 & \text{else} \end{cases} \tag{47}$$

As it is obvious, when discretizing time there is a lost in accuracy, when the measure is to be held to the infinity. Of course it is also possible to use more sophisticated approaches. But the basic stability properties of the method studied is the simplest case, the discretization chosen. It is not exclude that cause higher order shape functions be of unstable behavior. An important point is the approximation of the time derivative $\frac{\delta p}{\delta p}$ From the derivative definition:

$$\frac{\delta p}{\delta t} = \frac{p(x,t) - p(x, t - \Delta t)}{\Delta t} \tag{48}$$

In discrete form is obtained

$$\frac{\delta p}{\delta t} = \sum_{m=1}^{i} \frac{p_m - p_{m-1}}{\Delta t} \Psi(t_{ri}) \tag{49}$$

For a linear-time approach is used so that the derivative is not zero at the time.

$$p(x,t_{ri}) = \sum_{m=1}^{i} \left(\frac{t_m - t_{ri}}{\Delta t} p_{m-1} + \frac{t_{ri} - t_{m-1}}{\Delta t} pm \right) \Psi(t_{ri}) \tag{50}$$

For causality reasons, all variables prior to the time t_0 are set to zero:

$$p(y,t_i) = 0 \tag{51}$$
$$q(y,t_i) = 0 \tag{52}$$

Applying previous results, as it is demonstrated by M. Stütz [5] it is obtained the following:

$$\begin{aligned} &4\pi d(x_0) p_i(x_0) = \\ &\quad = -\int_S \left[\frac{q}{r} + \frac{\delta r}{\delta n} \left(\frac{p}{r^2} + \frac{1}{cr} \frac{\delta p}{\delta t} \right) \right]_{ret} dS \\ &\quad = \dots \\ &\quad = -\sum_{m=1}^{i} \int_S \left[\frac{q_m}{r} + \frac{\delta r}{\delta n} \frac{1}{r^2} [(i-m+1)p_m - (i-m)p_{m-1}] \right] \Psi(t_{ri}) dS \end{aligned} \tag{53}$$

Integration limits

As it can be seen in the solution of the linear equation, the formula has to be integrated for each time step. However t_m has not to be integrated over the whole boundary V. According to the following limits of integration

$$\begin{aligned} t_{m-1} \le t_i - \tfrac{r}{c} < t_m \\ (m-1)\Delta t \le i\Delta t - \tfrac{r}{c} < m\Delta t \\ (i-m)c\Delta t < r \le (i-m+1)c\Delta t \end{aligned} \tag{54}$$

Numerical results of the boundary element method show the whole boundary surface has to be integrated. However, there might be a simplification of the method in which only a shell may be integrated. Shell has an outer radius of $(i-m+1)c\Delta t$ and an inner radius $(i-m)c\Delta t$. For simplicity, a new index introduced by μ.

$$\mu = i - m + 1 \tag{55}$$

This shell may be referred as a μ spherical shell. By the time discretization, integration was set in source areas-shares, which have the form of spherical shells. Sources are located in one of these spherical shells, and their distance from the observation point will influence that there will be a time-delayed result. The total sound pressure is now obtained simply by adding up the individual sound pressure levels. Always, of course, taking into account the 'maturities' of the sound waves.

A bigger advantage is that integration does not depend on the sound pressure and the velocity. Of course this is only possible with having a constant time step Δ t, since otherwise this would change the area of integration.

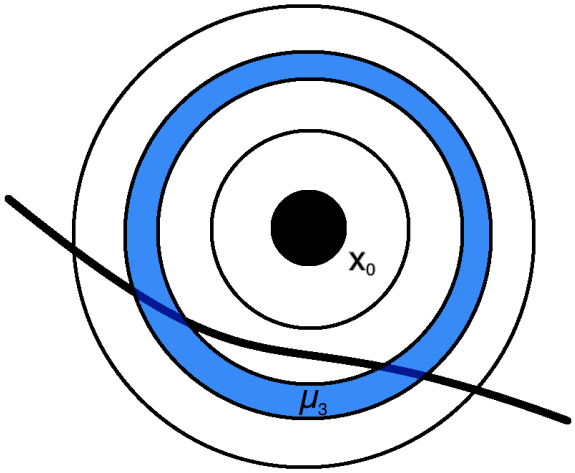

Figure 7: Spherical shells to be integrated

Spatial discretization

Because the BEM method treats points of the volume as monopoles, the space to be treated is a volume, whose boundaries will be divided into N planar elements.

$$V = \sum_{n=1}^{N} V_n \tag{56}$$

The sound pressure and the velocity are set each element as a locally constant

$$p(x,t) = \sum_{n=1}^{N} p^n(t) \tag{57}$$

$$q(x,t) = \sum_{n=1}^{N} q^n(t) \tag{58}$$

Collocation method

The solution of the boundary integral equation needs further numerical treatment in order to obtain a finite number of discrete equations so that the method can be used easily. One way of solution to solve approximately, the collocation method.

This method has the advantage of a relatively small numerical effort, since the fulfillment of the boundary integral equation is required only at certain collocation points. As collocation points are used for piecewise constant.

Matrix Lineup

As it has been explained, each time step has an own value which affects the integration. This time generates an matrix composed by integrals. The following equations can be therefore stated:

$$-2\pi p_1^i = \int_{V_1} \frac{1}{r_{i1}} \Psi(t_{r1}) dV q_q^1 + ... + \int V_1 \frac{1}{r_{iN}} \Psi(t_{r1}) dV q_1^N + \dots$$

where i = 1, 2, 3 , ... N

These equations may also be written in the following matricidal form:

$$-2\pi \underline{p}_1 = \underline{\underline{G}}_1 \underline{q}_1^1 + \underline{\underline{G}}_2 \underline{q}_1^2 + \dots + \underline{\underline{G}}_N \underline{q}_1^N \tag{59}$$

In order to simplify the system, new variables have been used, G and H:

$$g_{ab}^{\mu} = \int_{V_b} \frac{1}{r_{ab}} \Psi(t_{r\mu}) dV \tag{60}$$

$$h_{ab}^{\mu} = \int_{V_b} \frac{\delta r_{ab}}{\delta n} \frac{1}{r_{ab}^2} \Psi(t_{r\mu}) dV \tag{61}$$

And at last it may be obtained the following equation system:

$$-2\pi \underline{p}_i = \sum_{\mu=1}^{\mu_{max}} \underline{\underline{G}}_{\mu} \underline{q}_{i-\mu+1} + \sum_{\mu=1}^{\mu_{max}} \underline{\underline{H}}_{\mu} \left[\mu \underline{p}_{i-\mu+1} - (\mu - 1) \underline{p}_{i-\mu} \right] \tag{62}$$

The index μ_{max} specifies the maximum required number of matrices. For all $\mu > \mu_{max}$ the value of g_{ab}^{μ} and h_{ab}^{μ} equal zero. Since only a finite structures are considered, there is a r_{max} between collocation and observation point and the most distant source point.

$$\mu_{max-1} c\Delta t < r_{max} \leq \mu_{max} c\Delta t \tag{63}$$

Shells with $\mu > \mu_{max}$ are therefore neglected.

The main problem of BEM is that the resulting G and H matrices are very sparsely occupied. Because only a small fraction of the sources are in the observed area, one may obtain zeros for a large part of the data values $\Psi(t_{r\mu})$.

As a typical example is the filling of a starting from G matrix with $\mu = 5$ is shown. Equation 62 can also be rewritten in a large system of equations

$$-2\pi \begin{bmatrix} \underline{p}_1^1 \\ \underline{p}_1^2 \\ \vdots \\ \vdots \\ \underline{p}_1^N \end{bmatrix} = \begin{bmatrix} \underline{\underline{G}}_1 & 0 & \dots & & \dots & 0 \\ \underline{\underline{G}}_2 & \underline{\underline{G}}_1 & 0 & \dots & \dots & 0 \\ \underline{\underline{G}}_3 & \underline{\underline{G}}_2 & \underline{\underline{G}}_1 & \dots & \dots & \vdots \\ \vdots & & & \ddots & & \\ 0 & \dots & \underline{\underline{G}}_{\mu_{max}} & \dots & & \underline{\underline{G}}_1 \end{bmatrix} \begin{bmatrix} \underline{q}1 \\ \underline{q}2 \\ \vdots \\ \vdots \\ \underline{q}_i \end{bmatrix} +$$

$$+ \begin{bmatrix} \underline{\underline{H}}_1 & 0 & \dots & & \dots & 0 \\ 2\underline{\underline{H}}_2 & \underline{\underline{H}}_1 & 0 & \dots & \dots & 0 \\ 3\underline{\underline{H}}_3 - \underline{\underline{H}}_2 & 2\underline{\underline{H}}_2 & \underline{\underline{H}}_1 & \dots & \dots & \vdots \\ \vdots & & & \ddots & & \\ 0 & \dots & -(\mu_{max}-1)\underline{\underline{H}}_{\mu_{max}} & \dots & & \underline{\underline{H}}_1 \end{bmatrix} \begin{bmatrix} \underline{p}_1 \\ \underline{p}_2 \\ \vdots \\ \vdots \\ \underline{p}_i \end{bmatrix} \tag{64}$$

After this theoretical part, this section may be closed. It has been summarized the method for obtaining the theoretical values by using an accurate formula which obtains the eigenfrequencies. With this theoretical values, it might be interesting to contrast the results of the method, also previously stated, and compare the results for a future analyze.

3 Simulation of test rooms

Simulation is a very useful tool for evaluating the benefits of a specific method. However, in lots of cases the realization of the simulations can take long time and consume lots of resources of a computer. For example, they can take hours or even days so that results of a simulation can be obtained.

The objective of this thesis is to investigate about the efficient application of the method already described. The purpose is to prove how the method could be improved over other techniques, which nowadays are more developed, but on the other hand more limited. This is the reason why the method to be studied gains importance.

In this section will be described the procedure for the realization of the rooms simulation. To test the methods described in previous section a test room has been modeled and also has been meshed with a different order of number of elements, so that with the solution of the simulation it can be seen the difference of the parameters and find which solution is the most accurate as possible. It is also important to compare the results between different time-steps, so that the prediction consistency along contents of the acoustic quality method can be stated. In the following sections it will be also shown the results of the tests and analyzed which of the acoustic quality solution do perform better.

3.1 Description of the room to be measured

Before realizing any acoustic study it is necessary to generate the model that is going to be subject of study. This is a very important step in order to obtain a the most exact values as in the analytical case, so that next step will consist only in proving that the results are similar to real measured values. Simulation will then show the quality of the method, with its advantages and disadvantages over other methods.

The election of the room was influenced by some parameters. First of all is the limitation on the method. The TD-BEM needs to create big matrices to calculate the coefficients at the boundaries. According to this, the bigger the size of the room is, the more computational requirements there will be. For this reason, a small size of the room, will suit better with the measure. Another condition for the election is to have a room with hard walls. The method has been implemented for boundaries with total reflection. The Acoustic Faculty of the TU-Berlin disposes of a series of rooms, which are conditioned for this kind of measures. Because it is desired to contrast the numerical results with the empirical values, a test room will me be modeled. So that the model of the room is as exact as possible with the real

room, the room will be measured with laser measuring device. In the figure 8 it is represented the actual measured size of the room. It is about a rectangular room of size $L_x = 497cm$, $L_y = 324cm$ and $L_z = 300cm$ whose walls are made from concrete. Therefore it is called as a room with hard walls or with a lot of reflection.

Figure 8: Plans of room: top view

As it can be seen in this figure, in order to precise even more the quality of the method, four test points have been indicated in different locations of the room. As it has been mentioned before, this is an advantage of the boundary element method, because one the matrices coefficients have been calculated, BEM does not need more big calculations, when changing test points.

Now it is the turn to position the sound source, which will bein the following point of the map:

	Position x	Position y	Position z
Sound source	49	62	182

And the points in space desired to be measured:

	Position x	Position y	Position z
Position 1	193	188	144
Position 2	92	397	245
Position 3	103	245	167
Position 4	235	325	65

Positions are meant to be in centimeters.

Doing a model consists in creating a mesh. A mesh is a mapped grid of the desired object to be analyzed. For this case above described room will be meshed with COMSOL Multiphysics. However the quality of grid can be better or worse depending on the number of elements used. As a first point this means that the increase of the elements in a mesh, plays an important role that can affect results, when this value is increased. For this reason, the room to be simulated will have a big number of elements for the mesh, in order to have the most accurate results possible. In this case, the room will be meshed in approximately more than 5000, 8000 and 16000 elements. It is supposed that the time for computation for these simulations will be really high.

As it has been explained in the theoretical section, one of the main problems of the boundary element method is the handling of big matrices. These matrices have the coefficients in order to calculate the pressure. A finer discretization will increase the size of these matrices and this will cause that the computation requirements will increase exponentially. This is the motive that will encourage to realize the computation in a bigger computer. Because of the computational time, it is chosen that model is therefore simple; a simple rectangular room. With this it is achieved to control in the best way all the aspects of the room, what means that in case that a problem appears, a fast solution can be found.

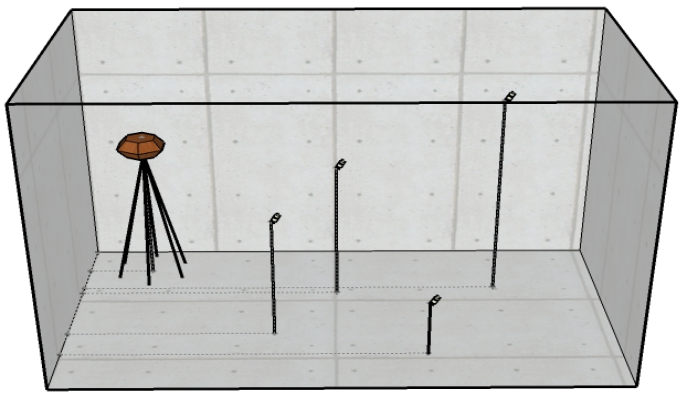

Figure 9: Model of room in 3D

Once the mesh is created, MATLAB will need diverse data to interpretate that model, and will as well provide that necessary data to the mesh in order to be able to use . It seems the method is able to apply the necessary excitation to calculate the room modes and check the response in a certain point of the room. Our method will analyze mostly low frequencies (from 16Hz up to a maximum of 2000Hz, when interesting) and will calculate the behavior of the structural radiant surfaces.

In the following section the process for obtaining the results of the simulation will be described step by step.

3.2 Parametrization of the room

As mentioned before, the first step is to create the mesh. The room to be modeled is indeed a three-dimensional space, so the first step of the process will be to create a 3D model. To create the mesh of the room, software capable of doing mesh is needed. A mesh, is the sum of polygons which, edges and faces define the shape of a polyhedral object in 3D computer graphics and solid modeling. The boundaries usually consist on triangles, quadrilaterals or other other simple convex polygons, since this simplifies rendering, but may also be composed of other general concave polygons, or polygons with holes.

For this case the description of the test rooms will be made by quad-edge meshes, which store edges, half-edges, and vertices without any reference to polygons. The polygons are implicit in the representation, and may be found by traversing the structure.

The first choice in meshing would always be a very regular shaped quadrilateral mesh. The 'perfect' quad is square. The 'perfect' triangle element is an equilateral triangle. As soon as the quad or triangle is distorted errors start to creep in.

Most real life shapes mean it is tough to have an all quad or very regular quad mesh. So an irregular quad mesh is usually produced. This is quite standard and should give reasonable results as long as the distortion of each element is within limits.

Purely triangular mesh is useful when model has very large amounts of double curvature. The three noded triangle fits the surface accurately. Although it is not he best solution, it avoids using planar quad elements which fit themselves to curved surfaces by internal rigid links between the flat element surface and the curved surface.

As in the case rooms are purely rectangular, best choice of use is to use a mapped quadrilateral mesh.

The number of elements in which the room is meshed will play an important role in the definition of the parameters, which will define later the system.
So that the room can have a parametrization coefficient, which can define them when comparing the accuracy of the simulation, the parameter β is established. This constant β is the coefficient between c, the speed of sound, multiplied by the period of time, in which our system will be discretized, and then divided by $L_{element}$, which is the length of one element of the mesh of the structure wanted to be measured. This means the equation will be as follows:

$$\beta = \frac{c \cdot dt}{L_{element}} \qquad \text{,where c} = 343\ \frac{m}{s}\ \text{(in room temperature: } 20^{\circ}C)$$

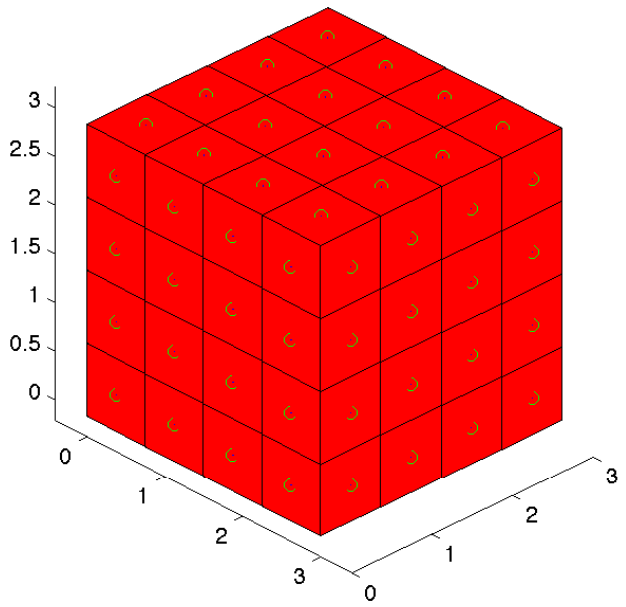

Figure 10: Example of a mesh from a cubical room of length 3 with 96 elements

As c is a constant parameter and $L_{element}$ depends on the quality of the mesh, this means the decision of dt will be the most important. As explained before, dt is the parameter which discretizes in time the system, also called time-steps. The value chosen for the parameter dt will be as low as possible to emulate analog time and have a better appreciation of the evolution of the system. This will make our response have better resolution and accuracy. But on the other hand, it must be taken into account that because of BEM stability problems and big sparse matrices, which take long calculation time, the value cannot be too low. By convention it is decided the value for the parameter β, which lies between 0,5 and 1,5.

Pressure in the interior of the room

After mesh has been created, next procedure will be to take surfaces from outsides so that we can analyze their boundary conditions. As BEM method consists basically in the boundary conditions, this step might be the most important for the whole procedure. A room, made by six rigid and parallel walls, will be divided into six surfaces, which surfaces will be later divided into even more smaller polygons. As it is to be analyzed the acoustics of a room, this means the source of sound pressure will be installed our model and the elements will have a normal vector pointing inside the room, representing the vector of pressure and vector of velocity of the

nodes in the meshed surface.

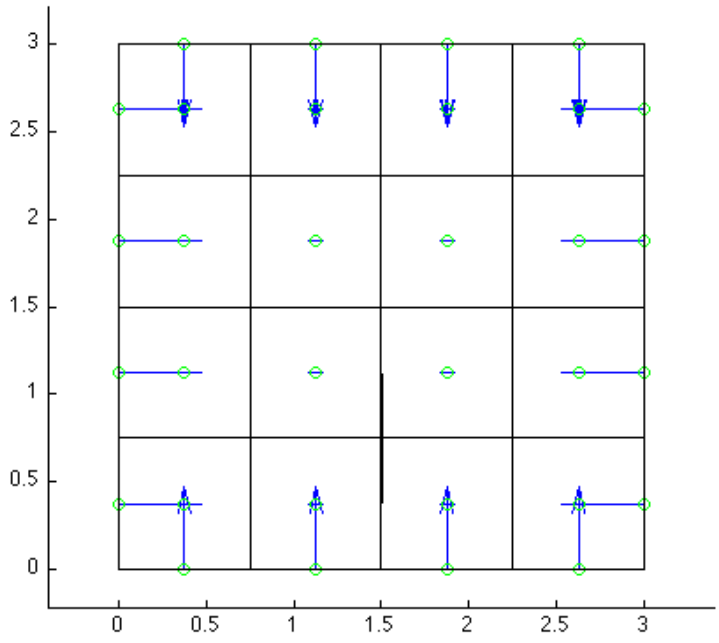

Figure 11: XZ plane of the cubical meshed room with normal vectors pointing to the inside

After this process, the first step of the BEM is already done. The surface being to be tested has been totally divided into small elements, where later the pressure will be calculated. As this condition is a lineal operation, to obtain it can be added. In the following episode the results of the simulation and of its parameters will be farther discussed.

3.3 Analysis of the room impulse response results

In this section there will be discussed the results from the simulation of the characterized test room, which in next section the measurement procedure with its results will be described. With the results of the calculated impulse response it will be tried to state the reason of the better or worse quality and performance and possible solutions.

3.4 Objective evaluation of the time-domain response results

This section shows the solution of the time-domain boundary element method (TD-BEM). In order to prove its liability , the method will be tested with different parameters. For example, show the difference between the results for a same space meshed with 3 different values.

Differences because of the Mesh

The following pictures 12, 13, 14 and 15, show the difference between a mesh with elements from 2030 up to 8280. Results higher than this value are difficult to manipulate and therefore they have not been plotted in the time domain. These results are the obtained directly without post-processing. All of the simulation results present instabilities as it can be seen on the illustrations. However for the presentation of the results in the frequency domain they have been filtered in order to diminish the big instability located at 0Hz.

As it can be seen, results improve depending on the β parameter used. With $\beta = 0.5$ the results happen to be too unstable. The time step is too small for the meshes used. As it can be seen, the solution with worst results is the one that uses both the less number of elements, although even using more than 8000 elements for the mesh is not enough.

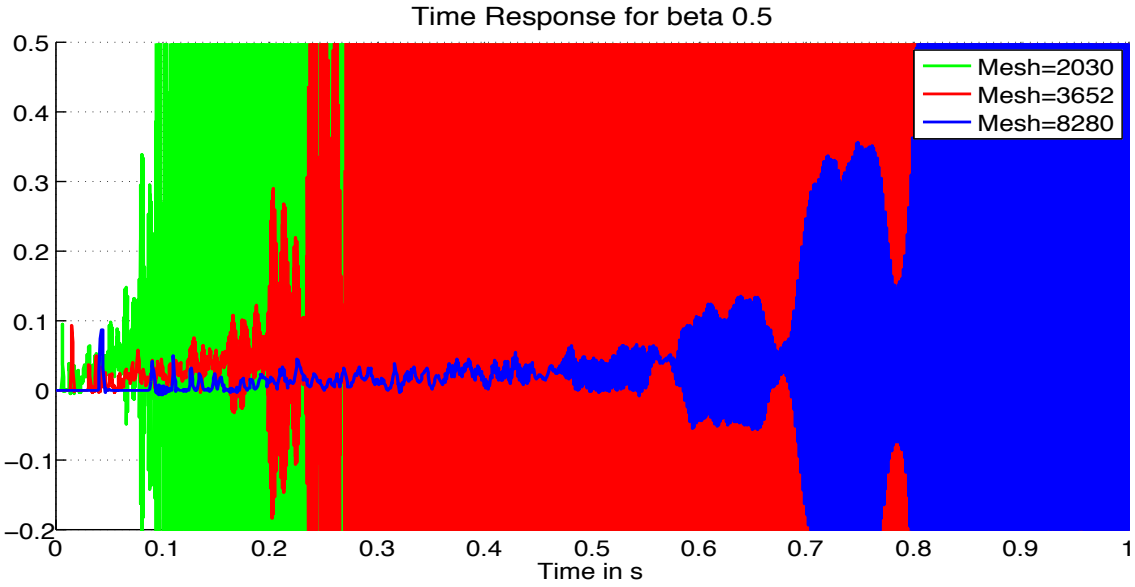

Figure 12: Room Impulse Response in Time Domain for different mesh with $\beta = 0.5$

Best results should happen when using a β parameter between 0.5 and 1.5. The simulation results obtained for $\beta = 0.8$ and for $\beta = 1$ are prove of this. Although the results still present instabilities it can be seen how the improvement of

the mesh, clearly improves the results. On the other hand, it can be seen in the results a simpler (or coarser) mesh, is more unstable.

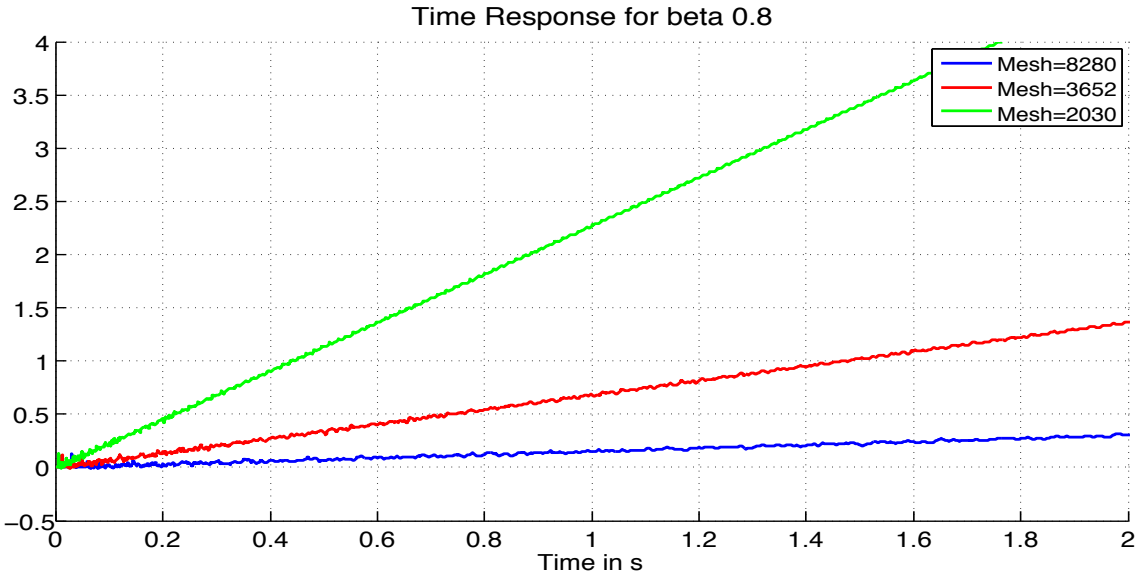

Figure 13: Room Impulse Response in Time Domain for different mesh with $\beta = 0.8$

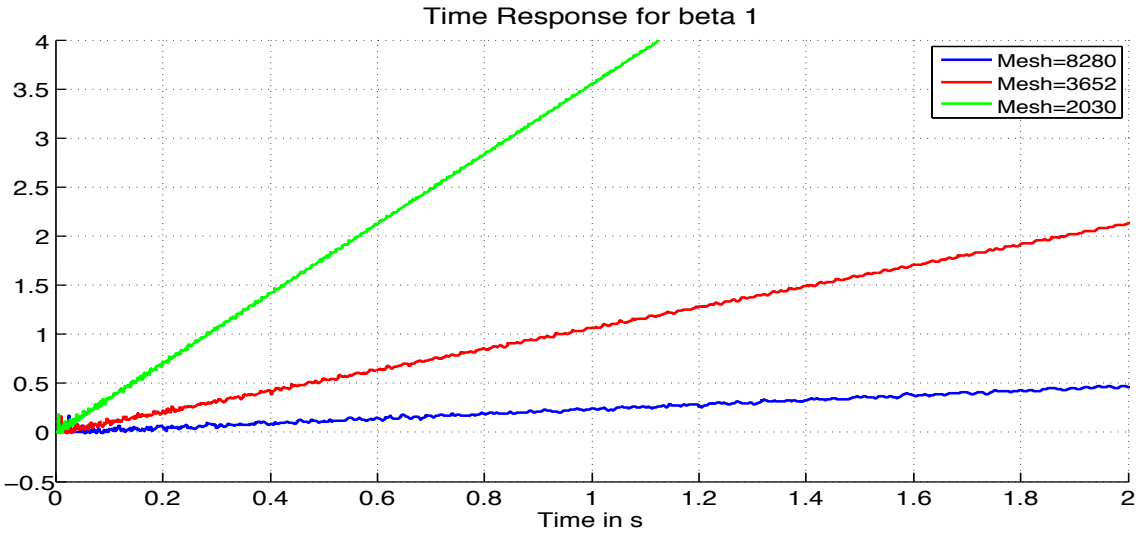

Figure 14: Room Impulse Response in Time Domain for different mesh with $\beta = 1$

As the results can prove, a smaller time-step indicates to give better results. Because when simulating with a smaller time-step means having a better discretization of time, results show to be less unstable.
The last case, for $\beta = 1.5$ it can be see, that because of the bad discretization, the results have a bigger slope because of the effects of the frequency at 0Hz.

A table afterwards shows the inclination for each case depending on the discretization of the mesh which states the improvement that affects a better mesh.

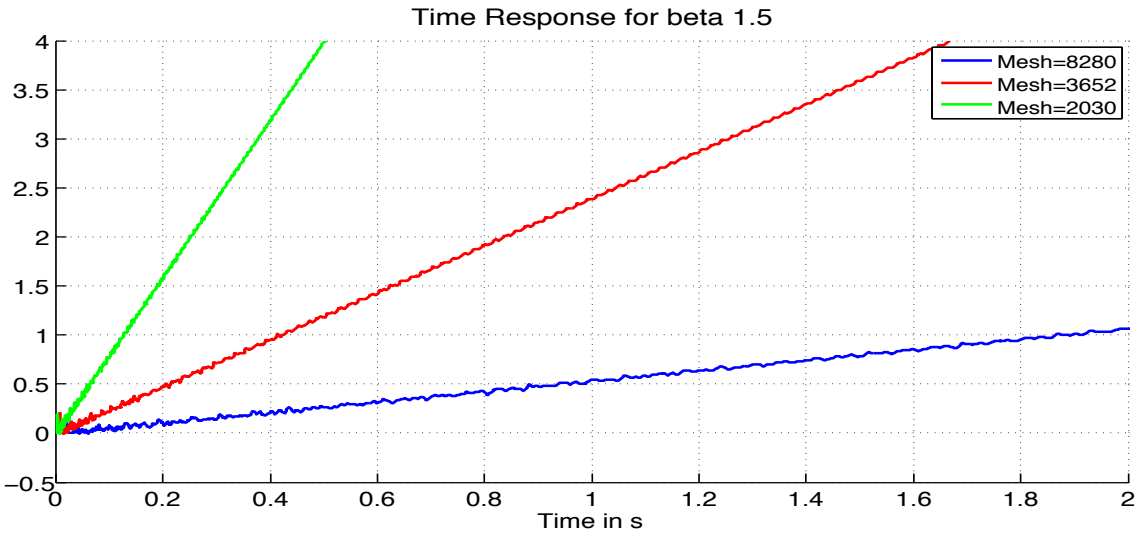

Figure 15: Room Impulse Response in Time Domain for different mesh with $\beta = 1.5$

	2030 Elements	**3652 Elements**	**8280 Elements**
β =**0.5**	not stable	not stable	not stable
β =**0.8**	2.2	0.7	0.14
β =**1.0**	3.5	1.06	0.16
β =**1.5**	8	2.4	1.9

Table 1: Inclination of results depending on mesh and β

Differences because of the time-discretization

Having proved that the first statement of the hypothesis was as expected, it will be tested the second one. In this case, solution is represented with different time steps. It will be denoted the parameter β, the coefficient of discretization depending on the number of mesh used. For four different βs it is interesting to see the results. Because the best results lay within $\beta = 0.5$ and $\beta = 1$ it has been chosen to use the four values 0.5, 0.8, 1 and 1.5.

Illustration number 16 shows clearly the instability depending on the election of the parameter β. Two different meshes have been used. Figure 16, meshed with 5046 elements, shows that a higher β improves the quality of the results, although on the other hand results show a bigger instability.

Increasing the number of elements, as seen may improve this result as it can be seen in the figure 17. With 10546 elements, a higher β shows to be stable for more time.

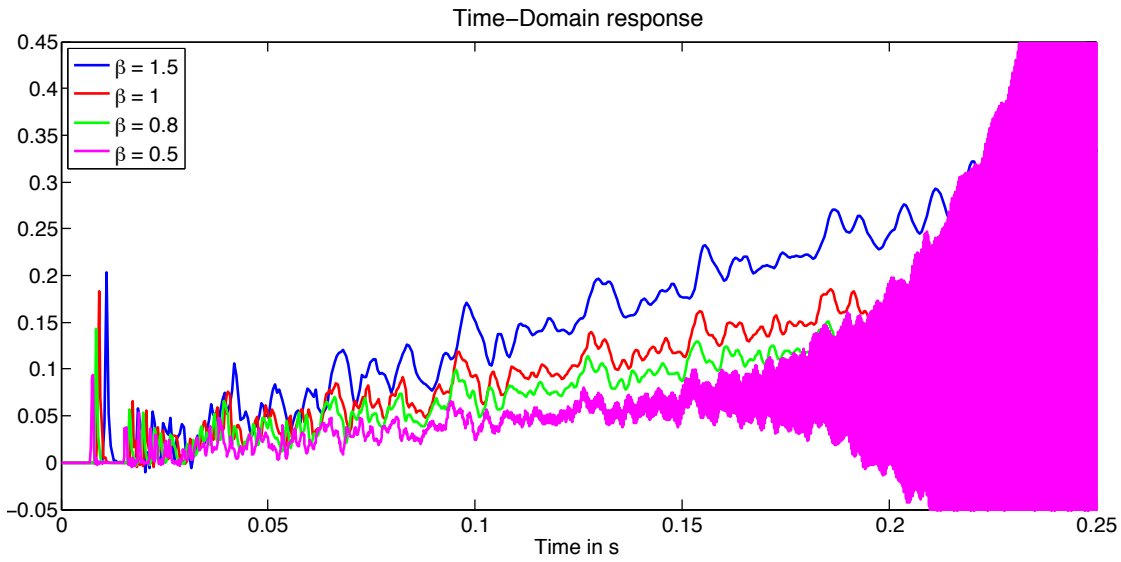

Figure 16: Room Impulse Response in Time Domain for different β with mesh of 5046 elements

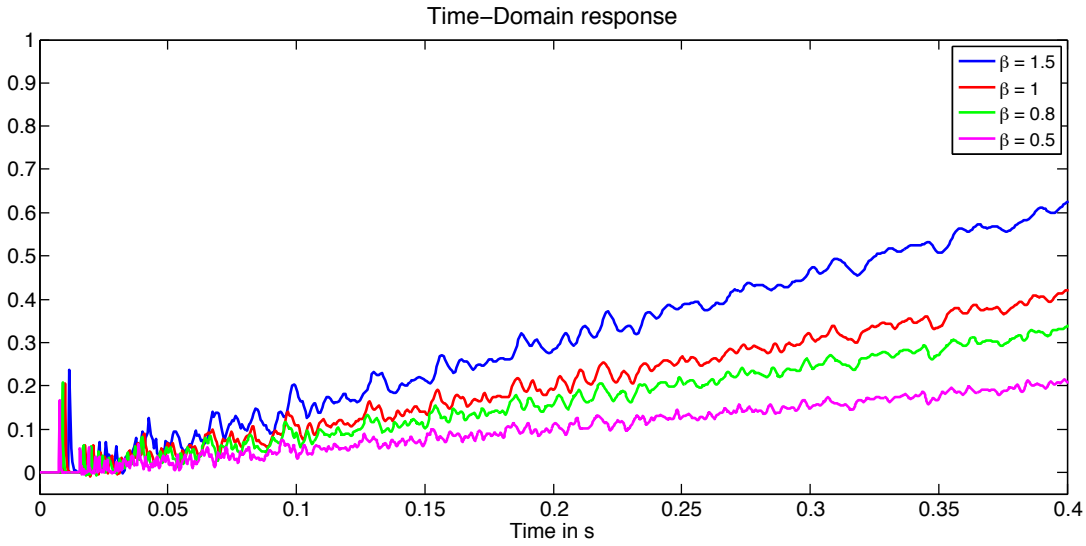

Figure 17: Room Impulse Response in Time Domain for different β with mesh of 10546 elements

3.4.1 Validation of the time-domain response results

As it has been demonstrated simulation needs to have a big number of mesh elements and also a big small value for the parameter in the time-discretization parameter in order to get the best solution.

BEM most problematic issue is the instability in the results. Because of the segmentation of the space to be treated there is always an error in the system. It seems to be beneficial to use more elements in the area so that the boundary is sat-

isfactorily represented. The instability problem can be solved in a very simple way by increasing the number of mesh elements, sufficient to approximate the results to the real values.

It is also clearly visible that there is an instability, which depends from the time-discretization parameter, Δt, chosen. It can be stated, that the smaller the time steps are, the more unstable are the results. A frequency in lower frequencies affects more in the results and therefore the slope of the results is bigger. On the other hand, there is a compromise in the election of β, because the higher the parameter is, the lower the slope is, but on the other hand, the faster it will become unstable. For this reason, it can be stated that because of the number of gauss points per element is not changed, when increasing the time-discretization parameter fewer gauss points are treated and for this reason the integration accuracy turn out to be worse. Figures have shown there is more instability in the results depending on the grade of time steps. The smaller the time steps are, the better the results are.

To validate the results of the calculated response it is desired to see the contrast between the results and theoretical values and also a frequency response measurement of the room, in order to see the differences and be able to state the causes of the results.

3.5 Objective evaluation of the frequency-domain response results

It is always desired to see the frequency response, in order to check the liability of the process. This section will show the illustration of the solution modes calculated with the previous theoretical basis. Using the Fast Fourier Transformation,

$$X(f) = \sum_{j=1}^{N} x(t)\omega_N^{(j-1)(k-1)}$$

where

$$\omega_N = e^{(-2\pi i)/N}$$

of the time-domain boundary element method results, one might obtain the results in the frequency domain.

When plotting the solution the obtained result is the following:

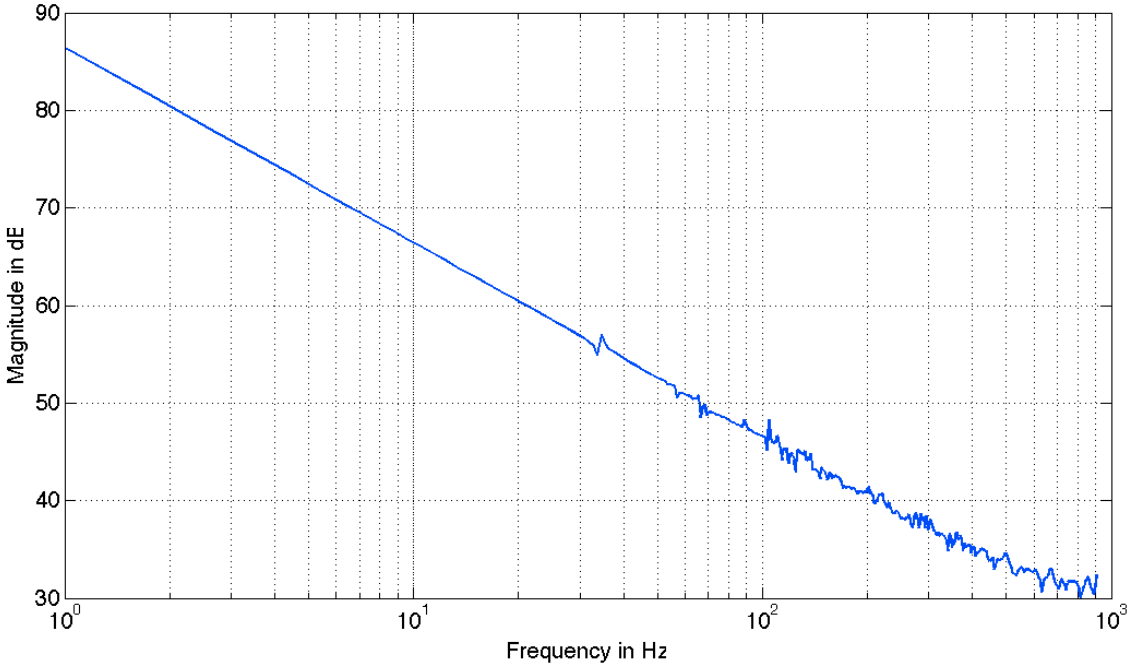

Figure 18: Room Impulse Response in Frequency Domain

Because of the instability problem a slope in the time-domain is transformed into a big peak on frequencies near to zero Hz. In order to eliminate this problem, two different methods have been tried.

- Damping of the matrix coefficients
- High-pass Filter at 16Hz

3.5.1 Damping the matrix coefficients

Results of the simulation show instability problems. The problem of instability in BEM simulations is not a new issue. It has been stated in many studies, that the boundary element method has difficulties at the frequencies of internal resonances in the closed structures, however just a pair solutions have been found for this instability problem.

The paper presented by H. Wang et.al. [12] takes an intensive study about this topic which shows the causes of this problem.

In previous results it as been shown that the corresponding time domain simulation presents instabilities depending on the time-step parameter. It is being investigated that there is a relation between instability and time-step parameter, and it can be related by the eigenvalues matrix of the time-stepping process.

Attenuation of eigenvectors

This citation indicates that instability comes from numerical errors imposed on a more fundamental problem and may be best avoided through a time domain technique corresponding to the methods already available in the frequency domain. It has been studied, that there is a difficulty in the form of the BEM when solving the exterior acoustic problem, that occurs at the set of frequencies at which the interior homogeneous problem has non-zero solutions. Therefore various methods are in development in order to create a modified boundary equation, so that a solution at all frequencies can be devised.

The inverse Fourier transform applied to the Boundary Integral Equation gives the time domain version, referred to as the retarded potential integral equation, which when discretized leads to a time-stepping scheme.

The connection between instability and internal resonances in scattering problems has been recognized for the exterior domain. It has been suggested that it could be rectified by an averaging of the time steps; Numerical evidence is given to establish the link through relating each eigenvalue of an iterative matrix with a particular frequency.

As it was shown in the theoretical section, applying the inverse Fourier transform to the BEM solution, one could obtain the time domain version. As a result of H being time dependent, as shown in previous section, the equation becomes modified into causing a time delay named Δt.

So remains the time domain equation:

$$\phi_i = \sum_{n=1}^{N} D^n \phi_{i-n} + y_i \tag{65}$$

where:

the vector ϕ contains the values of ϕ at the M nodal points and at the time $i\Delta t$. N is the number of time steps required to describe the system. The matrices Dδn come from the BEM. Finally, y_i comes from the given boundary values of $\frac{\delta\phi}{\delta n_q}$, where the surface velocity in this case has been treated as zero. For the analysis of stability, previous equation may be rewritten as an iterative form:

$$\Phi_i = H\Phi_{i-q} + g_i \tag{66}$$

where

$$\Phi_i = \begin{bmatrix} \phi_{i-N+1} \\ \phi_{i-N+2} \\ \vdots \\ \phi_{i-1} \\ \phi_i \end{bmatrix}, H = \begin{bmatrix} 0 & I & 0 & \dots & 0 \\ 0 & 0 & I & \dots & 0 \\ \vdots & \vdots & \vdots & \ddots & \vdots \\ 0 & 0 & 0 & \dots & I \\ D^{(N)} & D^{(N-1)} & D^{(N-2)} & \dots & D^{(1)} \end{bmatrix}, g_i = \begin{bmatrix} 0 \\ 0 \\ \vdots \\ 0 \\ y_i \end{bmatrix}. \tag{67}$$

The first M-1 rows merely state that $\phi_i = \phi_i$. Multiplying by the matrix H upgrades a set of surface values of ϕ at the structure node points, 1, 2,...M, and at

the set of times $(i-N)\Delta t, (i-N+1)\Delta t, ...(i-1)\Delta t$. In particular the homogeneous case where $g_i = 0$ after the forcing function has ceased to act, will be considered.

$$\phi_i = H\phi_{i-1} \tag{68}$$

For the analysis of stability, it will be supposed $\lambda = re^{(j\theta)}$ and U are an eigenvalue and vector of the iterative matrix H:

$$HU = \lambda U \tag{69}$$

Following the $NM \times 1$ vector structure of ϕ, U may be partitioned into N sets of M element values,

$$UT = [u_1T, u_2T, \ldots, u_NT,] \tag{70}$$

where u_i is a set of nodal values at a fixed time, $i\Delta t$. In full this is

$$\begin{bmatrix} 0 & I & 0 & \ldots & 0 \\ 0 & 0 & I & \ldots & 0 \\ \vdots & \vdots & \vdots & \ddots & \vdots \\ 0 & 0 & 0 & \ldots & I \\ D^{(N)} & D^{(N-1)} & D^{(N-2)} & \ldots & D^{(1)} \end{bmatrix} \begin{bmatrix} u_1 \\ u_2 \\ \vdots \\ u_{N-1} \\ u_N \end{bmatrix} = \lambda \begin{bmatrix} u_1 \\ u_2 \\ \vdots \\ u_{N-1} \end{bmatrix} \tag{71}$$

One obtains from the matrix rows:

$$u_2 = \lambda u_1, u_3 = \lambda u_2 = \lambda 2u_1, \ldots, u_N = \lambda u_{N-1} = \lambda N - 1u_1 \tag{72}$$

and for the last one:

$$D^{(N)}u_1 + D^{(N-1)}u_2 + \ldots + D^{(1)}u_N = \lambda u_N \tag{73}$$

Because it applies that $Y_i = 0$, forms the set of boundary pressures at the next time level, say u_{N+1} An the two successive pressure sets with the form of Φ are

$$U_{i-1} = \begin{bmatrix} u_1 \\ u_2 \\ \vdots \\ u_{N-1} \\ u_N \end{bmatrix}, U_i \begin{bmatrix} u_2 \\ u_3 \\ \vdots \\ u_N \\ u_{N+1} \end{bmatrix} = \lambda \begin{bmatrix} u_1 \\ u_2 \\ \vdots \\ u_{N-1} \\ u_N \end{bmatrix} \tag{74}$$

what satisfies

$$U_i = HU_{i-1} = \lambda U_{i-1} \tag{75}$$

This implies that from u_i the pressures at subsequent times may be generated by the simple iteration

$$u_i = \lambda u_{i-1} \tag{76}$$

So with

$$u_1 = [b_1 e^{j\alpha_1}, b_2 e^{j\alpha_2}, \ldots, b_M e^{j\alpha_M}]T, \tag{77}$$

then,

$$u_{i+1} = \lambda i u_1 = rj[b_1 e^{j\alpha_1 + i\theta}, b_2 e^{j\alpha_2 + i\theta}, \ldots, b_M e^{j\alpha_M + i\theta}]T \tag{78}$$

Since H is real, the eigenvalues and vectors are conjugate pairs, so real pressures may be taken from the real or imaginary part of equation 78

$$r^i[b_1 \cos\alpha_1 + i_\theta, b_2 \cos\alpha_2 + i_\theta, \ldots, b_M \cos\alpha_M + i_\theta]T$$

or

$$ri[b_1 \sin\alpha_1 + i_\theta, b_2 \sin\alpha_2 + i_\theta, \ldots, b_M \sin\alpha_M + i_\theta]T$$

Last equation shows the effect of progressing through time steps. Because of the discretization, the parameter Δt, moves the vector through an angle θ at a rate of $\frac{\theta}{c\Delta t}$ radians per second where c is the speed of sound. In this way a picture of the eigenvalues may be shown either as complex numbers. In next chapter, figures of the results will be shown,

Therefore, there is an association of eigenvalues with frequencies. And it may be obtained more formally by considering the effect of the Fourier transform on the sequence of vectors produced by the iterative scheme. From the start of u_1, the sequence $u_1, \lambda u_1, \lambda 2 u_1, \lambda 3 u_1, \ldots$ is produced. Taking $h_i u_i$ as i=0,1,2 ,... where $\lambda i = [re^{j\theta}]i$ the variation with time and u_1 will be constant through the iteration process. At this stage it is assumed that r<1. Since the times iΔt may be thought of as samples from continuous time t, h_i is sampled data from the following continuous function

$$h(t) = [re^{j\theta}]\frac{t}{\Delta t} = [e^{ln(r)+j\theta}]\frac{t}{\Delta t} = e\left[\left(-\frac{\alpha}{\Delta t} + j\frac{\theta}{\Delta t}\right)t\right] \tag{79}$$

$$\text{defining } f_a \text{ as } \frac{\theta}{2\pi\Delta t} \text{ and } \beta \text{ as } \frac{\alpha}{\Delta t} = e^{-\beta + j2\pi f_a t}$$

From this equation it can be stated that:

- If r=1 the amplitude of the oscillation does not decay but remains constant, which is clearly an undamped resonance.
- Clearly if r>1 the iteration process will be unstable and if r<1 then stable. A small change in r when r is approximately 1 may tip a resonance over from being stable to unstable or vice versa.

Application to the results of simulation

The analytical solution obtained from the simulation shows numerical evidence that the frequencies having $r \geq 1$ show instability in those frequencies.

Next figures show the analytic resonances and are indicated by circles. As it can be seen, eigenvalues are close to the value 1 and for that reason, there is an problem in stability:

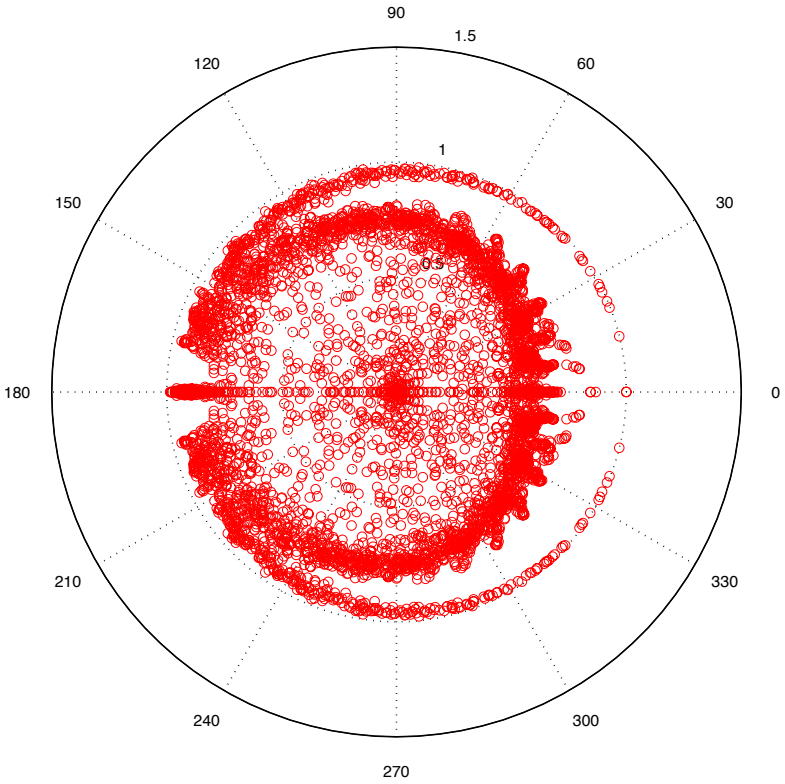

Figure 19: Polar form (r, θ) of the eigenvalues λ of room meshed with 1138 elements

It can be seen, that all solutions have values close to the unit circle. So it can be stated that interior resonances of the vibrating structure are causing difficulties when using the BEM for solving this acoustic problem in the frequency domain. This can be seen, because each eigenvalue of the iteration matrix is related to a frequency obtained by doing the Fourier transform of the discrete time solution. Numerical approximations are the cause of the decay rate to be smaller or bigger than 1 resulting in stability or instability, respectively.

For this reason a proper solution is thought to be implemented. In the paper written by Jean-Marc Parot and Christophe Tirard [14] a solution for this eigenvalue problem is presented. In order to minimize and make these eigenvalues have a lower value, it is explained that the iteration matrices which indicate the pressure coefficients can be stabilized, by damping them. The damping effect is created by multiplying the coefficient matrices by a constant smaller than 1. By doing this, all parameters of the matrices will decay and for this will lead to diminish the value of the eigenfrequencies.

Following illustrations 20 and 21 show the improvement of the results compared with the normal case. Those eigenvalues which fell before the damping outside the unit circle, lay afterwards inside of it. However, the eigenvalues are still to close to the unit circle and that may still show an unstable behavior.

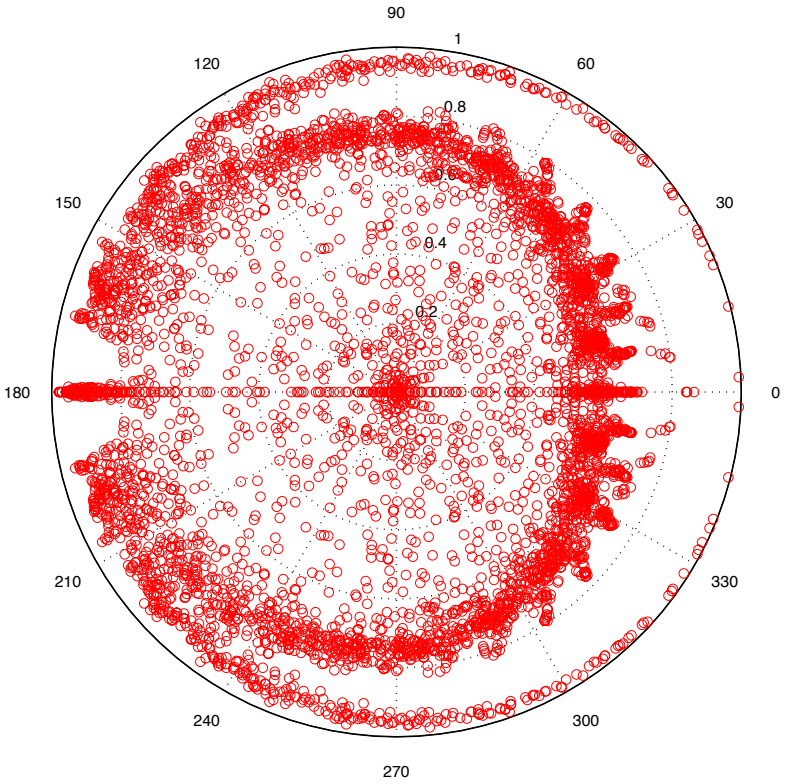

Figure 20: Polar form (r, θ) of the eigenvalues λ with a coefficient of 0.959

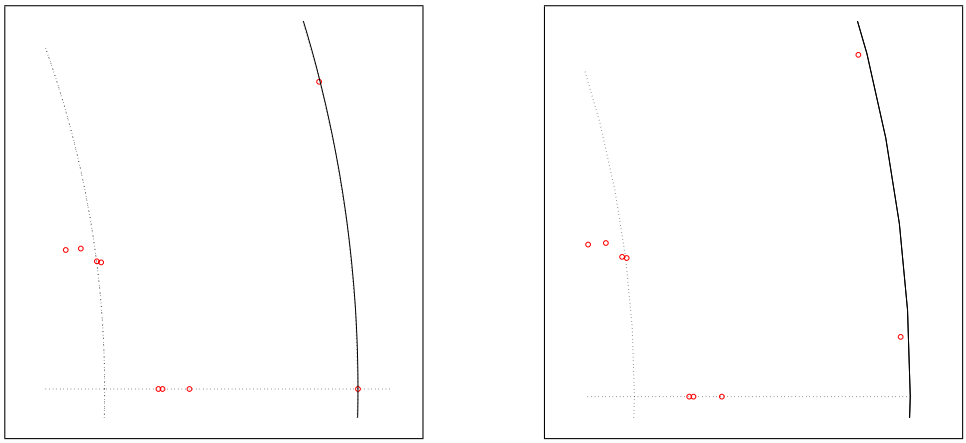

Figure 21: Comparison of eigenvalues (left:original, right:damped matrix by 0.959)

The actual behavior can be described with the following picture. When damping the sound pressure, the peak at 0Hz is damped. As figure 21 indicates, there the eigenfrequency at 1 in the unit circle, moves inside the unit circle when damped. However, because of the proximity to the boundary of the circle, there will still instability. This instability can be decreased by using a higher parameter for the damping. The more the results are damped, the more the eigenfrequency will be

closer to the center of the unit circle and therefore there will be less oscillation of the sound pressure at the output. As it can be seen in the figure 22, the frequency of oscillation is smaller the more the solution is damped, and that causes the results to be more stable.

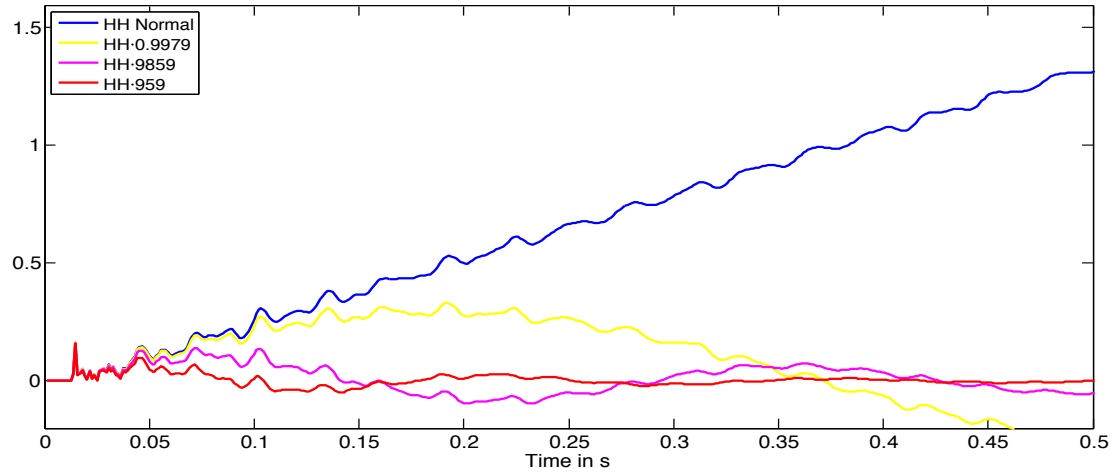

Figure 22: Comparison of different coefficients in time domain

However, because of this damping, the calculation is also damped and attenuated. This attenuation may affect when doing the transformation into the frequency domain. Picture 23 clearly states that there is a compromise between resolution and stability in the results. When solution is more damped, stability in time-domain is more assured, but on the other hand resolution in the frequency domain is lost. For this reason, for a better accuracy of the results compared with the analytical results, there is a compromise for election the damping coefficient that confronts stability versus accuracy of results.

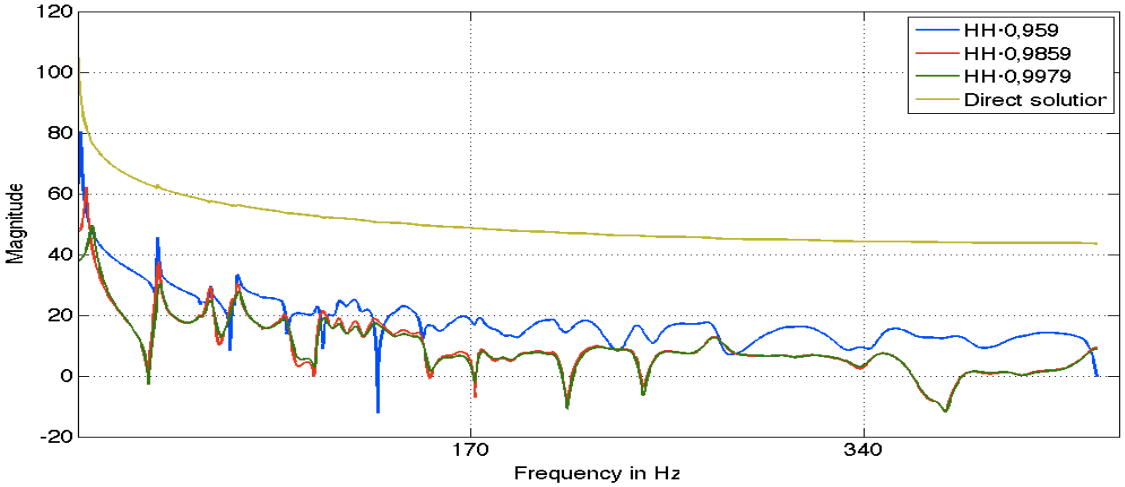

Figure 23: Comparison of different coefficients in frequency domain

3.5.2 Solution with high-pass filter at 16Hz

In order to minimize the level of desired peaks on low frequencies, there are other methods, for example, the digital filtering. Filters are used for the processing of signals. In acoustics and sound reproduction they serve as a basis for final adjustments. They are designed as a combinations of addition, multiplication and delay components. Depending on the level of combination, one may create a higher order of filters, that will have a better solution. However, when increasing the order of a filter supposed a big complicity in the construction of them for analogue circuits, what is no problem for digital filters.

There are two kinds of digital filters. FIR (Finite Impulse Response) and IIR(Infinite Impulse Response).

Finite impulse response filter is a type of a signal processing filter where its impulse response is of finite duration, because it settles to zero in finite time. This is in contrast to infinite impulse response filters, which have internal feedback and may continue to respond indefinitely, although its response after it will usually decay. Moreover IIR filters also require less effort and complexity than FIR filters and usually have a lower order.

Because of its infinite length and better response, an IIR will be used for filtering the obtained results. IIR filters make an approximation of a desired impulse response functions as possible. The filter transfer function is then:

$$H(z) = \frac{\sum_{n=0}^{N} b(n) z^{-n}}{\sum_{n=0}^{N} a(n) z^{-n}} \tag{80}$$

where the poles of the function is determined by a(n) and its zeros by b(n). This formula can be represented by the following block diagram:

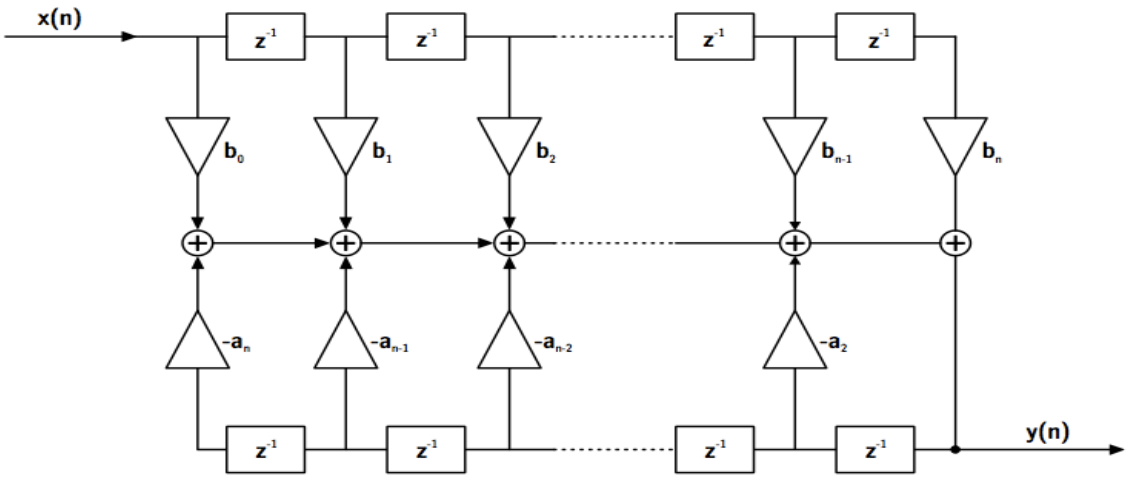

Figure 24: Block diagram of an IIR filter

As it can be seen in the illustration, the output signal, is created by amplifying and adding past samples. IIR filters can be optimized to produce a specific modulus

response, although the phase response cannot be controlled independently.

A discussion of digital filters is best illustrated with a plot of the complex transfer function. From 0 to 16Hz approximately, it appears an undesired solution. In order to eliminate that high peak, a high pass filter is used, which will try to eliminate values under 16Hz. A Butterworth Filter of order 6 will be taken for this purpose.

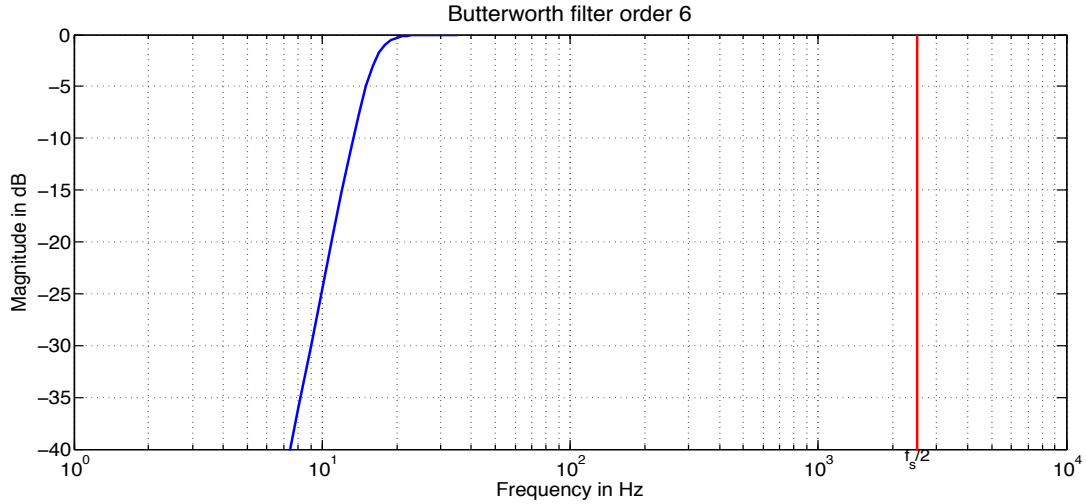

Figure 25: Butterworth Filter of order 6

Because of the boundary element method iteration for calculating the pressure coefficients in the surface, it is desired to filter the parameters after each iteration, so that the error created does not keep increasing in each iteration.

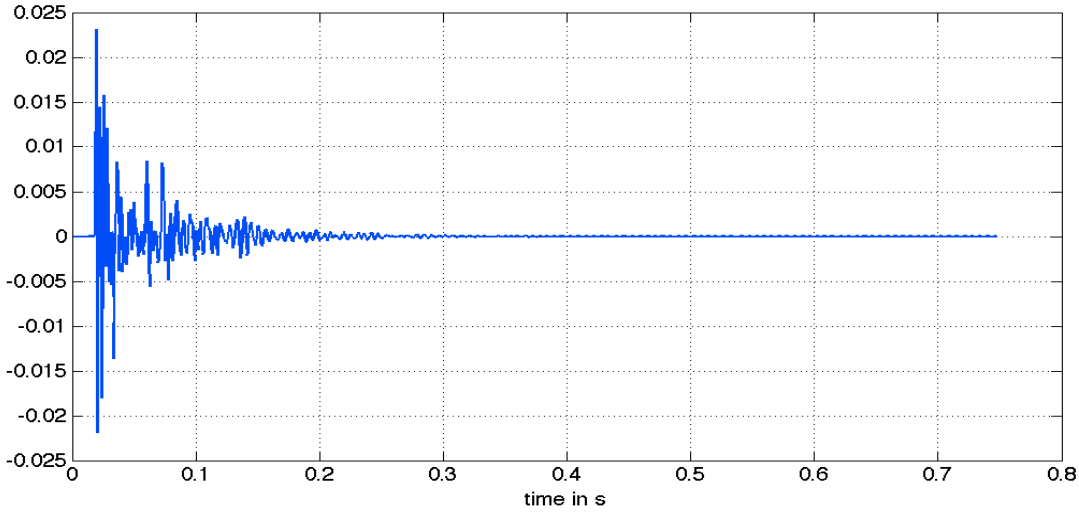

Figure 26: Filtering after each iteration

However, another option has been tried in order to see the filtering capabilities. Instead of filtering after every loop, a post-filter has been used. In this case, the resulting 'p' obtained from the method will be filtered afterwards and only once.

As it can be seen in the next illustration 27, the filter attenuates the signal's increase in time, lowering it, although not eliminating it completely. However, it is interesting to see the frequency solution. Because of this elimination of the band from 0-16Hz the result may be able to eliminate the high peak in the results near 0Hz.

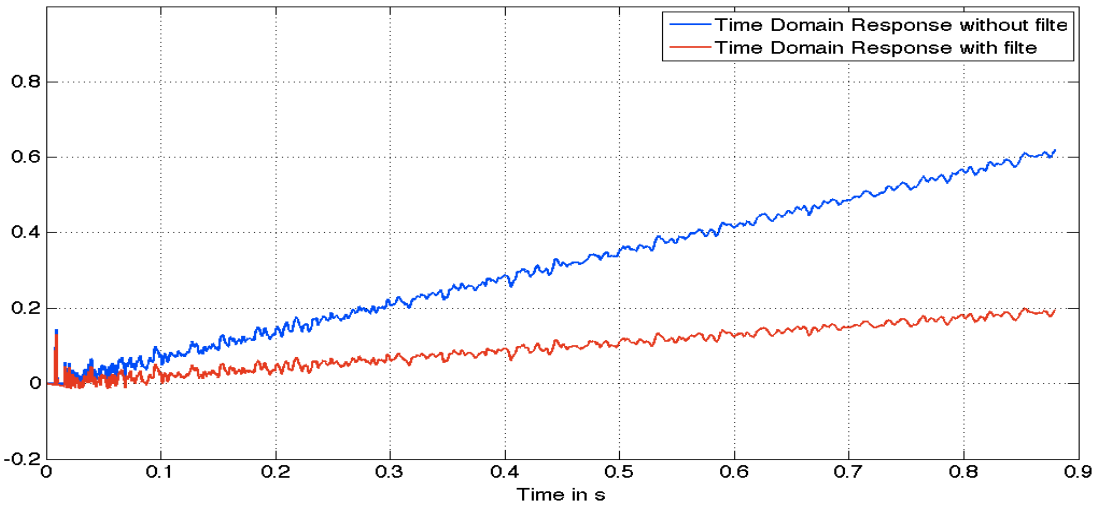

Figure 27: Comparison of filtered results

In order to see which solution has better performance, the results will be compared with the analytical results:

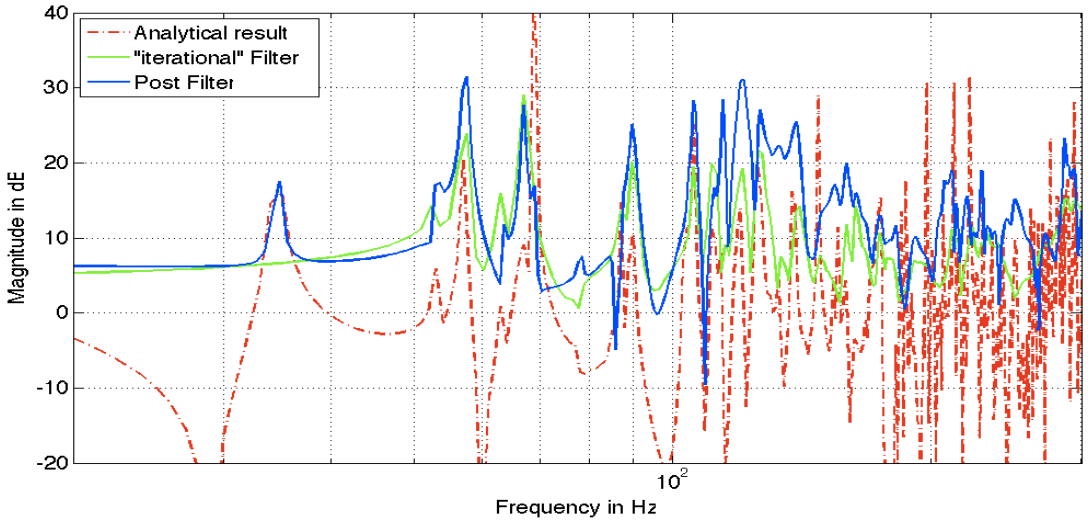

Figure 28: Comparison of results with Post-Filter and 'iterational Filter'

As it can be seen in the illustration 28, the iterational-filter does not have a god behavior over lower frequencies, as it eliminates the first frequency at 34,6Hz.

Also, this solution attenuates too much the results and does not have such a good behaviour like the post-filtering solution. Peaks can be better distinguished in this case.

For this reason, all of the following simulations of the test subject have been filtered with the presented filter. The results of the solution will be easily distinguished between the original and filtered sound, as it has been stated that these results have best performance.

3.6 Validation of the frequency-domain response results

This section will present the obtained results of the task realized. Results show the room impulse response of the room. The RIR will show how the room is affected by the input of acoustic energy into it. When introducing energy into the room, at modal frequencies and there will be standing waves. These standing are the eigenmodes (or eigenfrequencies), which are represented in the results by high resonance peaks because the amount of energy.

3.6.1 Results for the test point 1

For the simulation, 4 test points were situated in different places inside the whole boundary already described. Because of the capabilities of BEM it is really easy to calculate the results in a point of space or in another. However, this section will only present the results for one point of the test measure in order to see the similarities and differences of the results. More results will be presented in the appendix at the end of this work.

The first test point lays close to the sound source, so peaks or wells caused by constructive or destructive reverberations will not affect too much in the results. However, these results will always depend on two parameters: the definition of the mesh and the time-step used. As it has been seen in previous section, results in the time-domain are more or less stable, depending on the mesh used. A finer mesh presents more stability than a coarser and vice-versa. The other parameter is the β used. The results will be divided taking into account the parameter β. As it was mentioned before, the parameter β gives the coefficient of the time step created. A too small chosen β can lead to a faster instability of the result; however, as β depends from the time-step Δt, a to big choice may lead to bad results, due to the poor time discretization. Remember that the best choice of β is between 0.5 and 1.5

In order to see the relevance of the mesh points used, results are plotted with meshes of 2030, 3652, 8020 and 16594 elements respectively. Both resulting signals are compared with the analytical result commented in section number two.

Results in low frequencies (0-150Hz)

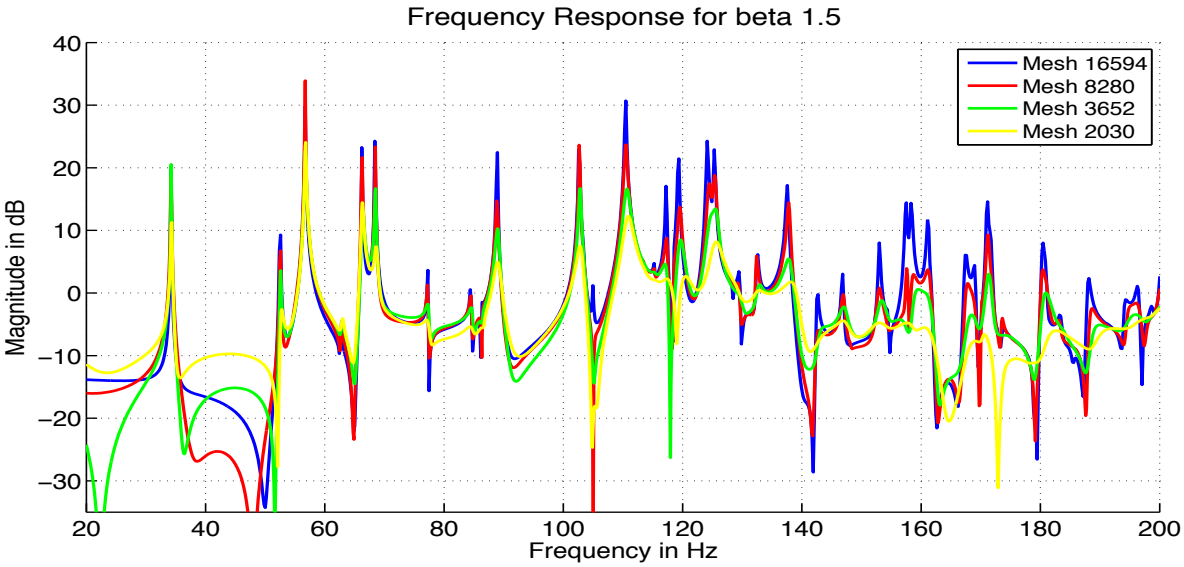

Figure 29: FD-RIR results for room with $\beta = 1.5$ at low frequencies

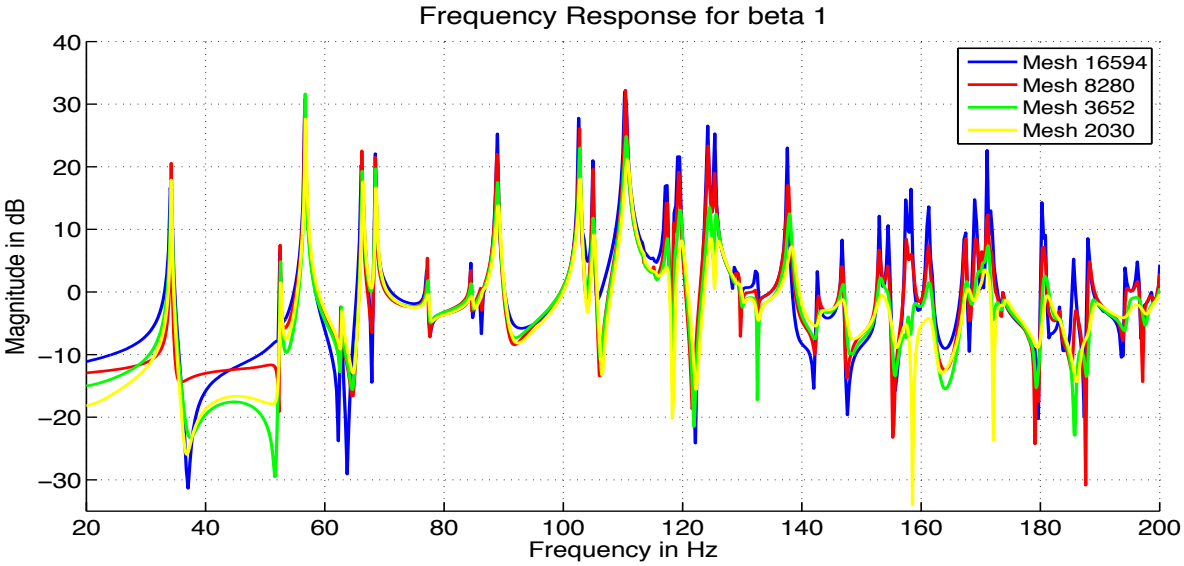

Figure 30: FD-RIR results for room with $\beta = 1$ at low frequencies

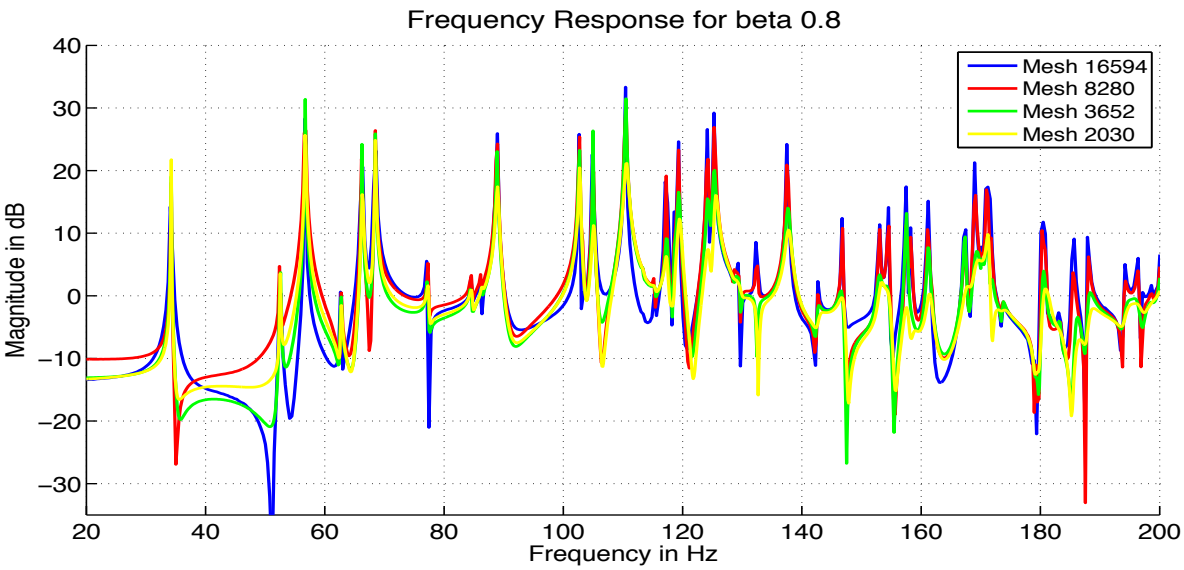

Figure 31: FD-RIR results for room with $\beta = 0.8$ at low frequencies

Results in high frequencies (300-420Hz)

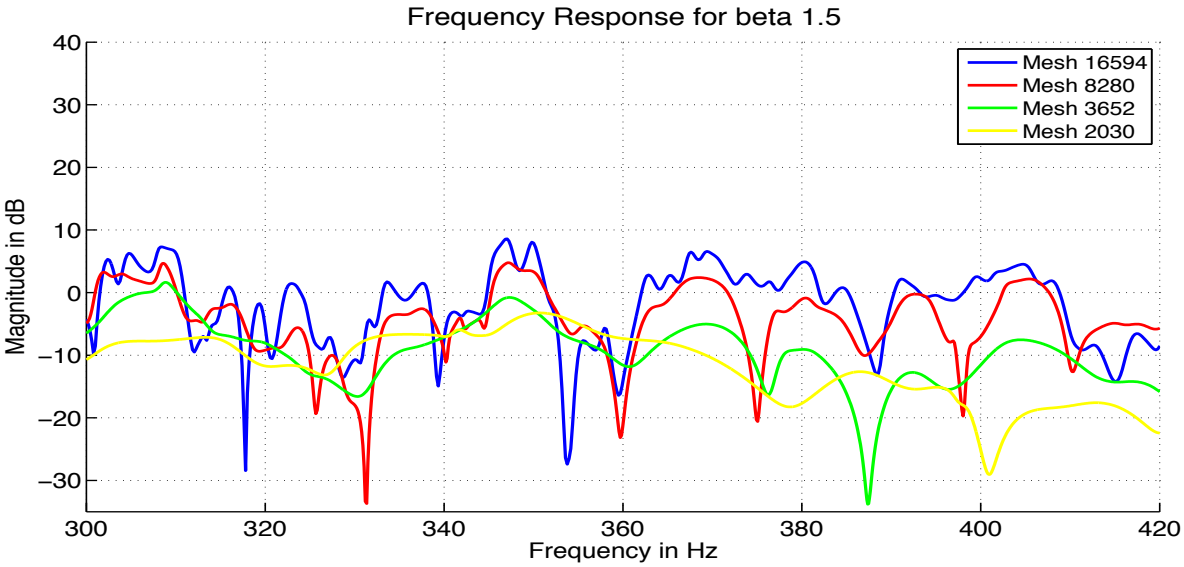

Figure 32: FD-RIR results for room with $\beta = 1.5$ at high frequencies

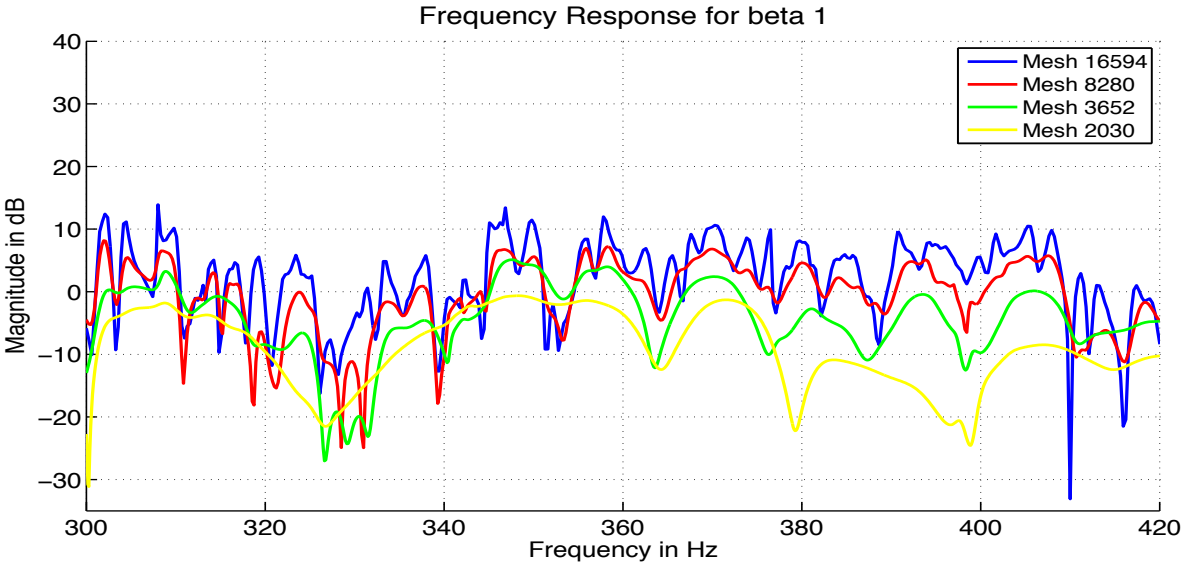

Figure 33: FD-RIR results for room with $\beta = 1$ at high frequencies

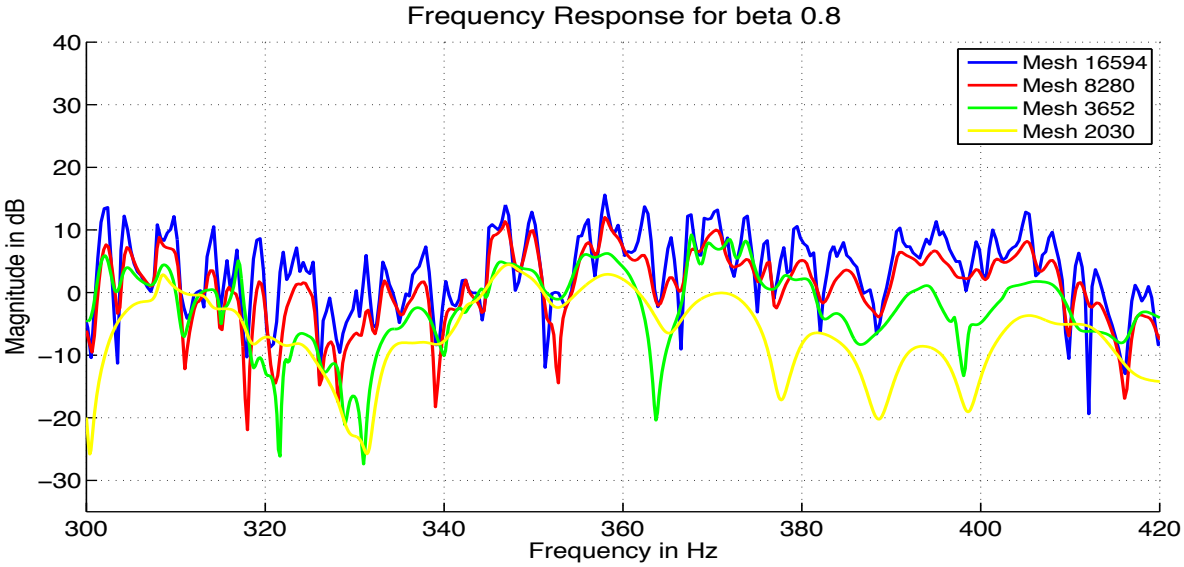

Figure 34: FD-RIR results for room with $\beta = 0.8$ at high frequencies

As it can be seen when observing the illustrations improving the quality of the mesh, leads to obtain results with a better resolution, as it was expected. It is presented the example of a poor mesh, which consists on more than 2000 elements. However, when observing the results of this case, it is appreciable that results have a good resolution until approximately 100Hz. Above this frequency, results start to be damped and peaks are not good differentiated. Figure 33 is a mesh that consists on more than 3500 elements and by watching the results it may be seen that in this case, the solution is only valuable until 160Hz.

When checking the results in steps, it is clearly more visible, that the solution with more mesh elements adjusts more to the energy values of the analytical case.

Improving the mesh up to 8280 and 16594 elements, shows that the results present good results above 200 Hz. In these cases, for example, the different types of modes explained in section 2 can be distinguished along this spectrum. Axial modes, for instance, can be easily detected when looking at the lowest frequencies. These resonance peaks are isolated and store a lot of energy. This fact shows that at these frequencies the eigenmodes will have a great impact on the sound reproduction in this room at certain listening positions. Tangential modes are located at higher frequencies. However, multiple isolated tangential modes can be observed for frequencies around approximately 150Hz. These isolated modes might superpose with each other, or additionally with isolated axial or oblique modes with the same frequency. Lastly, the oblique modes are as well illustrated. When looking above 150Hz a great number of eigenfrequencies can be seen. These isolated modes are located above this frequency and might superpose, as in previous cases, with axial or tangential modes. As a result it can be seen that increasing the frequency shows to have a lower effect on the sound reproduction.

Above mentioned was another parameter affecting on the quality of the results. The time-discretization parameter $\beta = \frac{\Delta t \cdot L}{c}$.

When watching in detail it can be noticed that results obtained with the parameter β set up as 0.5, are not shown on the illustrations. The reason of this, is that β has the smallest recommended, which means the time-discretization Δt is too small. This fact implies that results are not stable.

For the upper limit of $\beta = 1.5$ the results show on low frequencies a good performance. However also when moving onto higher frequencies resolution is lost and the results show up more damped. In this case the time-step is too big and it is interesting to make it smaller.

When improving the β parameter and setting it to 1, results start to show a much better finesse and accuracy for good frequencies. For this case results have a good performance, finesse and accuracy. The illustrations show a good has a better sensibility and results are much more consistent with the actual real result. However when going into higher frequencies, it can be seen that some of the eigenfrequencies are visible but for instance two near peaks are not often detected and distinguished.

Therefore there is a need on even improving the resolution and improving the discretization.

As it has been explained, optimal values lay within 0.5 and 1. However, it is preferable to choose a smaller parameter so that the time steps can be small and therefore accuracy in the obtention of the results, improved.

When improving the parameter β and setting it to 0.8 it can be seen that the results show a great performance. For this case, the results are the most consistent, even at higher frequencies results show up good.

By seeing the illustration, it is appreciable, that the peaks in lower frequencies are obtained correctly, however, the wells separating each peak are not so much. On the other hand, it can be seen that the increase in the results of the mesh elements affects in the accuracy of the results. It is expected that when meshing the room with even more elements, results will improve even more.
With this concludes the presentation of the results. It is now interesting to compare the actual results with the analytical case, in order to prove the quality of this method. In the appendix, more results in order to validate the results are shown. The results a frequency response simulation of the room performed in other test points. For the rest of the cases, the test points will be positioned close to a wall in the listening room opposite to the sound source. Radiation from the sound source is meant to be in all directions and for that reason, disturbing waves will be appearing in the results, which will cause solution to be different as in this first test point measure.

To conclude with this section, it will be sum up what it has been shown in with these results. There are two important factors when working with the TD-BEM. First of all is the time discretization and second of all the quality of the mesh used. Choosing a value in the middle of the limits for β increases the quality of the results. However it has been demonstrated, that between the ranges, choosing a smaller time-step than $\beta = 1$ will improve results, because of the better resolution.

Comparison with analytical case

In this section it will be discussed the results obtained in the simulation when compared with the analytical results. As the mesh composed by 16594 elements has proved to show the best performance, it has been used in following illustrations for the comparisons. Results are divided in two parts, one will present the results under the Schroeder frequency and the other one, the results in high frequencies above the Schroeder frequency.

Results for the low frequencies (0-150Hz)

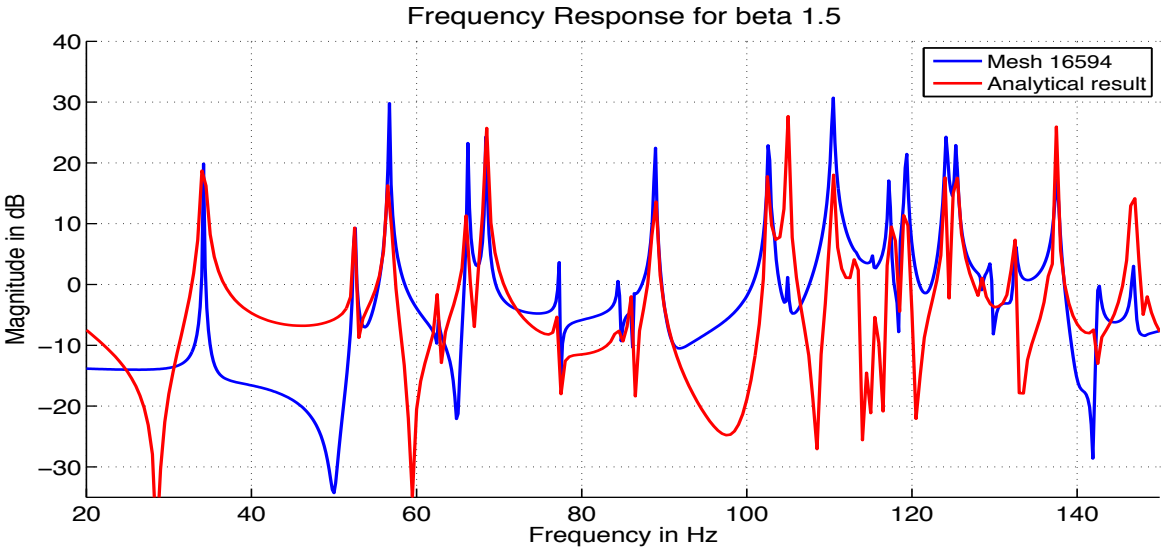

Figure 35: Comparison of results for room with $\beta = 1.5$ at low frequencies

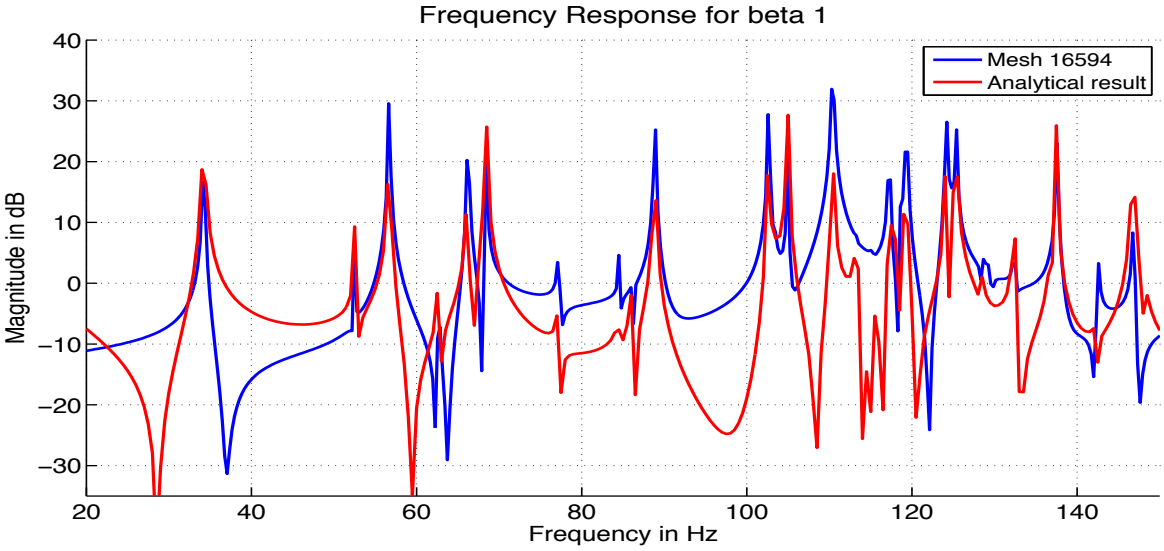

Figure 36: Comparison of results for room with $\beta = 1$ at low frequencies

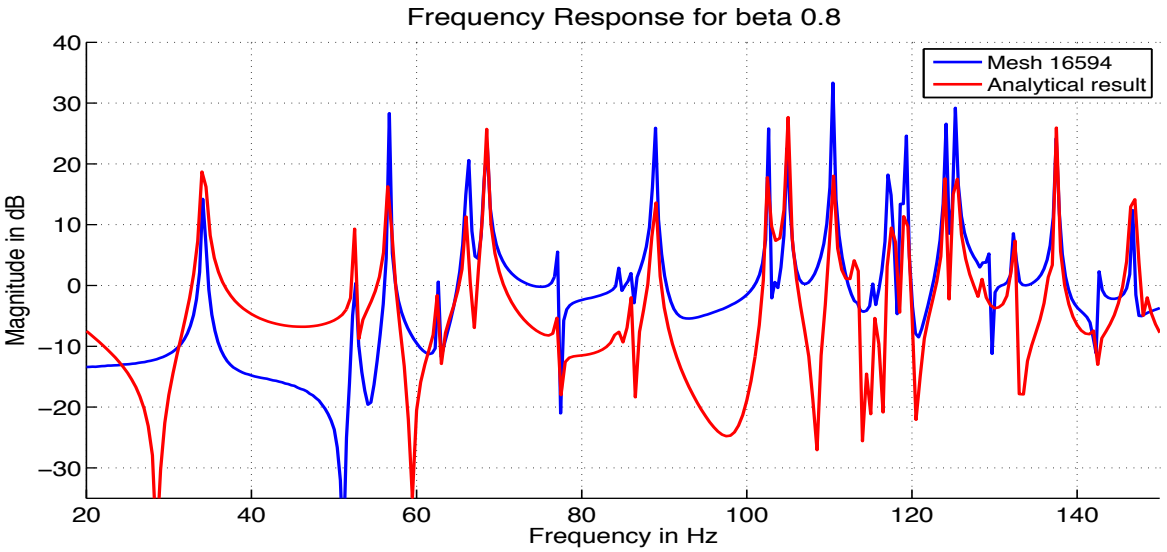

Figure 37: Comparison of results for room with $\beta = 0.8$ at low frequencies

Illustrations 35, 36 and 37 show the results for low frequencies. As it can be seen, the results adjust really good to most of the eigenmodes of the analytical result. Most of the peaks match perfectly as much as for the position in the frequency spectrum as for the energy. However, some peaks which are really close to each other are not defined by the simulation result. This could be because the discretization may be even needed to be improved. When comparing all of the three figures it can be seen that they show really similar results. There is a little improvement on resolution when adjusting the parameter β to a finer value. This is only due to the results are shown for low frequencies.

Results for the high frequencies (300-420Hz)

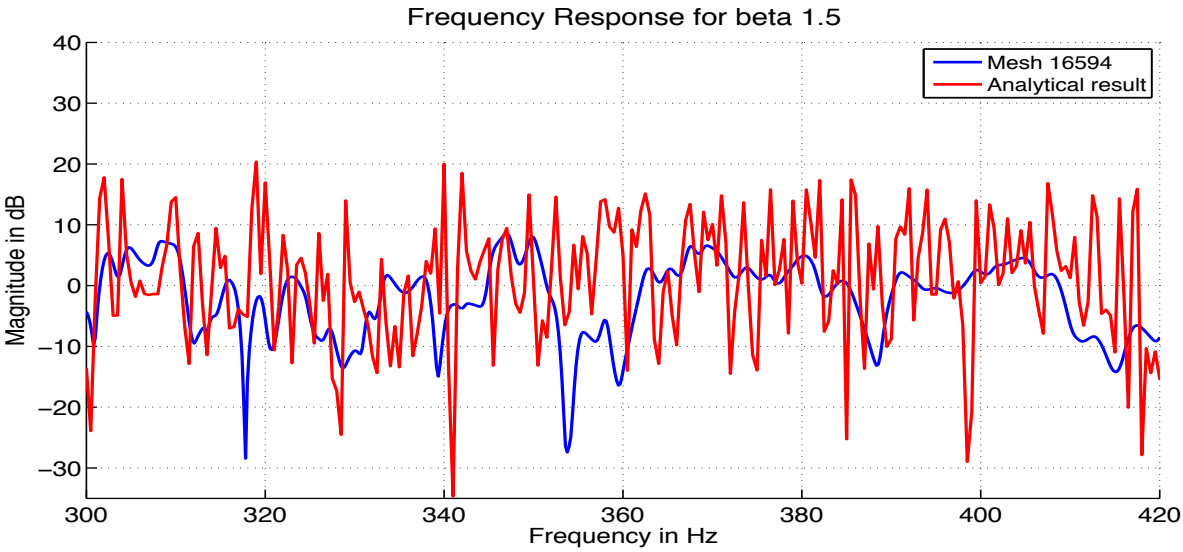

Figure 38: Comparison of results for room with $\beta = 1.5$ at high frequencies

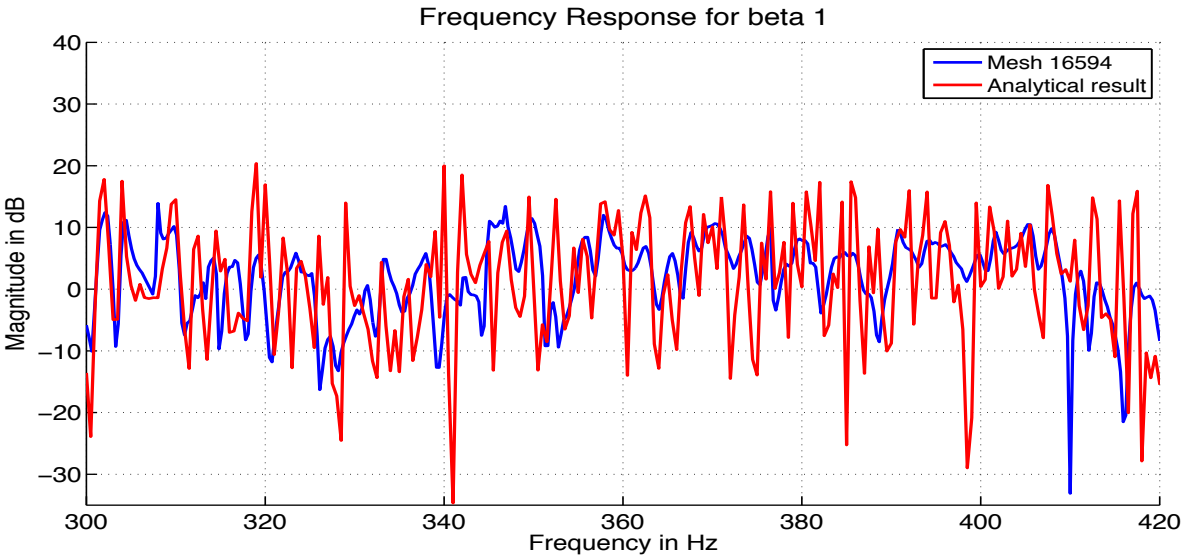

Figure 39: Comparison of results for room with $\beta = 1$ at high frequencies

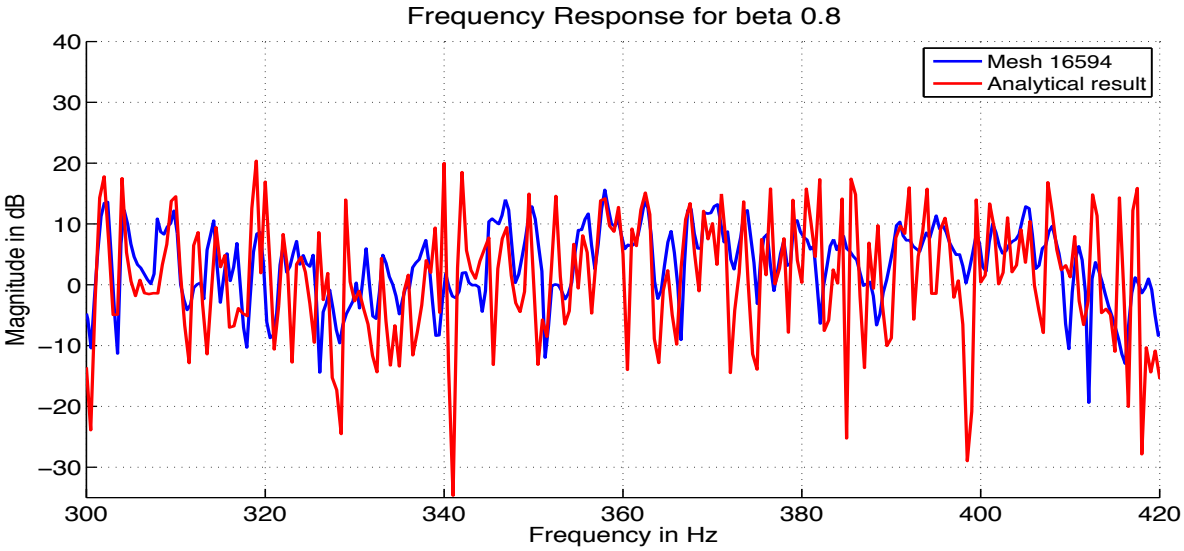

Figure 40: Comparison of results for room with $\beta = 0.8$ at high frequencies

Figures 38, 39 and 40 show the results of the simulation in higher frequencies. Results are not anymore precise and peaks cannot be identified anymore. Even though using a better time-step shows improves the results, when using $\beta = 0.8$ the results show that neither the amplitude nor the resolution correspond with the analytical case.

This shows that the TD-BEM is very limited when working in high frequencies and may be used to understand that wave based models are show good results at low frequencies.

3.7 Discussion of Simulation Results

This chapter has proved that the method described demonstrates the efficiency of boundary element methods by showing the impulse response of the room to be treated.

The discretization of a surface in small elements can create problems. An analytical calculation would interpretate infinite points from a surface and calculate with it a solution. In order to try to simulate reality, it is desire to have as much points as possible, what means more elements with smaller size and leading to an increase the accuracy of the results. So, as general rule, the element sizes for the mesh should be as small as possible across the boundary.

On the other hand, it may be taken into account, that the increase on the discretization of the mesh will suppose an increase on the computational expense.

However, there is another kind of discretization, which also could make problems appear. As explained in the theory, the system is discretized in time-steps. Time-steps divide the two points in time leaving a blank temporal gap in between. This value, controls therefore the time discretization. Leaving a big temporal gap in between could create instability in the solution. The more small the value of this parameter (or the more ”analog” the solution is), the more stable the results are.

After the reason for the simulation results have been stated, following chapter will show up the measures taken, in order to be able to compare the technique used, with the empirical values.

4 Measure of the Room Impulse Response

This section will discuss the procedure of taking the measures in order to obtain the empirical results of the method to be tested.

The measurements are divided into different measurement set-ups. In total there are two set-ups, each addressing to a certain type of the sound of the source. The impulse response was obtained from the saved measurements files done using the PC Software OROS System, a tool for measuring noise and vibration systems. The plots were afterwards produced by the Matlab software.

4.1 Measurement equipment

The following measurements were performed in a rectangular chamber of hard concrete walls in the Acoustic Faculty in the TU-Berlin. The dimension of the study room remains the same as for the test simulation:
4.97 meters of length by 3.0 meters wide and 3.24 meters of height.
The walls are from concrete, what means that the sound produces a noticeable reverberation and echoes when sound is generated inside the room. Once the room is set, it is to prepare the equipment to take the measure. It consists of:

- Four microphones
- Four Pre-Amplifiers
- One laptop PC running Windows XP with the OROS System Software
- One Noise generator
- One Sound Amplifier
- One air pistol - to create impulse
- OROS System measurement equipment

4.2 Measurement set-ups

All measurements were performed with the same disposition of the microphones. Their position

	Position x	Position y	Position z
Microphone 1	193	188	144
Microphone 2	92	397	245
Microphone 3	103	245	167
Microphone 4	235	325	65

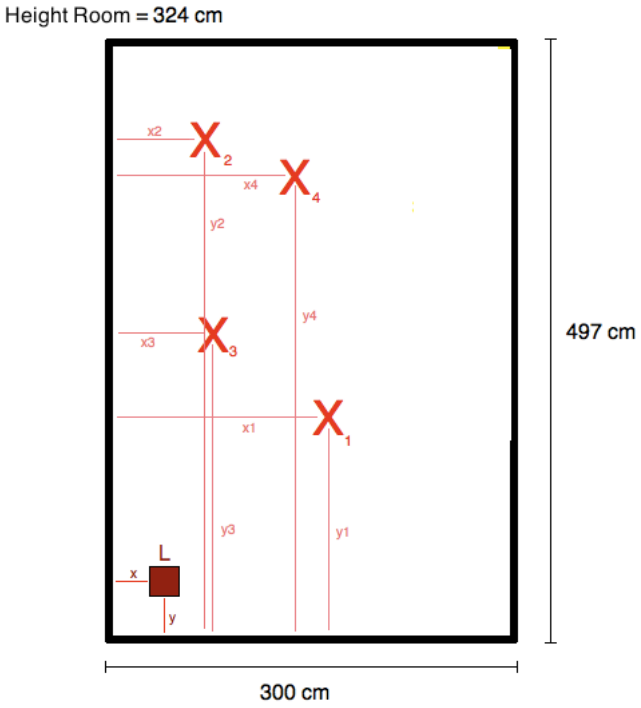

Figure 41: Collocation of microphones in room

in centimeters

As it can be seen, for the measurements, their collocation is the same as it was done for the simulation. Recordings have a length around 2s and 3s and are sampled at 44 kHz. For each measurement the RMS is calculated. The microphones are directly calibrated by a reference sound source after their positioning. The sound emitted from reference sound source has a stationary noise type spectrum As it was done with the microphones, the same occurs with the dodecahedron loudspeaker, which is placed in the same position as in the simulation, at one corner of the room. It's position in cartesian coordinates:

	Position x	Position y	Position z
Loudspeaker	49	62	182

Figure 42: Room with microphones

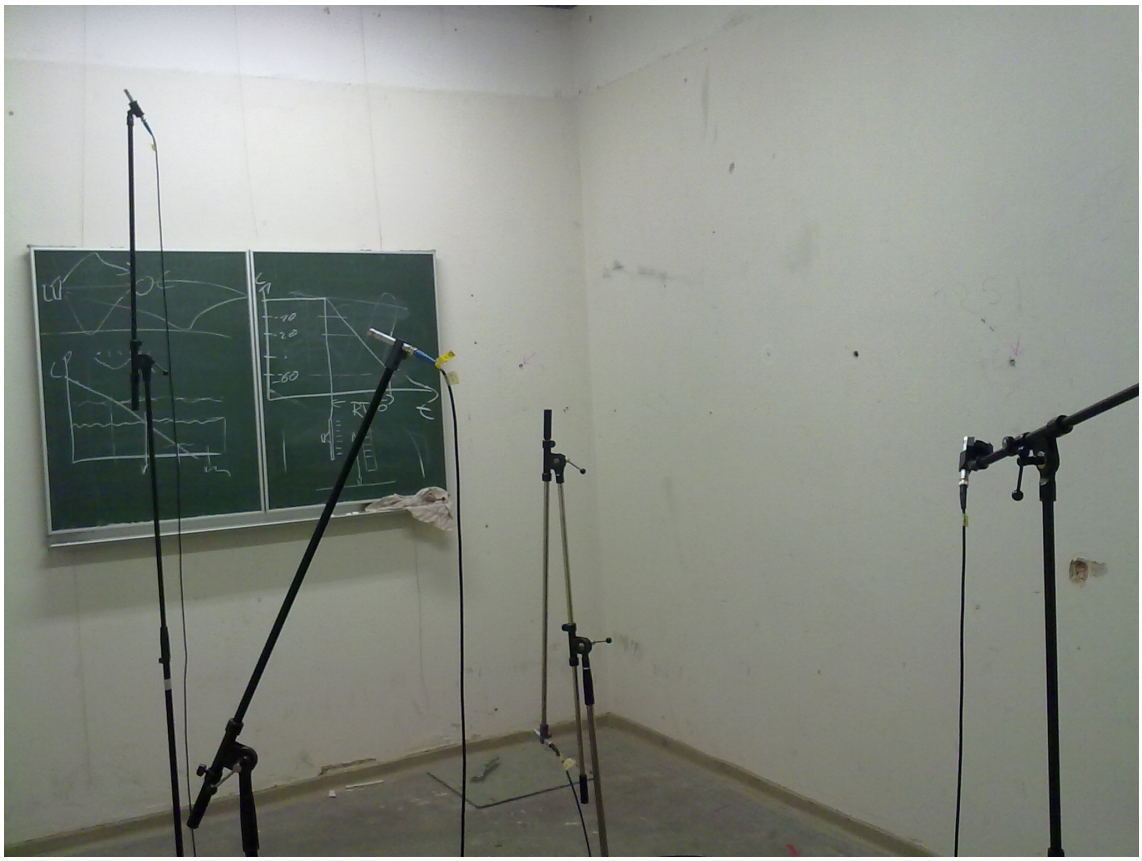

Figure 43: Room with microphones 2

For the set-up the positioning of the instruments (microphones and sound source) is the same as in first case. Unique difference lies in the element of the sound source. In this case, it will be an air pistol which will generate an impulse.

4.3 Methods for obtaining the Room Impulse Response

For obtaining the measured Room Impulse Response (RIR) of the room, a method designed by Edgar Berdahl and Julius Smith of their toolbox "Impulse Response Measurement" is used. Their method uses known sequences in the input, and calculates to obtain the most exact response from the liner system. There are two differents procedures, which differ in what is desired to be measured. Both of them will be explained in the following section.

4.3.1 Golay Complementary Sequences Theory

For characterizing the system, it is necessary to remember the fundamentals in signal processing. The system characterized is indeed a linear system. It is stimulated by an input signal s(n) which crosses a system with an impulse response h(n), and drives at the output a response signal r(n). However, problem is to estimate h(n). Given known input and output signals s(n) and r(n) respectively, a practical method for identifying finite impulse responses uses Golay complementary sequences to excite the linear system as described below.

The sequences a(n) and b(n) are Golay complementary sequences and it can be stated that:

$$a(n)a(n) + b(n)b(n) = 2L\delta(n) \tag{81}$$

If $a_L(n)$ and $b_L(n)$ are Golay, it can be demonstrated that a_{2L}(n) = [$a_L(n)$ $b_L(n)$] and $b_{2L(n)}$ =[$a_L(n)$ - $b_L(n)$] are also Golay. This means that Golay complementary sequences can be constructed recursively given seed sequences such as $a_2(n)$ = [1 1] and $b_2(n)$ = [1 -1].

So the solution of this will also be a Golay sequence:

$$a(-n) * a(n) + b(-n) * b(n) = 2L\delta(n) \tag{82}$$

As a result, the obtained sequences will consist of only 1's and -1's. This means that the signal contains the maximum possible power level given that $|s(n)| \leq 1 \forall n$. This property is helpful for minimizing measurement noise.

When there is a system in the middle, $r_a(n) = a(n) * h(n)$ is the response to the input a(n), and the same with $r_b(n) = b(n) * h(n)$. This will be the response due to an input b(n). So it is demonstrated that the impulse response is:

$$h(n) = \frac{1}{2L}(a(n)r_a(n) + b(n)r_b(n)) \tag{83}$$

With the concepts clear, it is desired to measure the impulse response of the

room. Once microphone are in position and calibrated, it is OROS System will play the Golay sequence created.

4.3.2 Golay Complementary Sequences Results

After doing the measure and processing the signals throughout the explained method, following results are obtained.

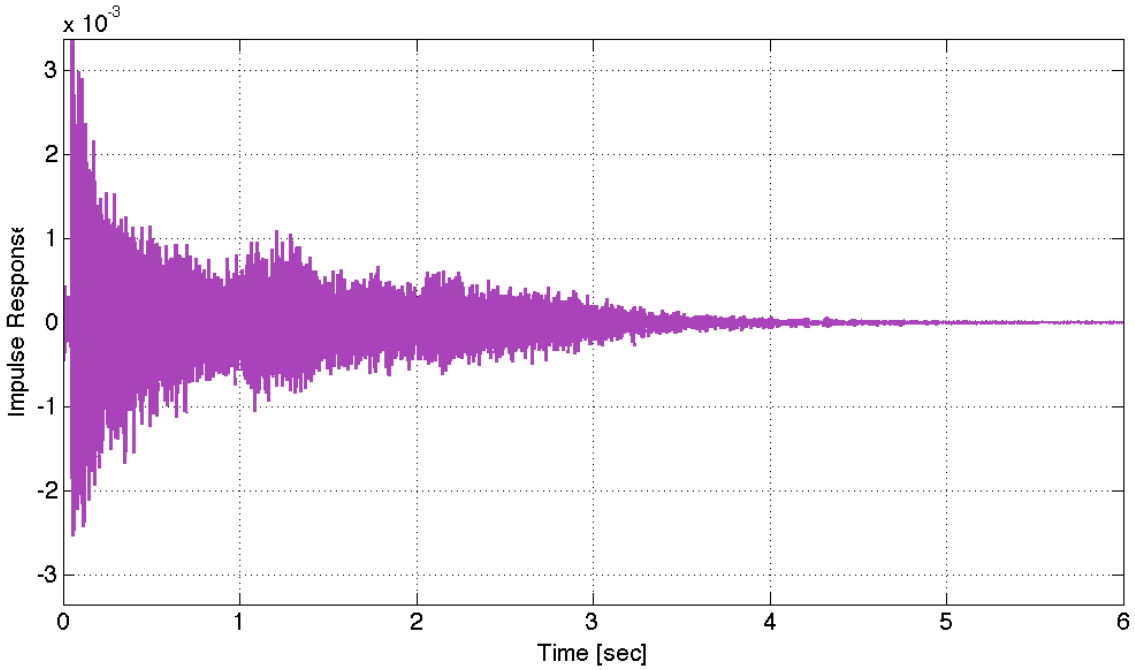

Figure 44: Golay impulse response in time domain

By using the Fast Fourier Transformation, one might obtain the results along the frequency spectrum.

Figure **??** shows peaks for the resonances and room modes from the room impulse response up to 10kHz.

However, because the Golay sequence method uses golay sequences and needs a pair of measures two obtain the results, the solution can vary a little depending on the localization of the measure point. For this reason, in the next illustration the measured impulse response is obtained and referred to different microphone positions.

The behavior of the room impulse response is really similar.

For the low frequencies, it can be clearly seen that measured eigenfrequencies correspond with the position of the theoretical room modes:

As it was stated in previous sections, these results show that lower frequencies have a greater effect on resonance on the appearance of room modes. For frequencies higher than 500Hz the effect is not so disturbable.

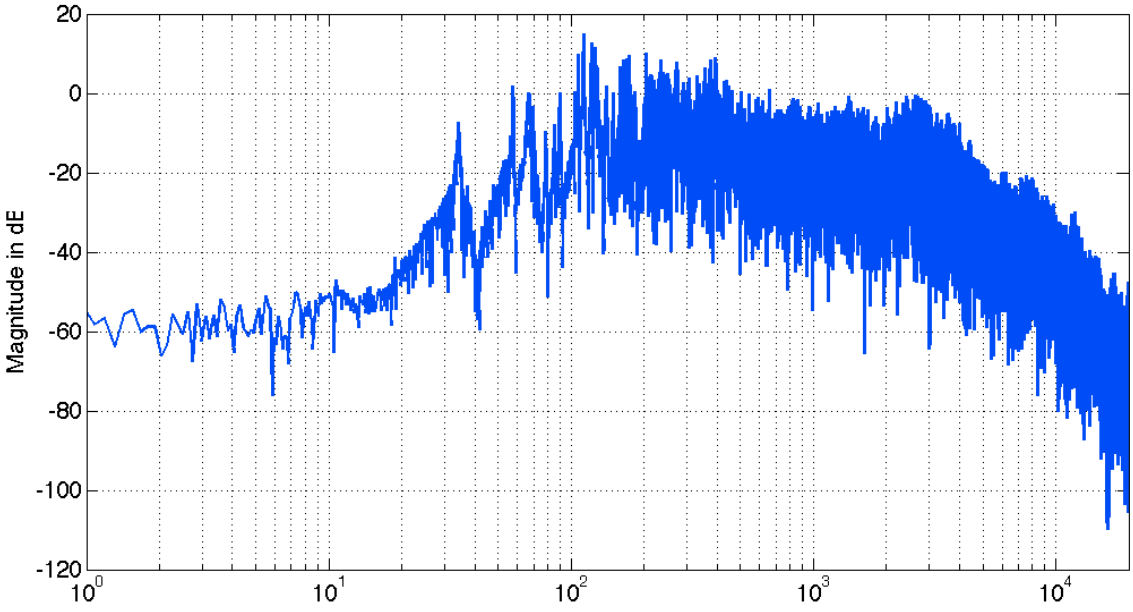

Figure 45: Golay impulse response in frequency domain

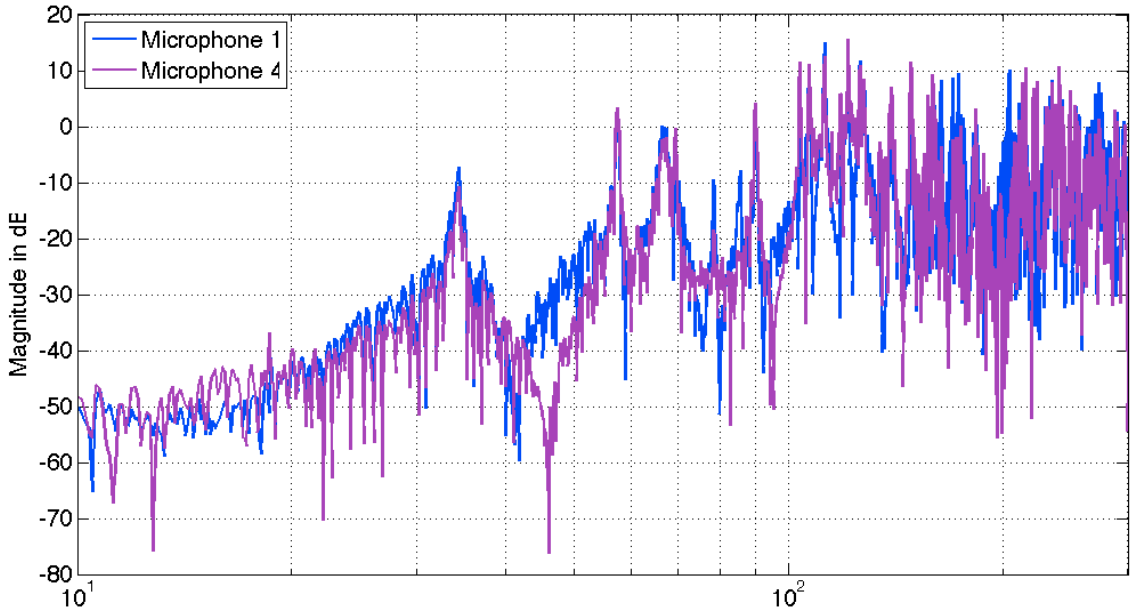

Figure 46: Comparision of different measure points

4.3.3 Sine Sweep Measurement Theory

Edgar Berdahl and Julius Smith on their toolbox "Impulse Response Measurement" present another another practical method for identifying impulse responses, it is the "swept-sine measurement". In some cases, it is desirable to relax the power-maximizing constraint $|s(n)| = 1 \forall n$ in favor of obtaining some other desirable measurement system properties. This method improves the accuracy of the measurement

at lower frequencies compared to higher frequencies. For this reason, the the excitation signal s(n) is not a Golay sequence, but a signal that contains more energy at lower frequencies.

$$r(n) = (f(s) * h)(n)$$

This property is only value in a memoryless and linear system. For this obtaining both of these desirable measurement system properties a new excitation signal s(n) will be used. This signal is a sine wave with a frequency that is exponentially increased from $\omega 1$ to $\omega 2$ over T seconds:

$$s(n) = sin\left[K\left(\exp^{-n/Lf_s} - 1\right)\right] \tag{84}$$

where K = $\frac{\omega_1 T}{ln\frac{\omega_2}{\omega_1}}$ and $L = \frac{T}{ln\frac{\omega_2}{\omega_1}}$.

Now it is needed to inverse the measurement by the excitation signal. To this end, we realize that a useful property of s (n) is that the time delay Δt_N between any sample n_0 and a later point with instantaneous frequency N times larger than the instantaneous frequency at $s(n_0)$ is constant:

$$\Delta t_N = T\frac{ln(N)}{ln\frac{\omega_2}{\omega_1}}$$

This characteristic implies that after inverse-filtering the measured response, the signals due to the nonlinear terms in f(s) are located at specific places in the final response signal. Consequently, the linear contribution to the response, which is proportional to h(n) can be separated from the other nonlinear terms. We can thus measure a linear system even if it is being driven by a weakly nonlinear motor.

Because the frequency of s(n) increases exponentially, the system is excited for longer periods of time at lower frequencies. This means that the inverse filter averages measurements at lower frequencies longer, so this measurement technique is better suited to especially low-pass noise sources.

4.3.4 Sine Sweep Measurement Results

In order to obtain the results the measurement will be following the same procedure as for the Golay sequences.

Following illustrations 47 and 48 show the response in time and frequency domain respectively. As studied in the theory, because of the signal used, the frequency response has a better performance in low frequencies than the Golay sequence method.

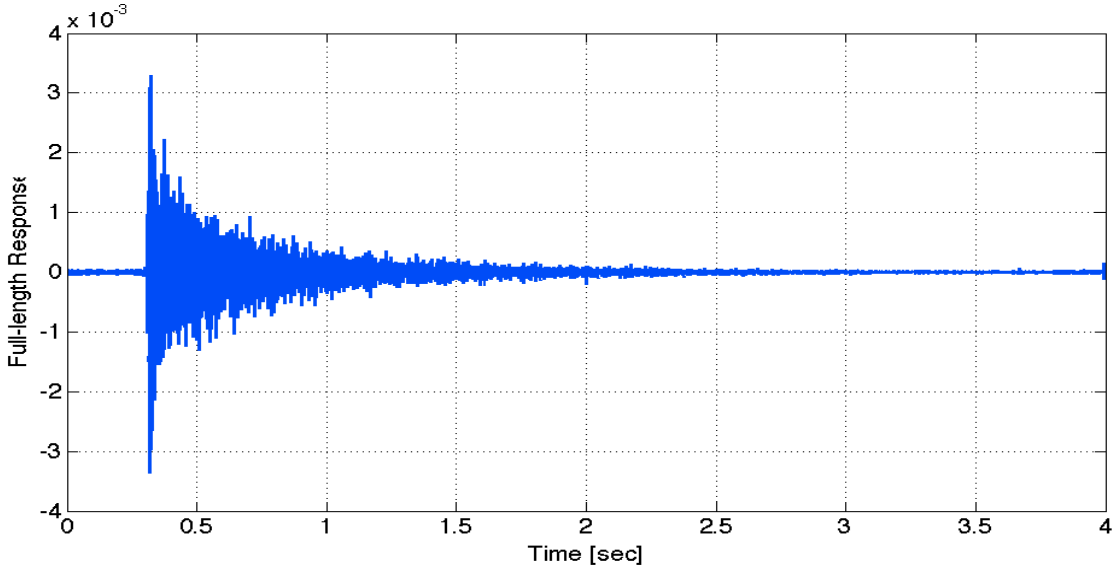

Figure 47: Time response of the sine sweep method

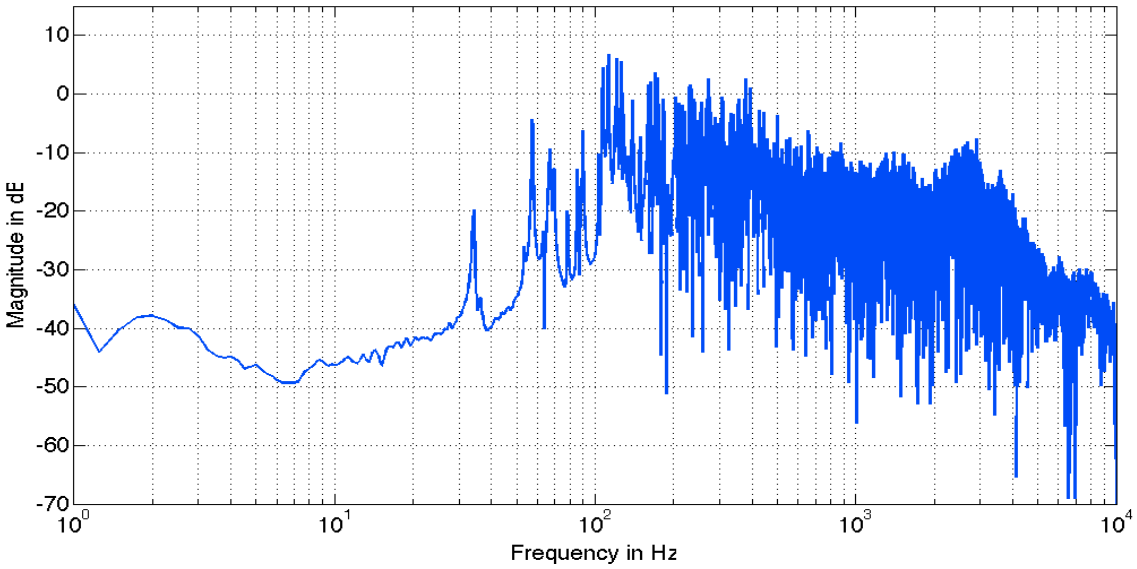

Figure 48: Frequency response of the sine sweep method

In order to be able to compare the peak detection, the sweep method has been compared with the analytical result calculated in the theoretical part. As the picture shows, the sensibility in this case is really high, and eigenmodes are well found by the sine sweep method.

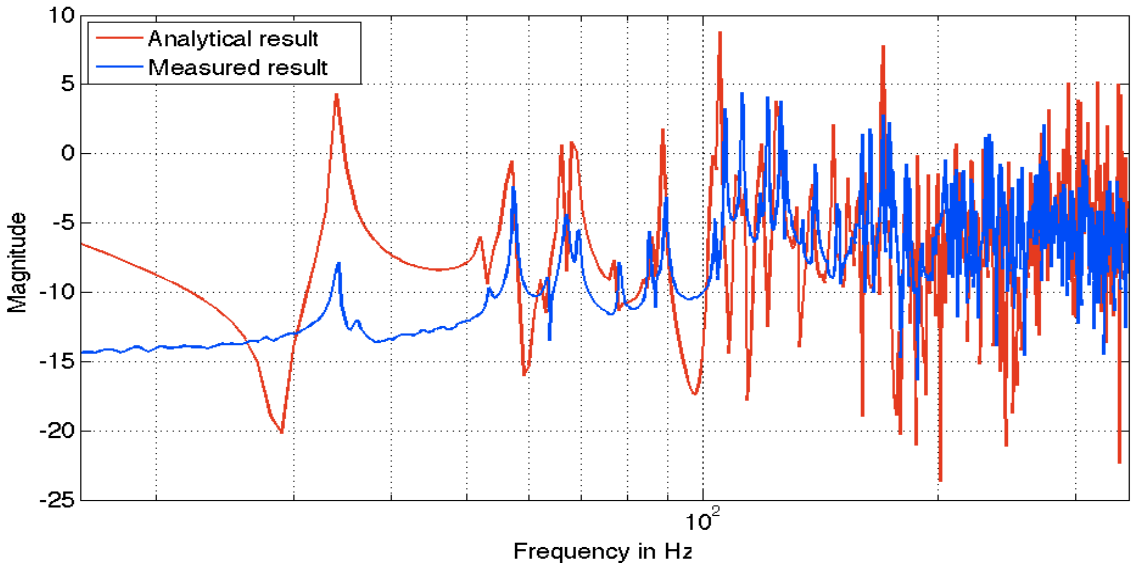

Figure 49: Comparison of sine sweep method vs analytical result

4.4 Comparison between both methods

This section shows the interest of comparing both measure methods in order to test the quality of both in order to acquire the room impulse response.
Results are shown both in time and frequency domain, so that their behaviors can be compared. As it can be seen on next image 50, the response is shown in time domain. Golay sequence shows reverberations and echoes in it. It can be seen, that when t=1 second a resonation appears that amplifies the signal. Again at 2 seconds there is another increase of amplitude. This echos effects can be better seen in the frequency domain, where the results are not so clear. Because of this, the swept sine response is much more clear and shows a better result.

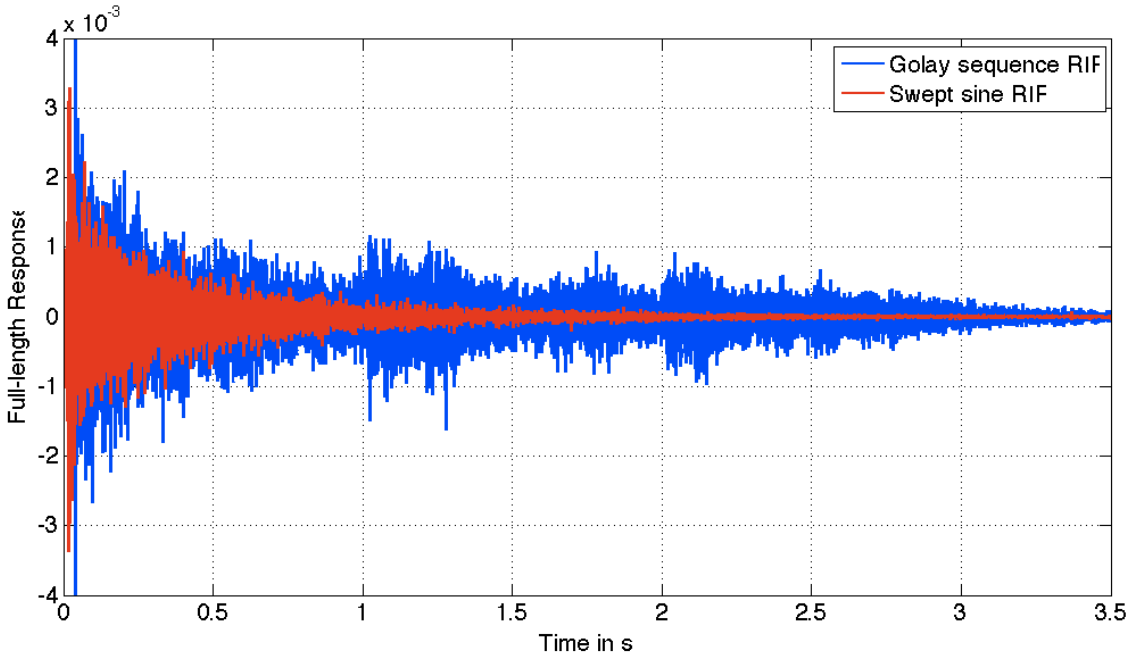

Figure 50: Comparison in time domain of sine sweep method vs golay method

Because of the interest of working in the low frequency, next illustrations 51 and 52 show the solutions in this domain. Results in the low range of the spectrum are zoomed in order to see that picture clearly indicates the sine sweep method is much more accurate in the low frequency range, because of the sensibility and peak detection, which moreover offers better results compared with the analytical result. For this reason, the sine swept method is used all along this thesis and for comparing the methods.

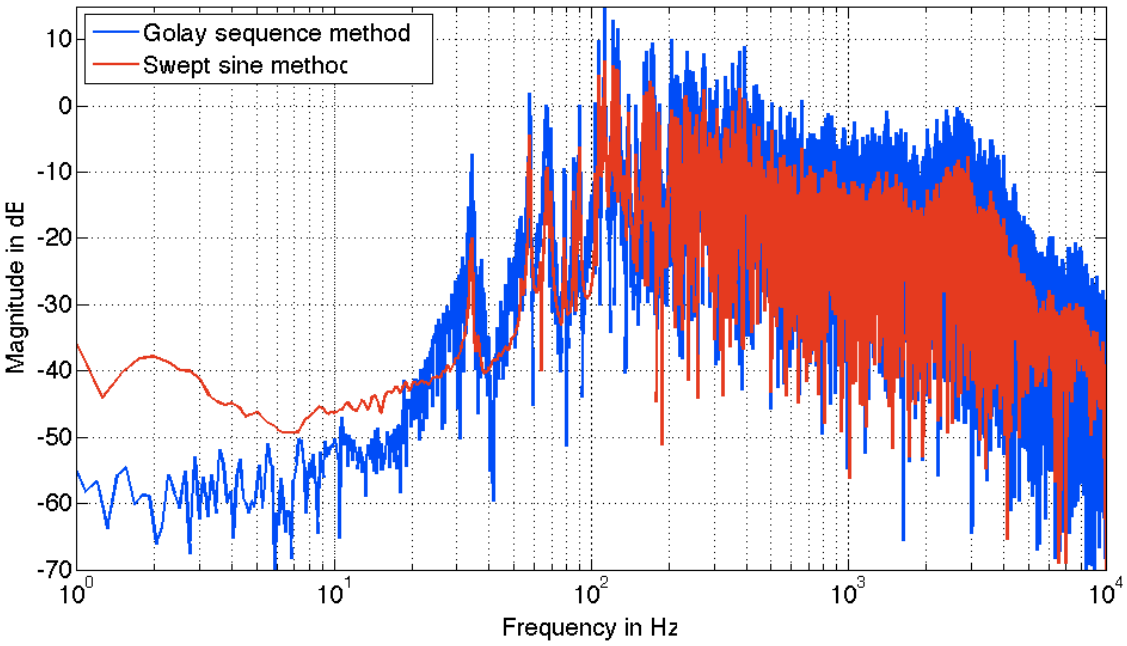

Figure 51: Whole spectrum of sine sweep method vs golay method

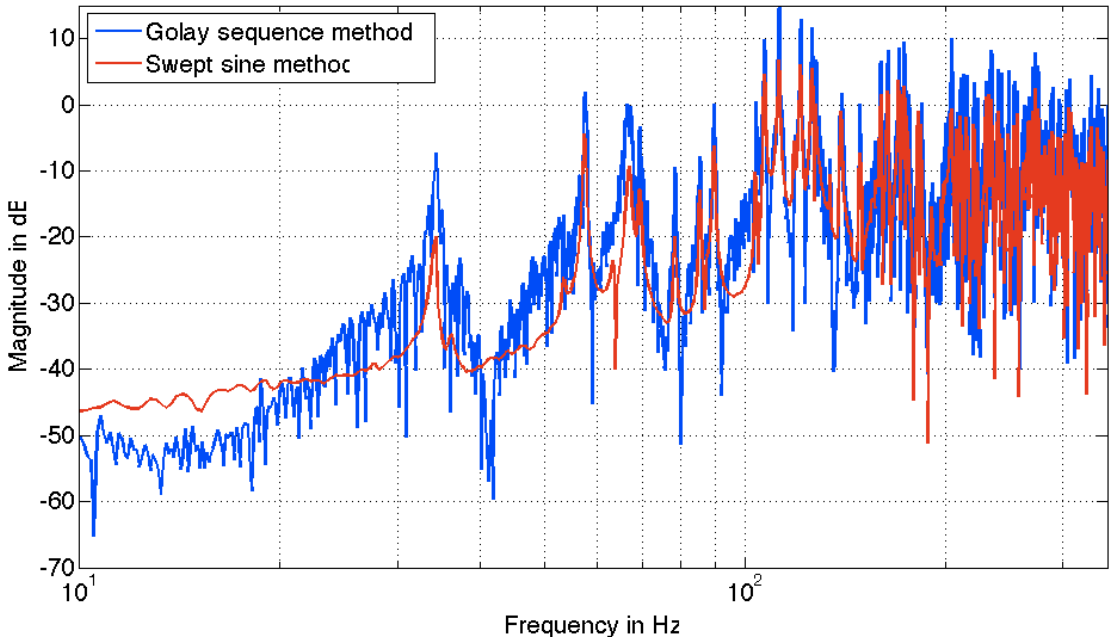

Figure 52: Comparison of sine sweep method vs golay method in the low frequency range

4.5 Comparison of Measure and Simulation Results

In this section it will be discussed the results obtained in the simulation when compared with the measure using the swept sine method. As seen in section 3, the mesh composed by 16594 elements will be used for the comparison, because it proved to be the one with the best results. For this reason, the measure results are also compared with the simulation results with the β parameter which gave the best performance in the previous section. So for this case, $\beta = 0.8$.

Results for the low frequencies (0-150Hz)

Following illustration 53 show the comparison of both of the results. When watching the results, two differences can be seen. The amplitude of the results and the position of the eigenfrequencies in the spectrum clearly differs. For the first statement, it can be seen,that the measure adjusts good when working in low frequencies. For example, the first peaks are positioned at the same frequencies of the spectrum as the results of the simulation. However, when increasing the frequency, problems appear and peaks start to differ. This separation seems to grow when increasing frequencies. The cause of this fact, has been mentioned in section 2. The eigenfrequencies are given by the relation of the wave number:

$$k = \frac{\omega}{c} \text{ with } \omega = 2\pi f \text{ and } c = 340\frac{m}{s} \text{ in room temperature: } T = 20°C$$

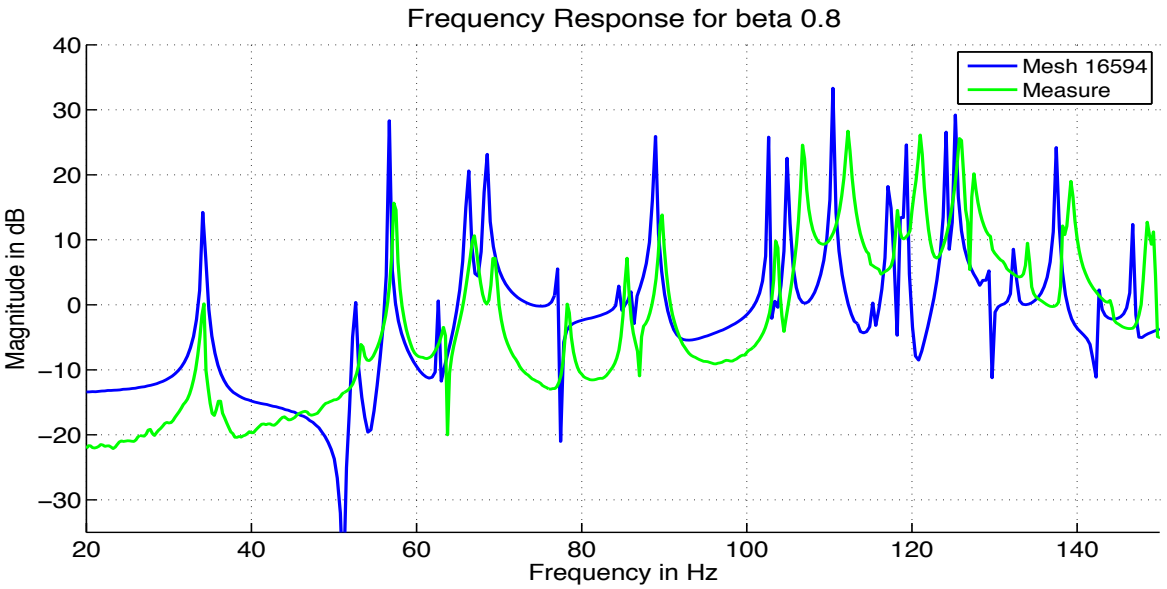

Figure 53: Comparison of results with $\beta = 0.8$ against measure

However, watching the results it can be stated that the temperature such as other parameters of the room are different from the ones used as for the simulation and for the analytical case and for this reason the eigenfrequencies are situated in a different position of the spectrum. For this reason, results for higher frequencies are not presented in this case, due to this problem.

As it was mentioned before, there is another noticeable difference when watching illustration 53. When watching the results below 100Hz, it can be seen that the amplitude of both of the results differ. First peaks are very attenuated and have really low energy. The reason of this lays in the response of the sound source. Because the measure was obtained from the measurement of a microphone the response of the loudspeaker actually shown in the results. The fact that the loudspeaker is not able to perform good in low frequencies can be observed when watching these results. For this reason, when moving into higher frequencies of the spectrum, the amplitude is more similar to the obtained in the results.

4.6 Evaluation of results

In order to see the quality of the method described in this work it is necessary to compare all of the three results that have been presented along this work. Different results have been obtained for the analytical case, for the measurement and also for the simulation.

Results in low frequencies (20-200Hz)

Figure 54 shows the results obtained below the Schroeder (or critical) frequency. Under these frequencies the eigenfrequencies obtained have a great effect on sound reverberation on the room and is the main cause of listening problems. When comparing the analytical result with the results obtained for the mesh of 16594 elements and $\beta = 0.8$. Because both of them have been calculated with the same parameter $c = 340\frac{m}{s}$ the peaks are placed exactly in the same position. However, because the room has a different propagation of the sound because of the various different parameters that affect on the propagation, the peaks are placed in another position.

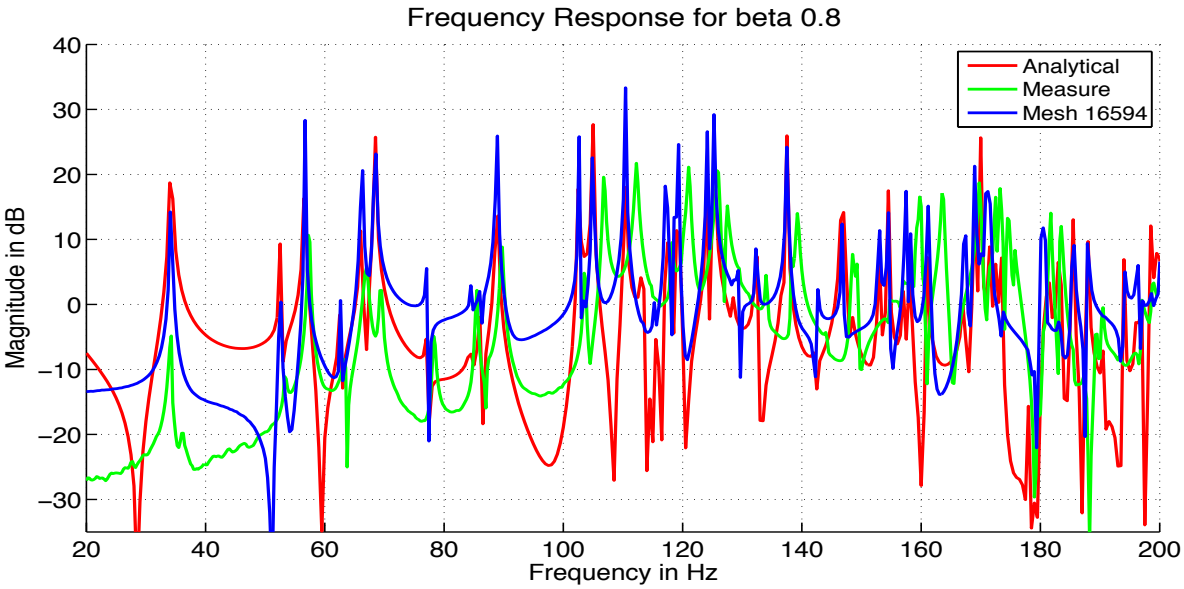

Figure 54: FD-RIR results in frequency-steps for $\beta = 1.5$

Results high frequencies (300-420Hz)

When working over the Schroeder frequency, the effect of eigenmodes is not so important. As it can be seen on figure 55, the peaks do not store so much energy as in low frequencies. When comparing the graphs obtained, it might be seen that

the analytical case still presents peaks, however, much more smaller than on low frequencies. In contrary, the results of the TD-BEM do not present a good resolution and peaks are no more good differentiated. However, it might be appreciated that the results have a similar behavior and results could correspond to the mean of the analytical result.

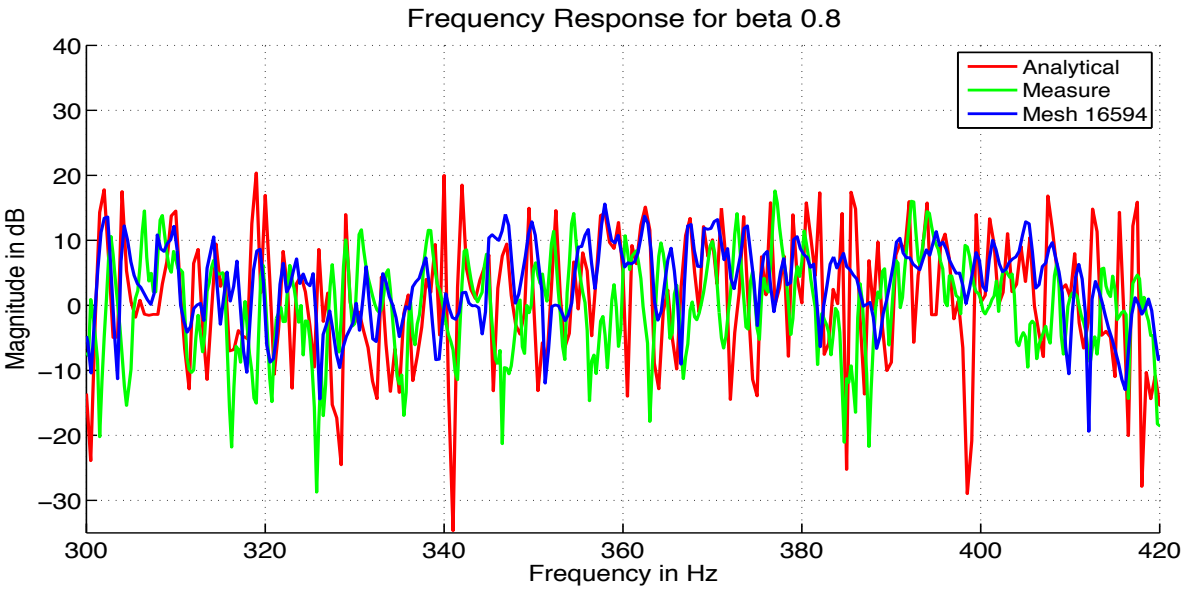

Figure 55: FD-RIR results in frequency-steps for $\beta = 1.5$

After having presented all the results obtained, next section 5 will sum up the main points of this thesis.

5 Conclusions

Room acoustics are gaining importance in the recent years. The computational expense, which was a problem on the last decades is getting overwhelmed by the potential of the new machinery. This has caused an interest in developing new methods in order be able to compare them with other various options that describe at its best the room impulse response, so that quality, precision and finesse in the results between them can be stated.

This master thesis has studied the BEM method working in the time domain, in order to obtain the Room Impulse Response. The theoretical fundaments for obtaining the analytical values, as well for the empirical values have been stated. A comparison between results has also been presented.

During this research various aspects related to the characterization of the room has been presented. It has been show that for a better accuracy in the results of the boundary element method there are key parameters to be adjusted, which can be further used by future researchers who are developing in this area. The two most important parameters presented in this study are:

- Discretization of the mesh
- Discretization of the time

First of all, it has been stated, for example, the importance of the discretization of the mesh. In the test simulation results it has been shown that meshes with less quantity of elements present a less accurate solution or even more it can be unstable. On the other hand, on other simulations where the number of elements is higher the solution appears to be more accurate.

Not only important is the discretization of the mesh, it also may have to be considered the discretization of the time. It has been demonstrated that the stability of the results depend on the correct decision of the parameter β (what has been proved to be taking a low discretization of time Δt). So it is important to focus on these parameter for obtaining better results.

On the other hand, it is important to state, that this simulations require big computation machinery. Because of the necessity of the BEM method to handle big matrices (depending on the size of the mesh of the system), simulations are required to be realized in a big computer with more than 90Gb RAM. Data, in order to obtain the room impulse responses for various scenarios, was simulated in a big computer and afterwards collected to be analyzed.

When obtaining this results, as some studies predicted, results in time domain resulted to be unstable. Instability can be produced because of the eigenvalues of

the matrix obtained by the BEM method. Eigenfrequencies whose eigenvalues are close to 1 show instabilities, and results have a tendency to grow.

This study has shown some solutions to this problem, which are been tested in actual time like the post-filtering of the signal or the damping of the eigenfrequencies solution. With both methods the instability problems are diminished and therefore the quality of results has increased, but despite of this, the instability problem has even so not been completely eliminated.

When comparing the final results with the theoretical values, it has been stated that all this factors, make the final solution to not give the best solution, although it is pretty close to the real one.

5.1 Future work

Room acoustics are still being investigated by several research groups in the world. The work done in this master thesis tries to reassemble the theory studied in this field. The procedure for obtaining the Room Impulse Response has been presented: The theory for the values of the eigenmodes, the theory of the BEM method for obtaining the RIR and the measurement methods known. It wants to help to contribute in further studies. There are still open topics in this field, that requires a study. As it has been seen, methods for correcting the stability problems are still in study and still those solutions bring side effects to the results, making them worse. For this reason, the improvement of stability problems which would follow to better results, is indeed a topic to deal with. As second points, the implementation of this method in other surroundings would be interesting. Adopting the study realized here and implementing it for rooms with other boundaries which are not hard, but have losses, would be interesting.

References

[1] Michael Vorländer., "Auralization,"Springer Verlag, 2010.

[2] Jens Blaeurt, Ning Xiang., "Acoustics for Engineers," *Springer Verlag*, 2009.

[3] Peter Hunter, Andrew Pullan, "Modeling Techniques for Virtual Acoustics," *Dissertation for Doctor Thesis*, February 21, 2001.

[4] Lauri Savioja., "FEM/BEM NOTES," Reading, 1999.

[5] Michael Stütz, "Disertation for Doctor Thesis,".

[6] M. Stütz, M.Ochmann "Simulation of a transient sound radiation using the Time Domain Boundary Element Method,".

[7] Jonathan A. Hargreaves, Trevor J. Cox., "A transient boundary element method model of Schröder diffuser scattering using well mouth impedance," *J. Acoust. Soc. Am.*, Vol. 124, No. 5, November 2008.

[8] Jonathan A. Hargreaves, Trevor J. Cox., "A transient boundary element method model for room acoustics," *J. Acoust. Soc. Am.*, Vol. 124, No. 5, November 2008.

[9] Jonathan A. Hargreaves, Trevor J. Cox., "A Transient Boundary Element Method for Acoustic Scattering from Mixed Regular and Thin Rigid Bodies," *Acta Acustica United with Acustica.*, Vol 95 p 678-689, 2009.

[10] Toufic Abboyd, Maxime Pallud, Xiaodong Zhou., "Time Domain Boundary Element Methods for Acoustics," *The International LMS Engineering Simulation Conference*, 2010.

[11] J.-M. Parot et al., Elimination of a non-oscillatory instability in a retarded potential integral equation. "Engineering Analysis with Boundary Elements (2006), doi::10.1016/j.enganabound.2006.09.014.

[12] H. Wang, D.J. Henwood, P.J. Harris, R. Chakrabarti, "Concerning the cause of instability in time-stepping boundary element methods applied to the exterior acoustic problem," *Journal of Sound and Vibration* 305 (2007) 289-29.

[13] Bjarne Büchmann, Jesper Skourup., "Stability of time-domain boundary elements models, theory and applications," *Journal of Sound and Vibration*

[14] Jean-Marc Parot, Christophe Tirard., "A numerical algorithm to damp instabilities of a retarded potential integral equation," *Engineering Analysis with Boundary Elements*, 2011.

[15] Edgar Berdahl, Julius Smith., "Impulse Response Measurement Toolbox ,Online Content, http://cnx.org/content/col10519/1.5/ .

A Appendix A

Frequency Hz	n_x	n_y	n_z	**Mode**
34.7	1	0	0	Axial
53.2	0	0	1	Axial
57.4	0	1	0	Axial
63.4	1	0	1	Tangential
67.1	1	1	0	Tangential
69.3	2	0	0	Axial
78.2	0	1	1	Tangential
85.6	1	1	1	Oblique
87.3	2	0	1	Tangential
90.0	2	1	0	Tangential
104.0	3	0	0	Axial
104.5	2	1	1	Oblique
106.3	0	0	2	Axial
111.8	1	0	2	Tangential
114.8	0	2	0	Axial
116.8	3	0	1	Tangential
118.7	3	1	0	Tangential
119.9	1	2	0	Tangential
120.8	0	1	2	Tangential
125.7	1	1	2	Oblique
126.5	0	2	1	Tangential
126.9	2	0	2	Tangential
130.1	3	1	1	Oblique
131.2	1	2	1	Oblique
134.1	2	2	0	Tangential
138.6	4	0	0	Axial
139.3	2	1	2	Oblique
144.3	2	2	1	Oblique
148.4	4	0	1	Tangential
148.7	3	0	2	Tangential
150.0	4	1	0	Tangential

Table 2: First 30 eigenfrequencies of the room

A Appendix B

Results for the test point position 1

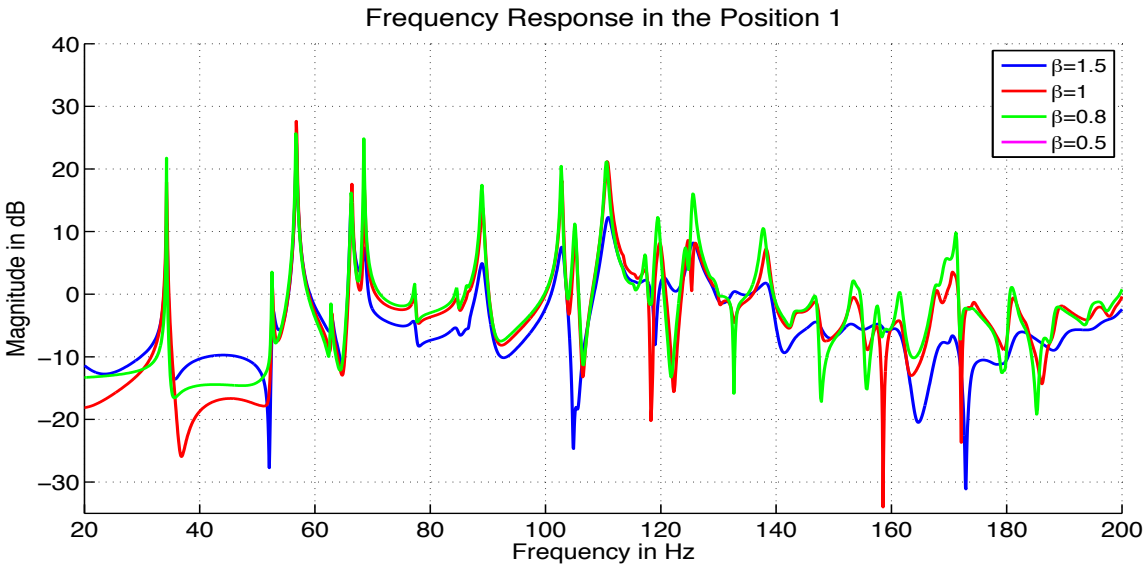

Figure 56: FD-RIR results for test point 1 meshed with 2030 elements

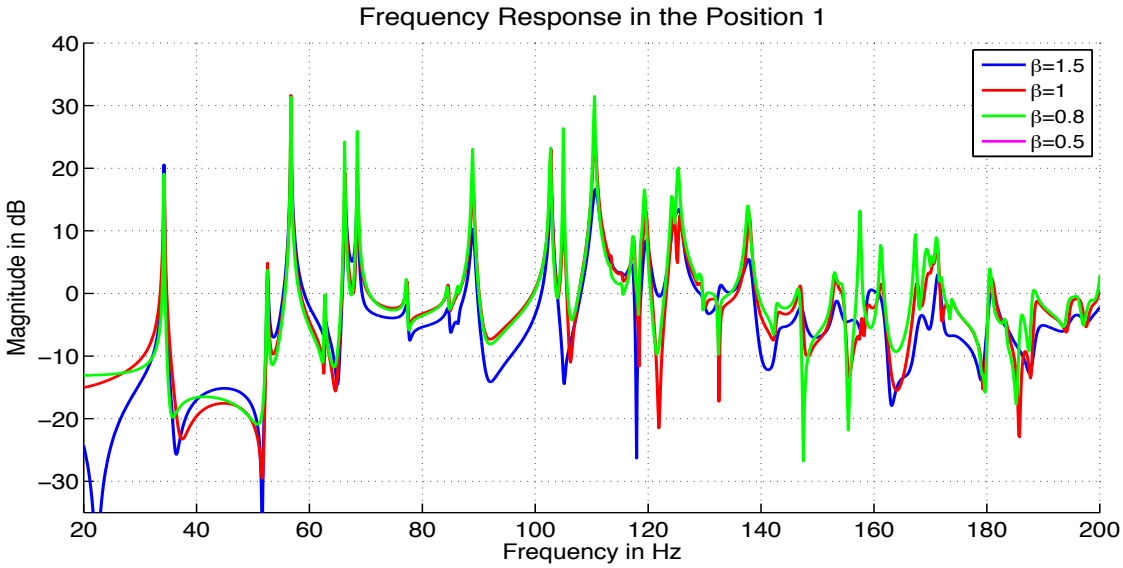

Figure 57: FD-RIR results for test point 1 meshed with 3652 elements

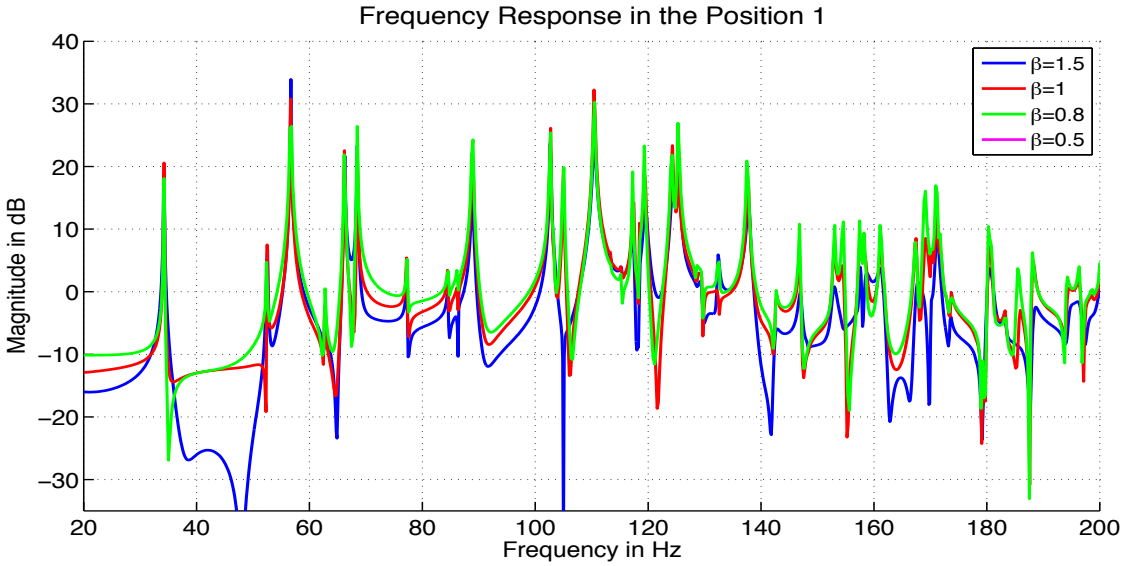

Figure 58: FD-RIR results for test point 1 meshed with 8280 elements

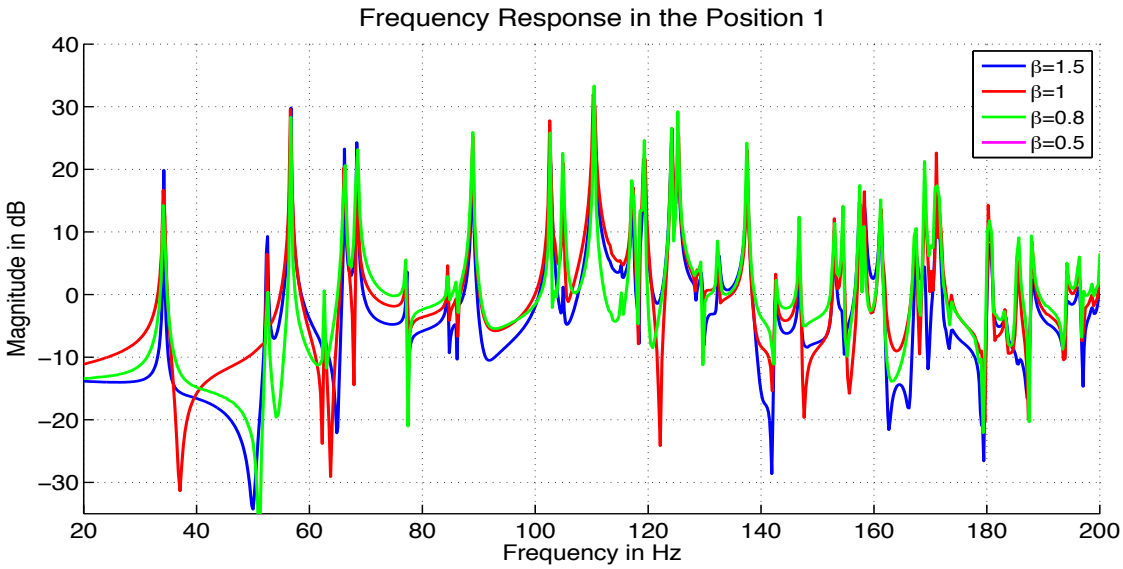

Figure 59: FD-RIR results for test point 1 meshed with 16594 elements

Results for the test point position 2

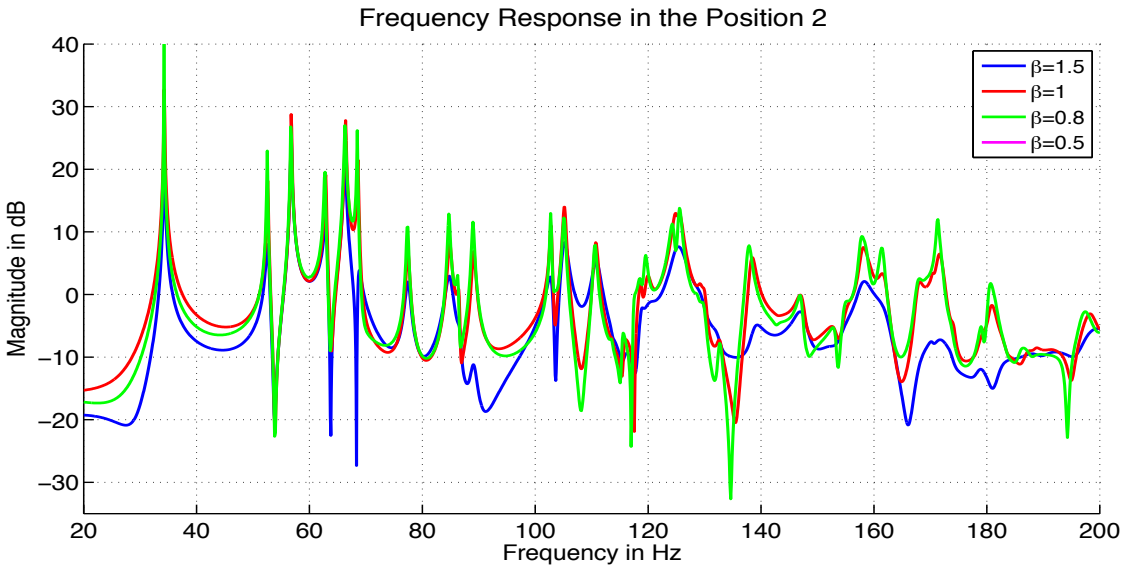

Figure 60: FD-RIR results for test point 2 meshed with 2030 elements

Figure 61: FD-RIR results for test point 2 meshed with 3652 elements

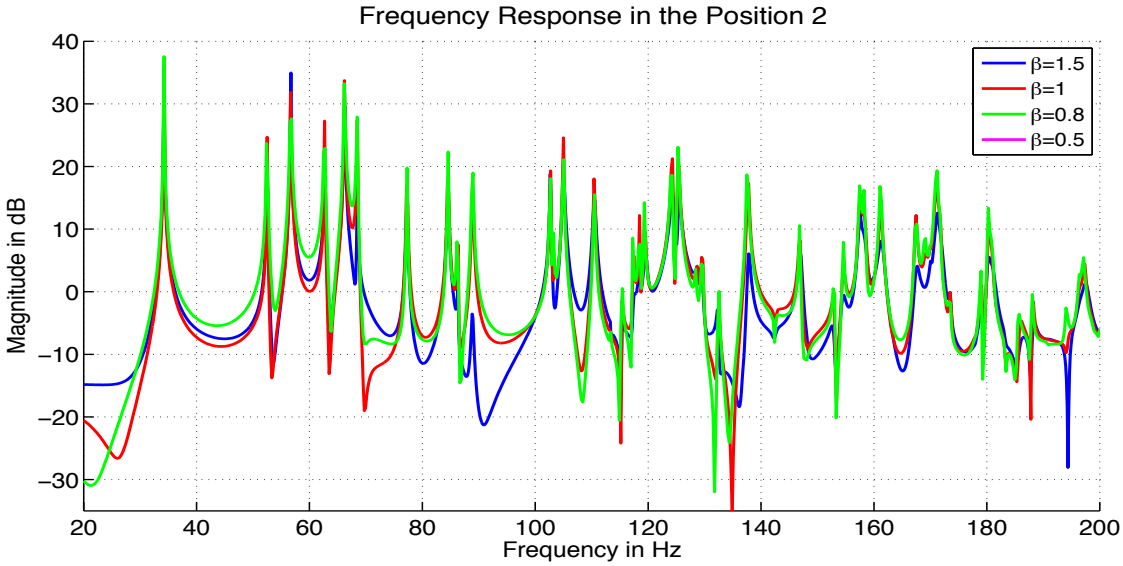

Figure 62: FD-RIR results for test point 2 meshed with 8280 elements

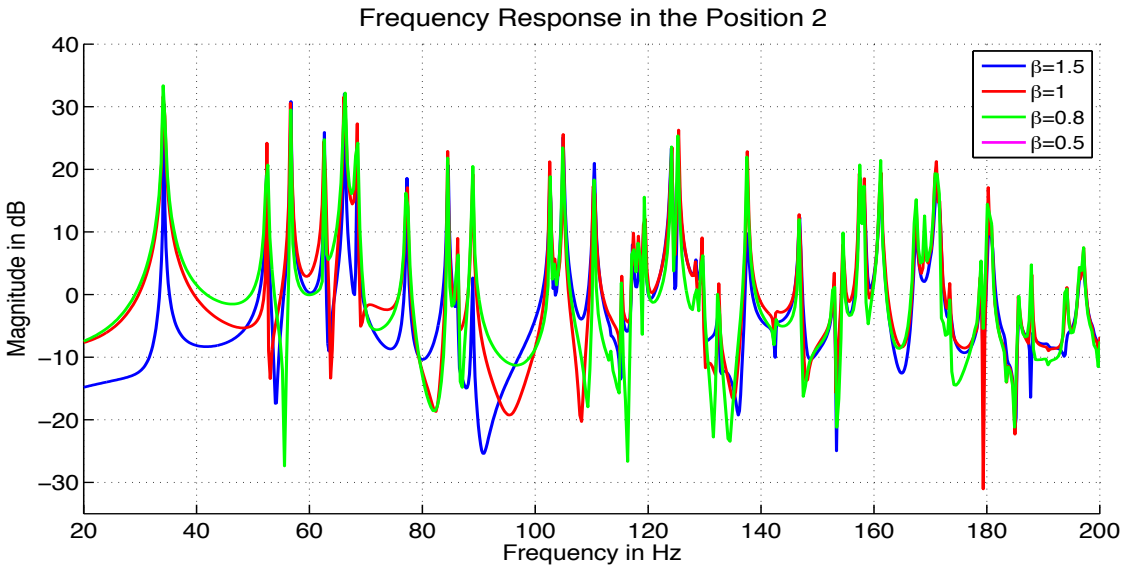

Figure 63: FD-RIR results for test point 2 meshed with 16594 elements

Results for the test point position 3

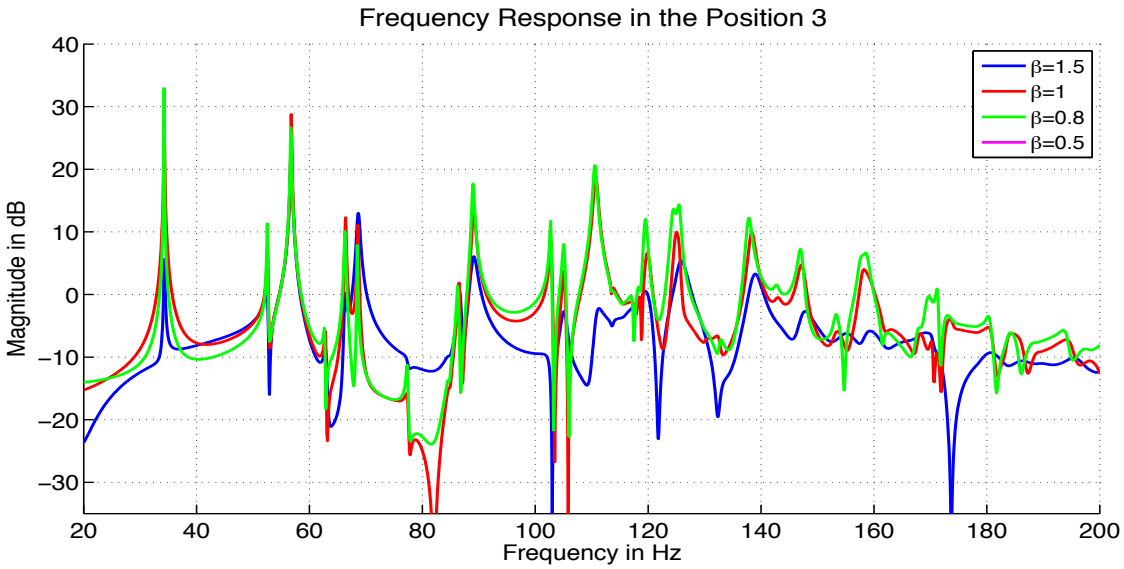

Figure 64: FD-RIR results for test point 3 meshed with 2030 elements

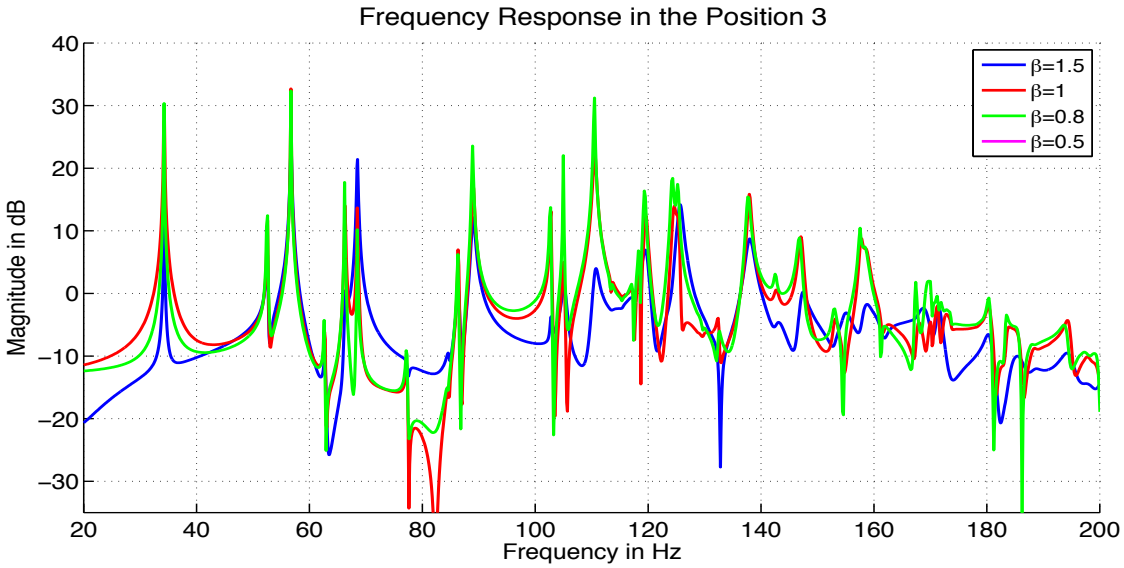

Figure 65: FD-RIR results for test point 3 meshed with 3652 elements

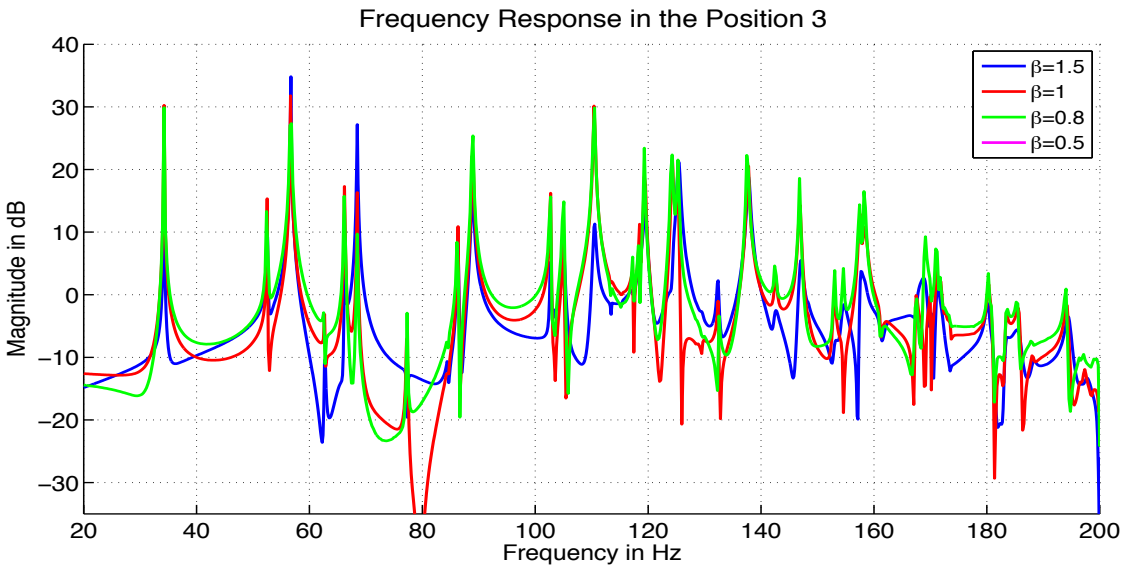

Figure 66: FD-RIR results for test point 3 meshed with 8280 elements

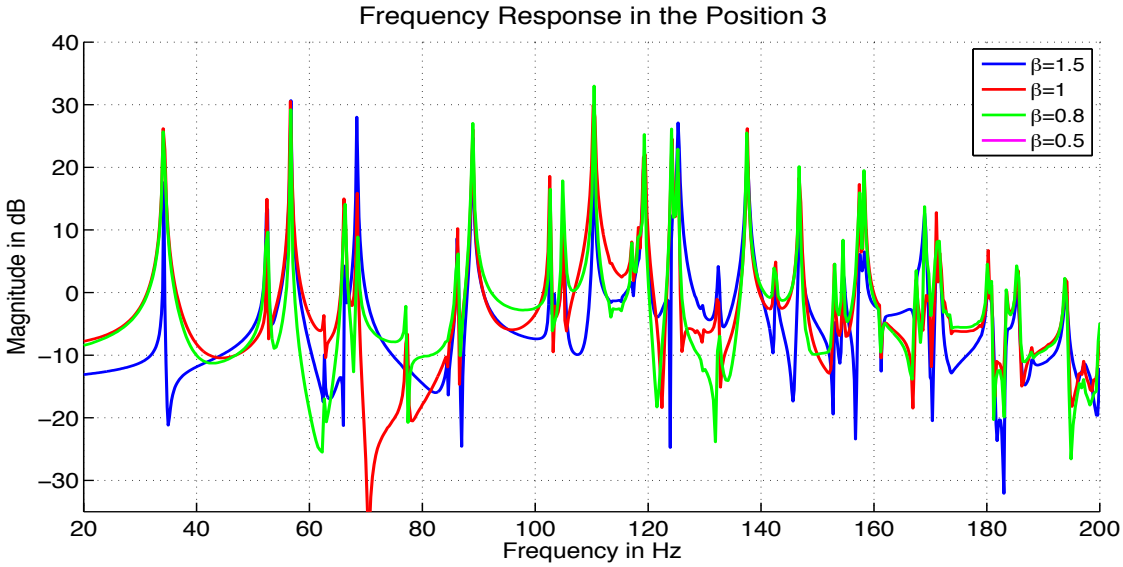

Figure 67: FD-RIR results for test point 3 meshed with 16594 elements

Results for the test point position 4

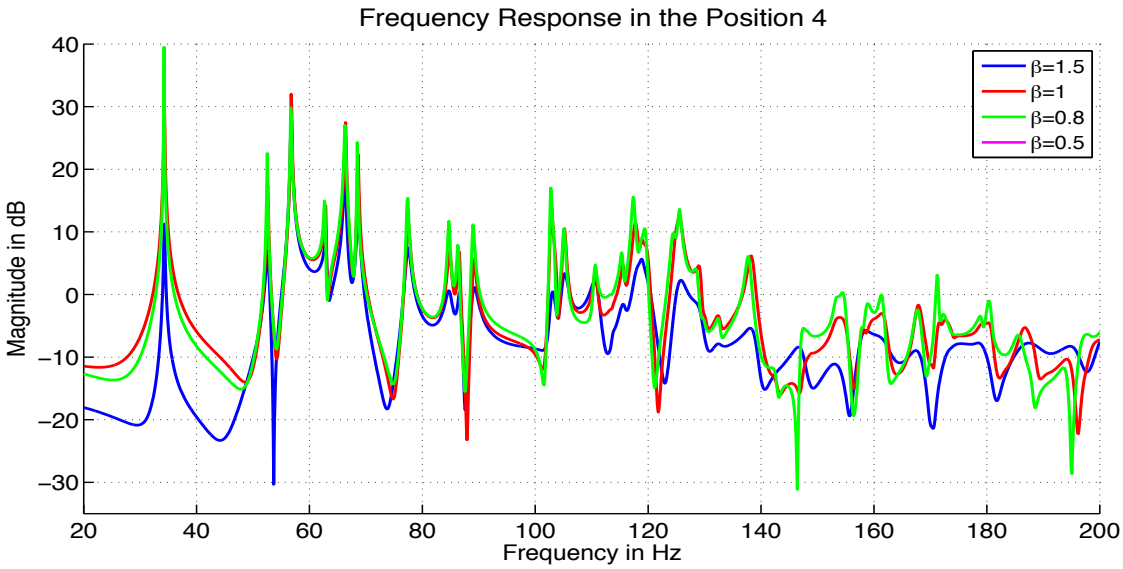

Figure 68: FD-RIR results for test point 4 meshed with 2030 elements

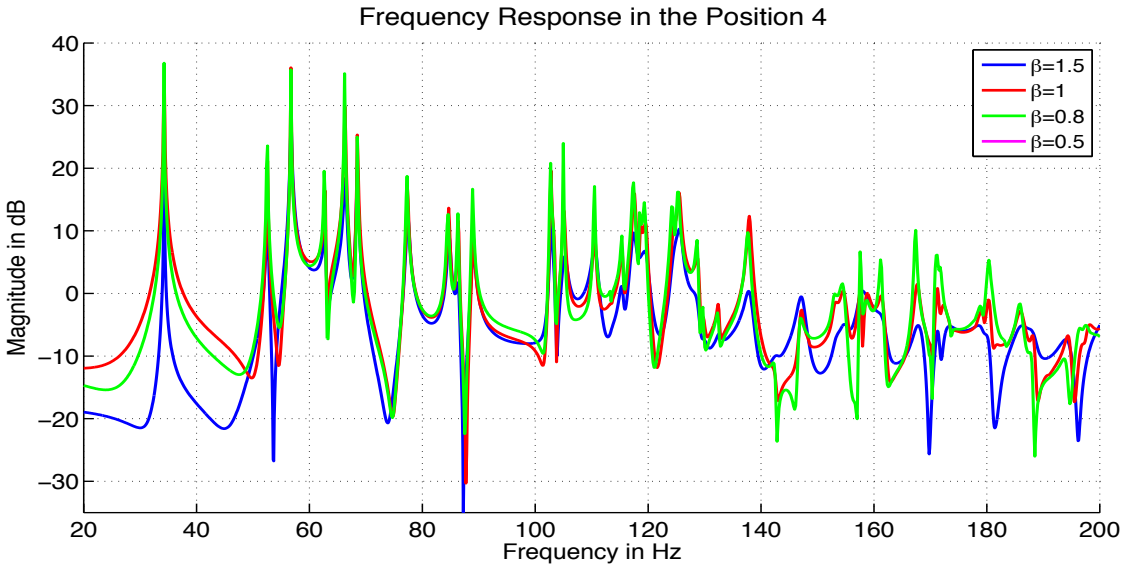

Figure 69: FD-RIR results for test point 4 meshed with 3652 elements

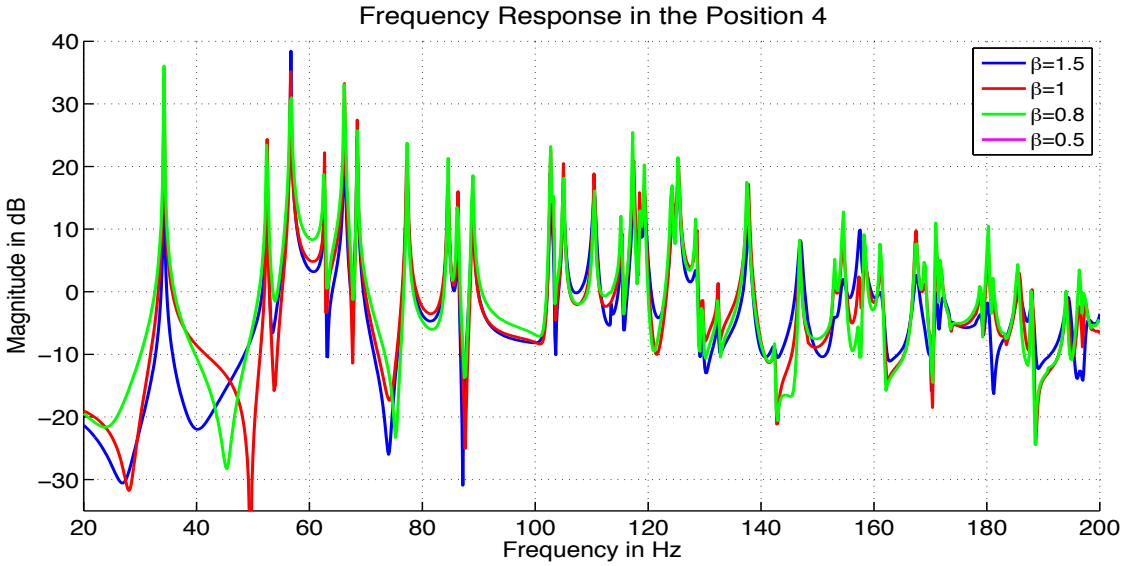

Figure 70: FD-RIR results for test point 4 meshed with 8280 elements

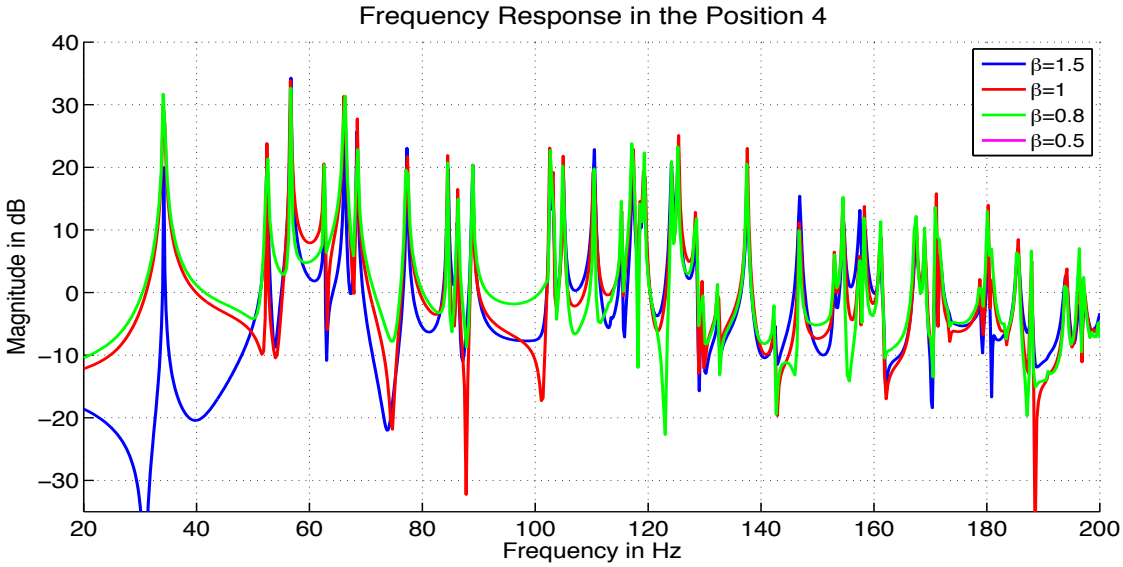

Figure 71: FD-RIR results for test point 4 meshed with 16594 elements